Geodynamics of the Lithosphere

GEO.916 WS2014/2015

Kurt Stüwe

Manuskript version 21.12.2014

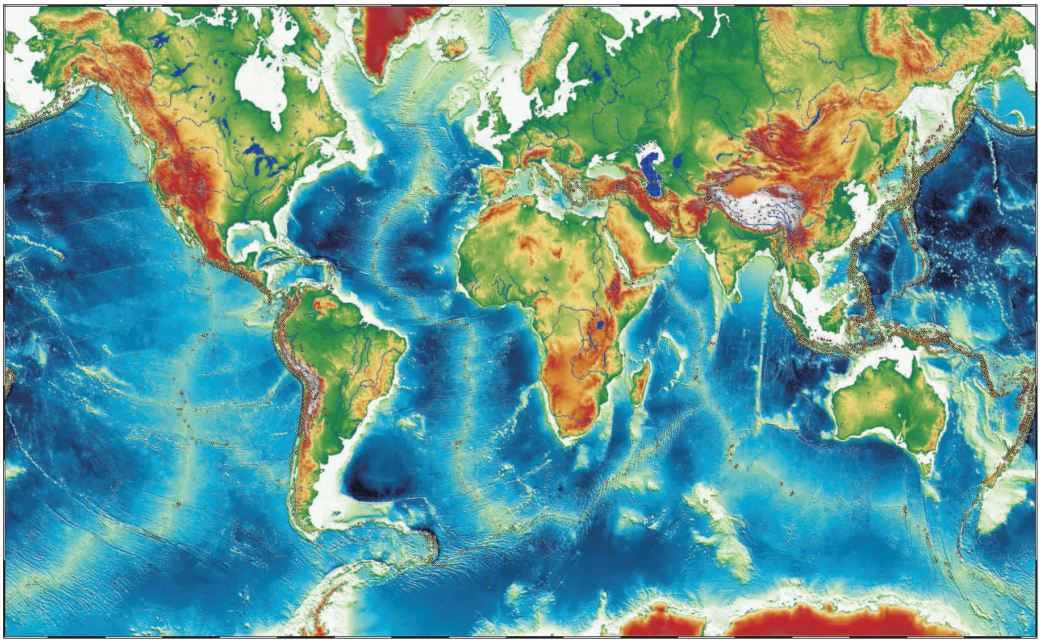

Introduction

This course (LV GEO.916) deals with quantitative estimate of processes in the Earth's lithosphere. As such, the *qualitative* processes and geometries of the lithosphere as discussed in the "geodynamics" course (LV GEO.524) of your curriculum are assumed to be known. In other words, it is expected that you have a basic qualitative understanding of the thermal and density structure of the lithosphere and how these rule fundamental plate tectonic processes like rifting, collision or subduction (e.g. Fig. 2.16 to Fig. 2.27 in my textbook "Geodynamics of the Lithosphere"). For this course, an extract of the subject of Geodynamics is made that fits a volume of a course incuding 13 Units taught in two hours per week over 1 semester. In the skript, each Unit is summarised in no more than 5 - 10 skript pages per Unit. The content of this course can be found in a series of textbooks. For those of you who want to understand this subject in more depth, I recommend the following three books:

- Turcotte D.L. and Schubert G. (2014): Geodynamics, 3rd ed., Cambridge University Press, 496 p.
- Fowler C.M.R. (1990): The Solid Earth. An Introduction to Global Geophysics. Cambridge University Press. 472 p.
- Stüwe K. (2007): Geodynamics of the Lithosphere. Springer Verlag, Berlin Heidelberg, 493 p.

The course script is made largely as an extract from Stüwe (2007), where more detail on each Unit can be found. I hope you enjoy the course and look forward to work with you!

21.12.2014 Kurt Stüwe

Content

1 Unit: The Diffusion Equation

The heat conduction equation - more commonly known as the diffusion equation - is fundamental for the understanding of the transport of heat in the lithosphere. It turns out that the very same equation cannot only be applied to the transport of thermal energy, but also to the diffusion of mass. It finds therefore application in many other fields, for example geomorphology, metamorphic petrology or hydrology. Thus, the diffusion equation is the first equation in this course that we will discuss in some detail. The fact that it is a second order partial differential equation should not scare us off. We will show that it is possible to understand it quite intuitively. The equation is a combination of two fundamental laws of heat conduction:

1.1 Fourier's Law of Heat Conduction

Fourier's 1. law is the basic law underlying the diffusion equation. This law states that the flow of heat q is directly proportional to the temperature gradient (Fourier 1816). This statement can easily be formulated in an equation:

$$q = -k\frac{\mathrm{d}T}{\mathrm{d}z} \quad . \tag{1}$$

In this equation q is short for heat flow, T stands for temperature and z for a spatial coordinate, for example depth in the crust. The ratio $\mathrm{d}T/\mathrm{d}z$ is the change of temperature in direction z. We call this ratio the temperature gradient. k is the proportionality constant between the gradient and the flow of heat. In order to understand this law better (and understand the units of k), let us consider a more familiar analogue: the flow of water in a river. The same law applies. In a river the flow of water can be described by the volume of water passing per unit of time and per area of cross section of the river (in SI-units: $\mathrm{m^3\,s^{-1}\,m^{-2} = m\,s^{-1}}$). This is called the volumetric flow. When normalized only to the width of the river and not to the cross sectional area of the river, the volumetric flow has the units of $\mathrm{m^2\,s^{-1}}$. In contrast, the flow of mass has the units $\mathrm{kg\,s^{-1}\,m^{-2}}$. Fourier's law – applied to our example of water flow – states that the flow of water is proportional to the topographic gradient of the river. This corresponds well to our observations in nature: The steeper a river bed, the faster the flow of water in the river (per square meter of cross sectional area). Fourier's law seems to be a good model description for this observation. This simple example also explains why there is a negative sign in eq. 1. The flow is against the gradient: it is *positive* in the *downwards* direction of the gradient.

In the theory of heat conduction, the flow of heat has obviously not the units of volume per time and area, but *energy* per time and area. (in SI units: $\mathrm{J\,s^{-1}\,m^{-2} = W\,m^{-2}}$). The thermal gradient now replaces the topographic gradient of the river. Because of historical reasons heat flow is sometimes given in heat flow units, or hfu. One hfu corresponds to 10^{-6} $\mathrm{cal\,s^{-1}\,cm^{-2}}$ and can easily be converted into $\mathrm{W\,m^{-2}}$. The units of the proportionality constant k, in eq. 1, follows now easily from the units of the other components of the equation: Because temperature has the units of K (or °C) and z has the unit m, k must have the units $\mathrm{J\,s^{-1}\,m^{-1}\,K^{-1}}$ so that the equation is consistent in its units. The constant k is called *thermal conductivity*. We can now try to read eq. 1. We can see that the flow of heat trends to zero if the conductivity is very low, regardless of the thermal gradient. Correspondingly, if the conductivity is very large, the flow of heat becomes large, even if the thermal gradient is very low. The equation may therefore be understood quite intuitively.

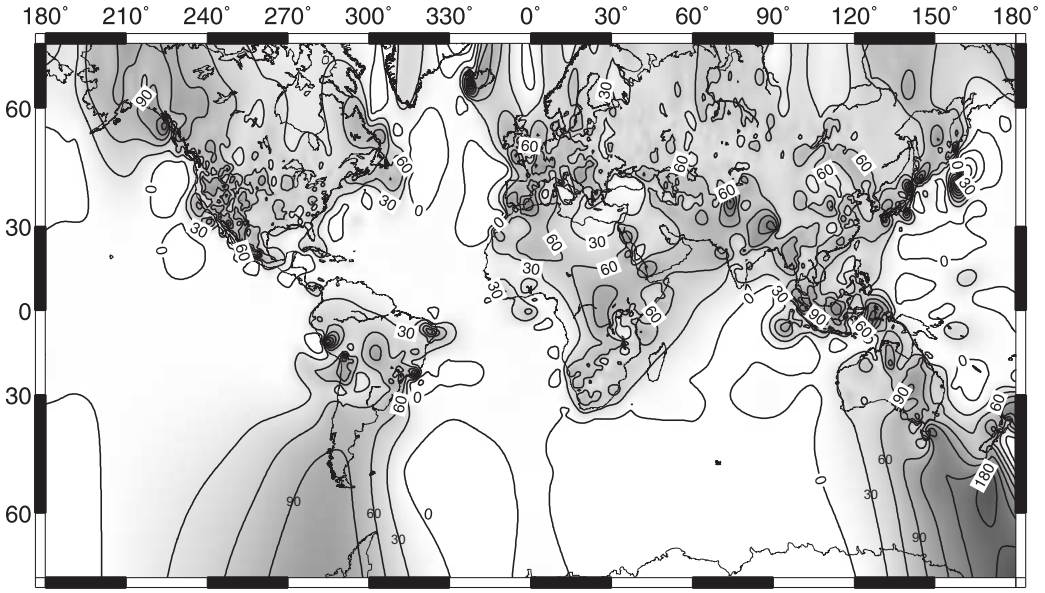

Figure 1: Map of global surface heat flow. The map is contoured in milli W m^{-2} and data above 300 mW^{-2} are omitted so that only a conductive response is shown. Nevertheless, because of the highly irregular distribution of the data, the contouring on a global scale is strongly dependent on the contouring algorithm and is associated with large uncertainties in areas of low data density. (made with the Global Heat Flow Data Base of the International Heat Flow Commission, W. Gosnold, Custodian pers. comm. 2006). As a consequence, this map is exclusively a representation of the data base with no consideration of the data distribution, its density or their reliability. As such, it appears (wrongly) that the heat flow on the oceans is lower than that of the continents. For a more considered heat flow map see Pollack et al. (1993) or Wei and Sandwell (2006).

Would the thermal gradient be constant everywhere, we could write it as $\Delta T/\Delta z$. However, in geological problems this gradient is never constant. Thus, we use the derivative $\mathrm{d}T/\mathrm{d}z$, which states that we want to be careful and consider our thermal gradient only to be constant within each infinitely small section of the thermal profile. If the gradient changes along the z direction, then eq. 1 states that the heat flow must also change.

1.2 Energy Balance

The second part of the diffusion equation (often called Fourier's 2. law) describes an energy balance. This energy balance relates heat and temperature and the change of heat flow with change in temperature. This relationship may be established independently from eq. 1 and may be written as:

$$\frac{\partial T}{\partial t} \propto -\frac{\partial q}{\partial z} \quad . \tag{2}$$

This equation states that the rate of temperature change of a rock must be proportional to the rate with which its heat content changes ($\propto$ is the symbol for "proportional to"). The rate with which the heat content of a rock changes ($\partial q/\partial z$) is given by the difference

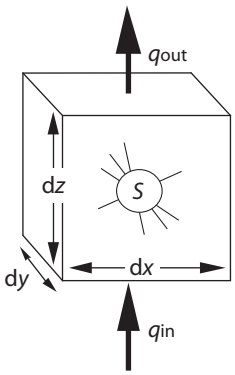

Figure 2: The flow of heat in a unity volume of rock. The heat production inside this volume S, is not considered until we discuss real continental geotherms.

between the flow of heat *into* the rock and the flow of heat *out of* the rock (Fig. 2). If the heat flow into the cube of Fig. 2 is larger than the flow of heat out of it, then the heat content of the cube will rise and its temperature will increase. If the heat flow into the volume is just as large as that that flows out, the temperature will remain constant. If more heat flows out of the cube than into it, then its temperature will decrease.

In the last sentences we have begun mixing the terms "temperature" and "heat". However, we have to remain careful no to confuse them as the rate of temperature change is not the same as the rate of heat content change. They relate by:

$$H = T\rho c_p \tag{3}$$

where H is the volumetric heat content in J m^{-3}. The rate, with which the temperature will change for a given change in heat content depends on another material specific proportionality constant. This is the *specific heat capacity* c_p. The specific heat capacity or short "*specific heat*" has the units of J kg^{-1} K^{-1} and defines how many Joules are required to heat the mass of one kg of rock by one degree Kelvin. The most common abbreviation for specific heat is c. The subscript p symbolizes the condition that the specific heat is measured at constant pressure. If the specific heat of a rock is large, we need many Joules to heat the rock and even a rapid increase of its heat content will lead to slow temperature increase and vice versa. Specific heat is formulated in terms of the *mass* that is heated. Considering that the energy balance in eq. 2 is formulated in terms of the *spatial* coordinate z, and heat capacity is formulated in terms of *mass*, we need to multiply c_p with the density ρ, so that the relationship between the spatial change of *heat flow* and the temporal change of *temperature* is consistent with the units. We can write the proportionality of eq. 2 as:

$$\rho c_p \frac{\partial T}{\partial t} = -\frac{\partial q}{\partial z} \quad . \tag{4}$$

(see also eq.41 for its equivalent in terms of heat). It should now be straight forward to understand eq. 4 intuitively using Fig. 2. The negative sign arises because the temperature *increase* when $\partial q = q_{\text{out}} - q_{\text{in}}$ is negative, that is, more heat flows into the rock volume than out of it. You may have noticed that the step from eq. 2 to eq. 4 was accompanied by the change from total- to partial differentials. This was necessary, because different parts of this equation are now differentiated with respect to different parameters.

1.3 The Diffusion Equation

If we substitute Fourier's law of heat conduction (eq. 1) into the thermal energy balance of eq. 4, we arrive at:

$$\rho c_p \frac{\partial T}{\partial t} = \frac{\partial \left(k \frac{\partial T}{\partial z}\right)}{\partial z} \quad . \tag{5}$$

Eq. 5 is the general form of the one-dimensional diffusion or heat conduction equation. If k is independent of z (e. g. if we consider heat conduction in an area without lithological contrasts), it is possible to simplify eq. 5 significantly. k can then be taken out of the differential and we can write:

$$\rho c_p \frac{\partial T}{\partial t} = k \frac{\partial \partial T}{\partial z \partial z} \qquad \text{or :} \qquad \frac{\partial T}{\partial t} = \kappa \frac{\partial^2 T}{\partial z^2} \quad . \tag{6}$$

The constants k, ρ and c_p are now summarized to $\kappa = k/(\rho c_p)$. κ is called thermal diffusivity. Eq. 6 can also be understood intuitively, without following the detailed derivation given above. Eq. 6 may be formulated in words as:

- *The rate of temperature change is proportional to the spatial curvature of the temperature profile.*

If you do not understand the relationship between this sentence and eq. 6, then remember that the first differential of a function describes its slope (or: "gradient", or: "rate") and the second its curvature.

Figure 3 illustrates this graphically. In our daily lives we encounter many examples that are described by this equation. Think for example that a piece of toast cools much quicker on its corners than along the edges or in its middle. This is because the *spatial curvature* of the isotherms in the toast is the largest at the corners! The same is true for the rapid cooling of the tip of a needle, the rapid erosion of ragged mountain tops and countless other examples in nature, all the way down to the rapid chemical equilibration of fine grained rocks in comparison with coarse grained rocks.

If we want to use eq. 6 we must solve it. For this we need boundary- and initial conditions. We also need some mathematical knowledge so that we can integrate this equation. Various methods how to go about this are discussed in sect. 6.0.1. A large part of this chapter will deal with various solutions of this equation. In this context we will often meet the terms "*boundary conditions*" and "*initial conditions*". Make sure you understand what they mean.

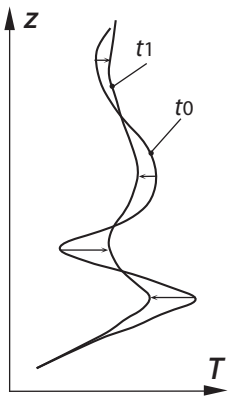

Figure 3: The thermal equilibration of a random temperature profile. The temperature profile is drawn at two different time steps t_0 and t_1. Note that the largest change in temperature between the two time steps has occurred in those places of the profile where the curvature of the profile is the largest (s. eq. 4). Where the curvature of the profile is zero (at the inflection points) the temperature does not change at all.

• **The magnitude of κ** A quantitative application of eq. 6 requires the knowledge of κ and therefore the knowledge of k, ρ and c_p. The specific heat of rocks is about $c_p = 1\,000 - 1\,200\ \mathrm{J\,kg^{-1}\,K^{-1}}$ (Oxburgh 1980). For most rocks c_p does not vary by more than 20 % around this value. Thus, the nice and even value of $c_p = 1\,000\ \mathrm{J\,kg^{-1}\,K^{-1}}$ is a sound assumption that can be used for many thermal problems. The density of many crustal rocks is of the order of $2\,750\ \mathrm{kg\,m^{-3}}$ and varies also not all that much around this value. However, thermal conductivity, varies by the factor 2 or 3 between different rocks types (Table 1). Fortunately, it is between 2 and 3 $\mathrm{J\,s^{-1}\,m^{-1}\,K^{-1}}$ for many rock types. For $k = 2.75\ \mathrm{J\,s^{-1}\,m^{-1}\,K^{-1}}$ and the values for specific heat and density from above the diffusivity is: $\kappa = 10^{-6}\,\mathrm{m^2\,s^{-1}}$. Because this value is easy to remember it is commonly used in the literature. Note, however, that κ may also be twice- or half as large if the thermal conductivity of rocks is twice or half as large.

1.3.1 Heat Refraction

If rocks of different thermal conductivity are in contact, the phenomenon of *heat refraction* may occur. What this is, is easily explained with eq. 1. In thermal equilibrium, the flow of heat in two adjacent rocks must be equal. Following from eq. 1 we can formulate:

$$-q = k_1 \frac{\Delta T_1}{\Delta z} = k_2 \frac{\Delta T_2}{\Delta z} \quad , \tag{7}$$

where the subscripts $_1$ and $_2$ denote two different rocks as shown in Fig. 4. We can see in this equation that, if the conductivities k_1 and k_2 are different, the temperature gradient in the rock with the higher conductivity must be lower and vice versa (Fig. 4). This is called heat refraction. Eq. 7 can also be written in differential form. This means, the temperature gradient must not change abruptly, but can also change continuously, if there are continuous changes in thermal conductivity.

Let us illustrate the phenomenon with an example. A rock with extremely high thermal conductivity, for example an iron ore body, will be practically isothermal, even if it stretches over many vertical kilometers in the crust. Its high conductivity will cause it to adapt some average temperature. Thus, the upper part the body may have a significantly higher temperature than its surroundings while its lowest part is colder than its surroundings. As a consequence, it is conceivable that the process of heat refraction will even leads to some kind of contact metamorphism.

Jaupart and Provost (1985) have noticed that there are some important differences in thermal conductivity between the sediments of the Tethys zone and the high Himalayan crystalline complex. They suggested that the process of heat refraction may have been

Table 1: Thermal conductivities and heat capacities of some rocks and common materials. k is given in J $\mathrm{s^{-1}}$ $\mathrm{m^{-1}K^{-1}}$ and c_p in J $\mathrm{kg^{-1}K^{-1}}$. The change of thermal conductivity as a function of pressure and temperature are negligible at geologically relevant temperatures in the crust (Cull 1976; Schatz and Simmons 1972).

rock type	k	c_p
sandstone	1.5-4.2	920
gneiss	2.1-4.2	800
amphibolite	2.5-3.8	840
granite	2.4-3.8	790
ice	2.2	1 800
water	0.58	4 200
salt	5.4-7.2	880
iron	73	460

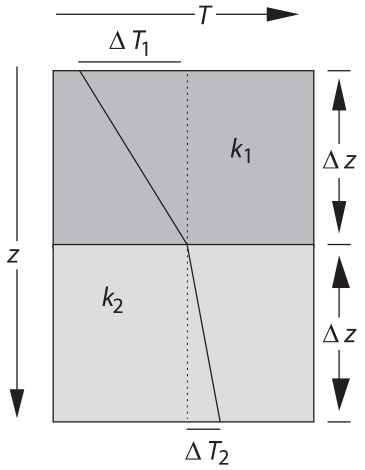

Figure 4: Illustration of the process of heat refraction. The flow of heat in the dark and the light shaded bodies is the same. However, the temperature gradient in the dark shaded body is larger, because its thermal conductivity k_1 is smaller. The subscripts $_1$ and $_2$ denote the dark and the light shaded body, respectively.

of relevance in connection with the melting of the Himalayan leucogranites. The process has also been discussed as the cause for high grade metamorphism in several Australian provinces (e.g. Mildren and Sandiford 1995) and as the trigger for a range of tectonic processes (Sandiford 1999). In fact, several exploration companies currently explore for geothermal energy sources in Australia by looking for regions where rocks of low thermal conductivity insulate underlying rocks of high thermal conductivity (Hillis et al. 2004).

If we want to describe the process of heat refraction quantitatively, we can not assume the simplification that we have made in going from eq. 5 to eq. 6. We must stick with eq. 5 to describe conductive equilibration.

2 Unit: Stable Continental Geotherms

Three fundamental processes create and redistribute heat in the continental lithosphere: *conduction*, *advection* and *production*. If we add heat advection and heat production terms to the diffusion equation discussed above, then a full one-dimensional description of the thermal energy balance for the lithosphere has the form:

$$\frac{\partial T}{\partial t} = \left(\frac{k}{\rho c_p}\right)\frac{\partial^2 T}{\partial z^2} + u\frac{\partial T}{\partial z} + \left(\frac{S}{\rho c_p}\right) \quad , \tag{8}$$

where the diffusivity is the ratio of conductivity and density × heat capacity: $\kappa = k/\rho c_p$. The central term on the right hand side of this equation describes advection (at the rate u) and advection may be due to transport of mass by *erosion, deformation, magma* or *fluid* and we will discuss some of these later in this course. In the most right term on the right side of the equation above, the heat production S may have *mechanical, chemical* and *radioactive* contributions. In this section we learn to describe aspects of the thermal structure of the continental lithosphere.

2.1 Thermal Definition of the Lithosphere

The lithosphere may be defined thermally or mechanically. According to the thermal definition, the lithosphere is the outer shell of Earth, in which heat is transported primarily by *conduction*. In contrast, in the asthenosphere, heat is transported primarily by *convection*. Thus, the lithosphere itself is nothing but a *thermal boundary layer* of Earth. This boundary layer looses heat at all times through the Earth's surface into the atmosphere and further – by radiation – into space. The average heat flow through the surface of the continents is 0.065 $\mathrm{W\,m^{-2}}$. The total surface area of the continents is about $A_c = 2 \cdot 10^8$ $\mathrm{km^2}$. Thus, the total heat loss of earth from the continents is $1.3 \cdot 10^{13}$ $\mathrm{J\,s^{-1}}$. This heat loss is balanced by radioactive heat production within the lithosphere and by heat flow into the lithosphere from the asthenosphere, so that this thermal boundary layer has a largely constant temperature profile, if it is not disturbed by orogenesis. Thermally stabilized lithosphere has a thickness between 100 and 200 km (Pollack and Chapman 1977).

2.2 Definition of Geotherms

The function that describes temperature in the lithosphere as a function of depth is what we call a *geotherm*. We discern:

– stable or steady state geotherms,

– transient geotherms.

• **Stable geotherms** Stable or *steady state* geotherms form by long term thermal equilibration of the lithosphere. In general, this is understood that the term "steady state" refers to a geotherm in a stationary lithosphere and we shall use it in this way in this section. However, in other reference frames, steady state geotherms may also occur in a moving lithosphere (for example a lithosphere that moves upwards relative to the surface during erosion).

In most geological situations, the temperatures of steady state geotherms increase steadily with depth. Stable geotherms are only found in regions that have had at least

about 100 my time for equilibration and have not changed in thickness during this time. The origin of this number is discussed in sect. 3.1.1. Thus, active orogens are *not* characterized by stable geotherms. Regardless, the calculation of steady state geotherms in orogens may help us to estimate the maximum or minimum temperatures that can be attained during an orogenic process at a given depth. This maximum or minimum possible temperature is often called *potential temperature* (e.g. Sandiford and Powell 1990).

• **Transient geotherms** Transient geotherms are only valid for a particular point in time. In some geological situations, transient geotherms do *not* increase steadily with depth and the change of the geotherm with time can be different in different depths. For example, after rapid stacking of nappes, rocks may simultaneously heat above a major thrust, but cool below it.

In this section we calculate the quantitative shape of stable continental geotherms.

2.3 Stable Geotherms: The Relevant Equation

For the stable or steady state case, the heat conduction equation (eq. 6) or the full thermal energy balance (eq. 8) can be simplified enough so that it is possible to find simple analytical solutions that provide useful tools to understand the thermal structure of the lithosphere, even without a lot of mathematical knowledge. This is therefore a good example to familiarize ourselves with the involved thought process. Neglecting advection (because we deal with *stable* geotherms) eq.8 simplifies to:

$$\frac{\partial T}{\partial t} = \left(\frac{k}{\rho c_p}\right) \frac{\partial^2 T}{\partial z^2} + \frac{S}{\rho c_p} \quad . \tag{9}$$

We need the heat production term to account for radioactivity, which is of substantial importance to stable geotherms. For *steady state* geotherms, there is no change of the temperature with time. This means:

$$\frac{\partial T}{\partial t} = 0 \quad .$$

Eq. 9 simplifies to:

$$\left(\frac{k}{\rho c_p}\right) \frac{\mathrm{d}^2 T}{\mathrm{d}z^2} + \frac{S}{\rho c_p} = 0 \quad . \tag{10}$$

Note that eq. 10 is no *partial* differential equation anymore. By canceling out of the constants we get:

$$k \frac{\mathrm{d}^2 T}{\mathrm{d}z^2} = -S \quad . \tag{11}$$

The integration of this equation forms the basis for all calculations of stable geotherms.

2.3.1 Geotherms Without Radioactivity

Equation 11 may be integrated the easiest, if we neglect radioactive heat production all together: $S = 0$. Eq. 11 then simplifies to:

$$k\frac{\mathrm{d}^2T}{\mathrm{d}z^2} = 0 \qquad \text{or even:} \qquad \frac{\mathrm{d}^2T}{\mathrm{d}z^2} = 0 \quad . \tag{12}$$

As this still is a differential equation of the second order, me must integrate it twice to solve it. A first integration gives:

$$\frac{\mathrm{d}T}{\mathrm{d}z} = C_1 \tag{13}$$

and a second:

$$T = C_1 z + C_2 \quad . \tag{14}$$

The two integration constants C_1 and C_2 must be determined by the geological boundary conditions. For example, we can assume that we know that the temperature at the surface of Earth (at $z = 0$) is constant and has the value $T = 0$. Then, for eq. 14 to hold, C_2 must be zero so that the temperature is zero at $z = 0$. It we assume a thermal definition of the lithosphere, then we can determine the other constant with the assumption that $T = T_\mathrm{l}$ at depth $z = z_\mathrm{l}$ where T_l and z_l are the temperature and the depth of the base of the lithosphere. With this assumption C_1 must have the value $C_1 = T_\mathrm{l}/z_\mathrm{l}$. The temperature as a function of depth is therefore described by:

$$T = z\frac{T_\mathrm{l}}{z_\mathrm{l}} \quad . \tag{15}$$

Other common assumptions (instead of $T = T_\mathrm{l}$ at $z = z_\mathrm{l}$) at the model base are the assumption of constant mantle heat flow at the Moho: $q = q_\mathrm{m}$ at $z = z_\mathrm{c}$). Equation 15 describes a linear temperature profile between the surface and the base of the lithosphere. This is not very surprising as we have assumed no heat production and no other reasons why the temperature profile should be anything else but a straight line between the assumptions at the boundaries. With a thermal conductivity of $k = 2$–$3\ \mathrm{W\,m^{-1}\,{}^\circ C^{-1}}$, and $T_\mathrm{l} = 1\,200\,^\circ\mathrm{C}$ as well as a lithospheric thickness of $z_\mathrm{l} = 100$ km, our equation describes a surface heat flow of 0.024–0.036 $\mathrm{W\,m^{-2}}$. This value is much lower than the average surface heat flow of the continents which is between 0.04 and 0.08 $\mathrm{W\,m^{-2}}$. This is one of the proofs of the existence of radioactivity in the lithosphere. We can easily conclude that eq. 12 is not a very good model description and that it is wiser to integrate eq. 11 using a meaningful function that describes S as a function of depth. When we do so, we will always assume that $S = S_\mathrm{rad}$, i.e. there is no other heat production sources but the radiogenic ones. In the steady state mechanical or chemical heat production sources are irrelevant.

2.4 Radioactive Heat Production

Radioactive (or: radiogenic) heat is produced in the Earth predominantly by the naturally occurring radioactive isotopes ^{238}U, ^{235}U, ^{232}Th and ^{40}K. Of the two naturally occurring uranium isotopes 99.28% is ^{238}U and only 0.72% is ^{235}U. All of the naturally occurring thorium is ^{232}Th and only 0.0119% of the natural potassium is ^{40}K (Turcotte and Schubert

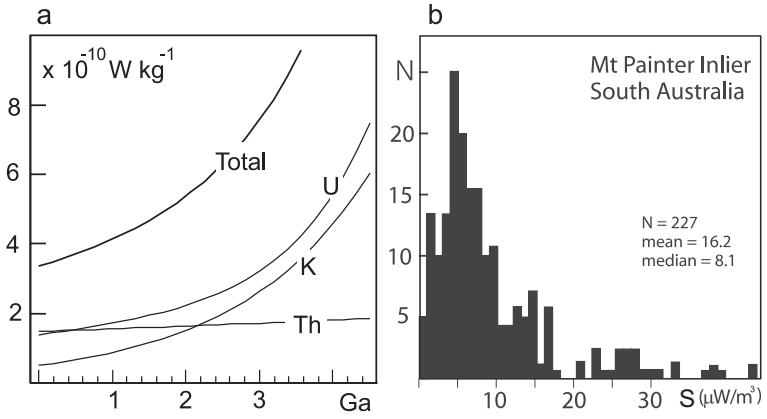

Figure 5: **a** Radioactive heat production in the crust through time. Note that the heat production in the Archaean 3 Ga ago was about twice as high as today. Also note that U and Th are the primary heat producing elements today, but it was U an K in the past. **b** Rates of radiogenic heat production in granites from the Mt Painter province, a low-pressure high-temperature metamorphic terrain in Australia (after Sandiford and Hand 1998b). Heat production rates in other Proterozoic terrains of Australia are similar. N is the number of data points.

element	**U**	**Th**	**K**
mean mantle concentration (kg/kg)	31×10^{-9}	124×10^{-9}	31×10^{-5}
mean crustal concentration	1.24×10^{-6}	5.6×10^{-6}	1.43×10^{-2}
mantle heat production (W/kg)	3×10^{-12}	3.2×10^{-12}	1.1×10^{-12}
crustal heat production (W/kg)	1.4×10^{-10}	1.5×10^{-10}	0.5×10^{-10}

Table 2: Concentrations of heat producing elements in the crust and undepleted mantle (after Turcotte and Schubert 2002). In granites, the heat production is about 2–3 times higher than the values listed here. The heat productions are per kg of rock, i.e. the values come from concentrations given in the first two rows multiplied with the heat productions given in the text.

2002). As pure metals, these 4 isotopes produce the following amounts of heat: ^{238}U = 9.46×10^{-5}W kg^{-1}; ^{235}U = 5.69×10^{-4}W kg^{-1}; ^{232}Th = 2.64×10^{-5}W kg^{-1} and ^{40}K = 2.92×10^{-5}W kg^{-1}. Fortunately, the concentrations of these elements in rocks are quite low so that substantially less heat is produced per cubic meter of rock. Table 2 lists some average concentrations of the heat producing elements in the continental crust and in the mantle. We can see that the Earth's mantle (oceanic crust has comparable values) contains about 2 orders of magnitude less radioactive elements than the crust. These concentrations are still important when considering problems related to cooling of earth as a whole or when thinking about the vigor of mantle convection in the Archaean, but for considerations of the heat budget of the Phanerozoic crust we need not consider radioactivity in the mantle. However, the crustal heat production is significant: The sum

of the values listed in this table is about 3.4×10^{-10} W kg^{-1}, which corresponds roughly to a heat production rate of about one μW m^{-3} (see eq. 43). Using typical values for heat capacity and density of crustal rocks, S= 1 μW m^{-3} converts to a heating rate of of about 10°C per million years. So the burial of highly radiogenic bodies by deformation can cause significant heating ! In fact, most granites have substantially higher heat productions than those listed in Table 2 and there are many terrains around the world where radiogenic heat production rates is significantly higher than some μW m^{-3} (Fig. 5b; Sandiford and Hand 1998b). Radiogenic heat production in the continental crust is responsible for about half of the heat flow that we can measure at the surface of the Earth.

2.5 The Contribution of Radioactivity to Stable Geotherms

The radioactive heat production rate of rocks is of the order of some microwatts per cubic meter. A typical value measured from samples at the Earth's surface is: $S = 2-5\mu\mathrm{W\,m^{-3}} \equiv 2-5\cdot10^{-6}\ \mathrm{W\,m^{-3}}$. The contribution of this value to the surface heat flow is simply the heat production times its depth extent. For example, if the heat production were constant in the entire crust of 30 km thickness (z_c = 30 km) then the surface heat flow caused by radioactivity is:

$$q = q_s = S \cdot z_c = 0.03\mathrm{Wm^{-2}} \quad . \tag{16}$$

This can be converted into a temperature gradient using eq. 1 where we have seen that the thermal gradient has the units of heat flow divided by the thermal conductivity. If the thermal conductivity is $k = 3\ \mathrm{W\,m^{-1}\,K^{-1}}$, then the assumptions from above indicate: $\mathrm{d}T/\mathrm{d}z = q/k = 0.05\,^{\circ}\mathrm{C\,m^{-1}} = 50\,^{\circ}\mathrm{C\,km^{-1}}$. This geothermal gradient of 50 °C per kilometer is only due to the contribution of radioactivity. The mantle heat flow would have to be added to this. Since the resulting thermal gradient would be much higher than just about all thermal gradients measured on earth, we can conclude that the radioactivity of rocks measured at the Earth's surface must be higher than that of the rest of the crust.

2.5.1 The Distribution of Heat Production

The considerations above have shown that the radioactive heat production of the crust is unlikely to be that of the surface in the entire crust. Various studies have therefore explored the vertical distribution of heat producing elements (e.g. Cermak and Rybach 1989; Pinet and Jaupart 1987; Pribnow and Hurter 1998; Heier and Brown 1978). The most simple model for a heat source distribution is that the heat production is constant to the depth z_{rad} and zero below that. This model depth, to which the crust produces radioactive heat at the same rate as on the surface, has been elegantly determined using the relationship of two independent sets of data that can be measured at the surface: The surface heat flow and the heat production rate at the surface, S_0. Roy et al. (1968) explored this relationship in the eastern US and its significance was described by Lachenbruch (1968; 1970; 1971). They found a roughly linear relationship between these two parameters (Fig. 6). The straight line that fits these data has the form:

$$q_s = q_m + q_{\mathrm{rad}} = q_m + z_{\mathrm{rad}} S_0 \quad . \tag{17}$$

In this equation, q_s is the surface heat flow, q_m is the mantle heat flow, q_{rad} the radiogenically produced heat flow and z_{rad} is the thickness of a hypothetical layer in which radioactive heat is produced at the same rate as on the surface. q_m can be measured from the intersection of the line with the heat flow axis and the value of z_{rad} is given by

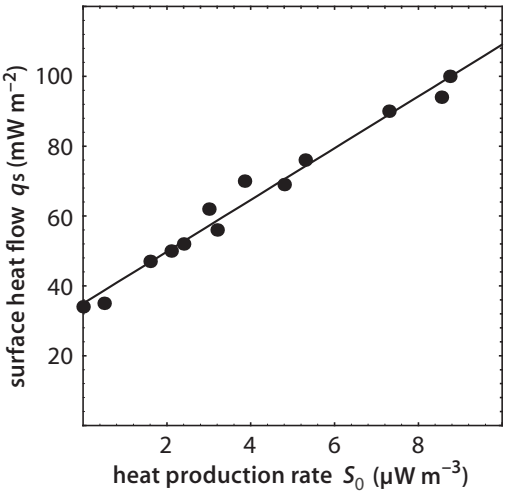

Figure 6: Measured data of surface heat flow q_s and surface heat production S_0 in the eastern US. The best line that fits the data is described by the equation $q_s = 0.035 + 7\,413 S_0$. Accordingly, the thickness of the layer that produces heat at a rate S is 7 413 m thick and the contribution of mantle heat flow to the total heat flow is 0.035 W m^{-2} (after Roy et al. 1968).

its slope. The data of Roy et al. (1968) show that $z_{\rm rad}$ is about 7 km in the eastern US. Similar considerations in other areas indicate thicknesses of 10–15 km. Of course, the crust does not produce heat constantly in this layer and no heat at all below it, but the relationship is useful to estimate the total heat production in the crust. This is given by the product $z_{\rm rad} S_0$. This product corresponds to the area underneath the different model curves in Fig. 7.

In order to obtain a continuous function for the rate of heat production with depth, the most elegant assumption is the assumption that there is a continuous exponential drop off in radioactive heat production with depth (model *c* in Fig. 7). This model has the great advantage that there is no discontinuity in the heat production in the crust at z_{rad} and we do therefore not need several equations to describe a single geotherm. We assume that:

$$S_{(z)} = S_0 \mathrm{e}^{\left(-\frac{z}{h_{\rm r}}\right)} \quad . \tag{18}$$

The variable $h_{\rm r}$ is called the *characteristic drop off* or *skin depth* of heat production. According to eq. 18, the heat production at depth $z = h_{\rm r}$ is only the 1/e part of the heat production at the surface S_0. Our new starting equation to calculate a geotherm is therefore:

$$k \frac{\mathrm{d}^2 T}{\mathrm{d}z^2} = -S_0 \mathrm{e}^{\left(-\frac{z}{h_{\rm r}}\right)} \quad . \tag{19}$$

Before we use this equation, we make some further qualitative considerations of the behaviour of surface heat flow during lithospheric thickening or thinning.

• **Heat flow relationships** The relationship between surface heat flow, mantle heat flow and radioactive heat production can be illustrated clearly by interpreting the surface heat flow q_s as the sum of the mantle heat flow q_m and the heat flow caused by radiogenic heat production $q_{\rm rad}$:

$$q_s = q_m + q_{\rm rad} \quad . \tag{20}$$

In this equation, the radiogenic heat flow is given by: $q_{\rm rad} = S_{\rm rad} z_{\rm rad}$, as we explained when we discussed Fig. 6 (see also eq. 17). England and Thompson (1984) assumed that

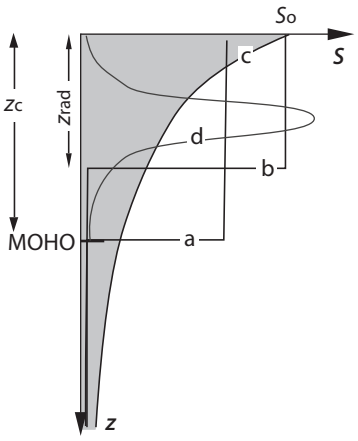

Figure 7: Four simple models describing the distribution of heat production with depth in the crust (s. Haack 1983). The total heat production of the crust is given by the area underneath the model curves. It is the same for all four models and is shaded for model *c*. *a* Constant concentration in the entire crust and no heat production in the mantle. *b* Constant concentration in the upper crust in a layer with the thickness $z_{\rm rad}$ and no heat production below that. *c* Exponential drop off of the heat production with depth. *d* Heat production peaking in the middle crust.

the radiogenically caused heat flow is comparable to the mantle heat flow ($q_{\rm rad} \approx q_{\rm m}$) and that the mantle heat flow remains unchanged, regardless of the thickness of the crust.

Thickening of the crust without thickening of the mantle part of the lithosphere doubles the radiogenic heat flow (because $z_{\rm rad}$ is doubled) but does nothing to the mantle heat flow. We can write:

$$q_{\rm s} = q_{\rm m} + 2q_{\rm rad} \quad . \tag{21}$$

Thus, the surface heat flow in thermal equilibrium after thickening is expected to be of the order of 1.5 times as high as before if $q_{\rm rad} = q_{\rm m}$ (Eq. 20).

However, if the mantle part of the lithosphere thickens together with the crust (homogeneous lithospheric thickening), then this halves the heat flow through the Moho (as the mantle lithosphere is thermally defined). We can then write:

$$q_{\rm s} = \frac{q_{\rm m}}{2} + 2q_{\rm rad} \quad . \tag{22}$$

Thus, if $q_{\rm rad} = q_{\rm m}$ and the entire lithosphere thickens to double thickness, the surface heat flow in thermal equilibrium and after thickening would be only 1.25 times as large as the value given by Eq. 20. If $q_{\rm rad} = q_{\rm m}/2$, then thickening or thinning of the lithosphere as a whole does not change the surface heat flow at all.

2.6 Realistic Continental Geotherms

If we define the lithosphere thermally, we implicitly state that we know the temperature at its base. An obvious choice for a lower boundary condition may therefore be: $T = T_{\rm l}$ at the depth $z = z_{\rm l}$. This choice allows us to describe temperatures in the entire lithosphere.

2.6.1 Constant Heat Production

In a model where we assume constant heat production rate in the crust and no heat production in the mantle part of the lithosphere, density *and* heat production are discontinuous at the Moho. This complicates the integration of eq. 11 dramatically. We will

not present the equations here and refer the interested reader to the original works of Sandiford and Powell (1990) or Zhou and Sandiford (1992). However, for comparison with the thermal model of England and Thompson (1984) we show an example of a geotherm calculated with these assumptions as curve *a* in Fig. 8. We see that this model results in unrealistically high temperatures if we assume the surface heat production rate to be representative for the whole crust.

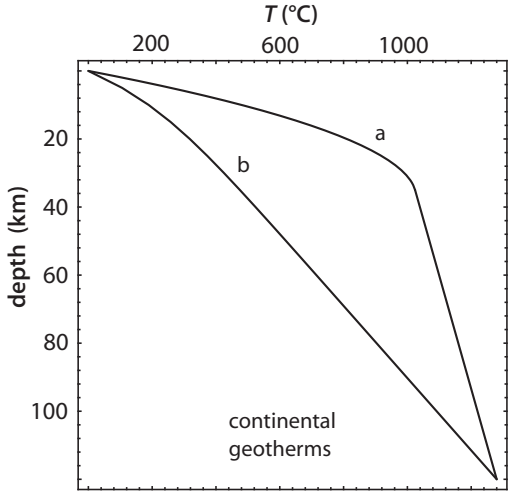

Figure 8: Examples of continental geotherms calculated with a lower boundary condition of a fixed temperature at the base of the lithosphere. Geotherm *a* was calculated assuming constant heat production in the crust and no heat production in the mantle lithosphere. Geotherm *b* was calculated for a continuous, exponentially decreasing heat production using eq. 26. The temperature T_l is assumed to be 1 280 °C.

2.6.2 Exponential Heat Production

If we assume a continuous heat production in the whole lithosphere that decreases exponentially with depth, then we can derive from eq. 19 an elegant and simple description of stable continental geotherms. After two integrations we get:

$$kT = -h_\mathrm{r}^2 S_0 \mathrm{e}^{\left(-\frac{z}{h_\mathrm{r}}\right)} + C_1 z + C_2 \quad . \tag{23}$$

Both constants of integration can only be evaluated after this second integration. The second integration constant C_2 is fairly easy to determine if we assume again that $T = 0$ at the surface where $z = 0$. At $z = 0$ the exponential term in eq. 23 goes to 1 so that C_2 must be:

$$C_2 = h_\mathrm{r}^2 S_0 \quad . \tag{24}$$

The lower boundary condition of $T = T_\mathrm{l}$ at the depth $z = z_\mathrm{l}$ can be evaluated by rearranging eq. 23:

$$C_1 = \frac{kT_\mathrm{l}}{z_\mathrm{l}} + \frac{h_\mathrm{r}^2 S_0 \mathrm{e}^{\left(-\frac{z_\mathrm{l}}{h_\mathrm{r}}\right)}}{z_\mathrm{l}} - \frac{C_2}{z_\mathrm{l}} \quad . \tag{25}$$

After inserting both constants into eq. 23 we get:

$$T = \frac{zT_\mathrm{l}}{z_\mathrm{l}} + \frac{h_\mathrm{r}^2 S_0}{k}\left(\left(1 - \mathrm{e}^{\left(-\frac{z}{h_\mathrm{r}}\right)}\right) - \left(1 - \mathrm{e}^{\left(-\frac{z_\mathrm{l}}{h_\mathrm{r}}\right)}\right)\frac{z}{z_\mathrm{l}}\right) \quad . \tag{26}$$

Curve *b* in Fig. 8 is an example of a geotherm calculated with this relationship. Eq. 26 provides a realistic and useful description of stable continental geotherms and has been presented and used by many authors.

2.6.3 More General Formulations

In order to use eq. 26 more efficiently, it is useful to introduce two new parameters: the vertical thickening (or thinning) strain of the crust f_c and that of the lithosphere f_l. A value of $f_c = 2$ means that the crust is twice as thick as in the reference state. Using these parameters, eq. 26 can be generalized. All we need to do is multiply the reference crustal and lithospheric thicknesses z_c and z_l with their respective thickening strains. We get:

$$T = \frac{zT_l}{f_l z_l} + \frac{f_c^2 h_r^2 S_0}{k} \left(\left(1 - e^{\left(-\frac{z}{f_c h_r}\right)} \right) - \left(1 - e^{\left(-\frac{z_l f_l}{f_c h_r}\right)} \right) \frac{z}{f_l z_l} \right) \quad . \tag{27}$$

This equation can be used to calculate the equilibrium temperatures at any depth for any thickness ratio of crust and mantle part of the lithosphere.

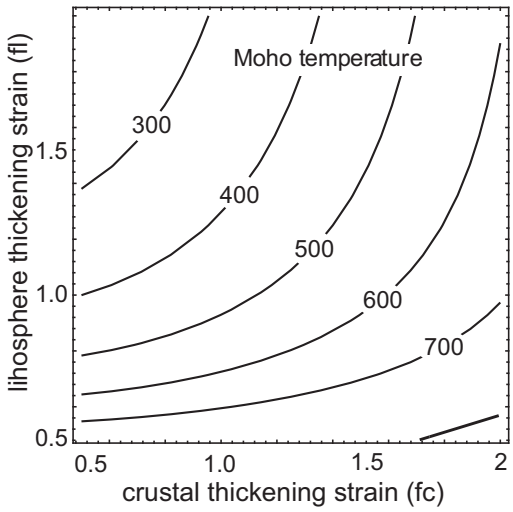

Figure 9: Moho-temperatures of continental lithosphere for different crustal thickening strains (expressed by f_c) and for different total thickening strains of the lithosphere (expressed by f_l). The diagram was calculated with eq. 27 assuming $z = z_c$. The assumption of the parameters are the same as in Fig. 8.

3 Unit: Heat in Oceanic Lithosphere

Oceanic lithosphere contains practically no radioactive elements. Thus, one could think that it is simple to describe stable oceanic geotherms. In analogy to continental geotherms we might want to formulate the geotherm equation as:

$$k\frac{\mathrm{d}^2T}{\mathrm{d}z^2} = 0 \quad . \tag{28}$$

After one integration we get:

$$k\frac{\mathrm{d}T}{\mathrm{d}z} = C_1 \quad .$$

Using as a boundary conditions that: $q = q_\mathrm{m}$ at the depth $z = z_\mathrm{c}$, (i.e. that the mantle heat flow q_m at the Moho (z_c) is fixed and known) we get:

$$kT = q_\mathrm{m} z + C_2 \quad .$$

If we also assume that $T = 0$ at the surface $z = 0$, then $C_2 = 0$ and we can write:

$$T = z\frac{q_\mathrm{m}}{k} \quad , \tag{29}$$

Eq.29 is our solution. However, eq. 29 is not a very good model to describe oceanic lithosphere. A simple consideration of the time scale of conductive equilibration will show us why: oceanic lithosphere is produced at the mid-oceanic ridges and it gets its thickness only by its increasing age. The oldest oceanic lithosphere is about 150 my old (Fig. 10). However, we will soon show that the time for thermal equilibration of the lithosphere is of the order of 150 my or more! We can conclude that oceanic lithosphere is *not* thermally stabilized. The assumption underlying eq. 28 is wrong. There is no thermally stabilized oceanic lithosphere! We can not assume that $\mathrm{d}T\,/\,\mathrm{d}t = 0$ and we must solve the time dependent diffusion equation (eq. 6). This is by far not as trivial as the simple integrations we have done for stable (time independent) geotherms above and we need to make a little excursion into the dealing with time dependent problems.

3.1 Handling Time Dependent Problems

If we want to use eq. 6 to describe a time dependent conduction problem, we must solve it for a given set of boundary- and initial conditions. If we try this, we would quickly realize that this is only possible for a very few boundary- and initial conditions. Periodic problems are some of those for which there are "real" solutions of this equation (see unit 6). For most problems there are simply no solutions of eq. 6 possible. For example, for many geological problems we will see that it is useful to assume that the boundary conditions lie at infinity (at distances that are far away compared to the scale of the problem). In all such problems, the results of integrating eq. 6 will contain a term of the form:

$$\frac{2}{\sqrt{\pi}}\int_0^n \mathrm{e}^{-n^2}\mathrm{d}n = \mathrm{erf}\,(n) \tag{30}$$

This integral cannot be solved. However, because it occurs so often in solutions of the heat flow equation, it has its own name: the *error function*. The values of the error function for different values of n have been determined numerically and can be looked up on tables,

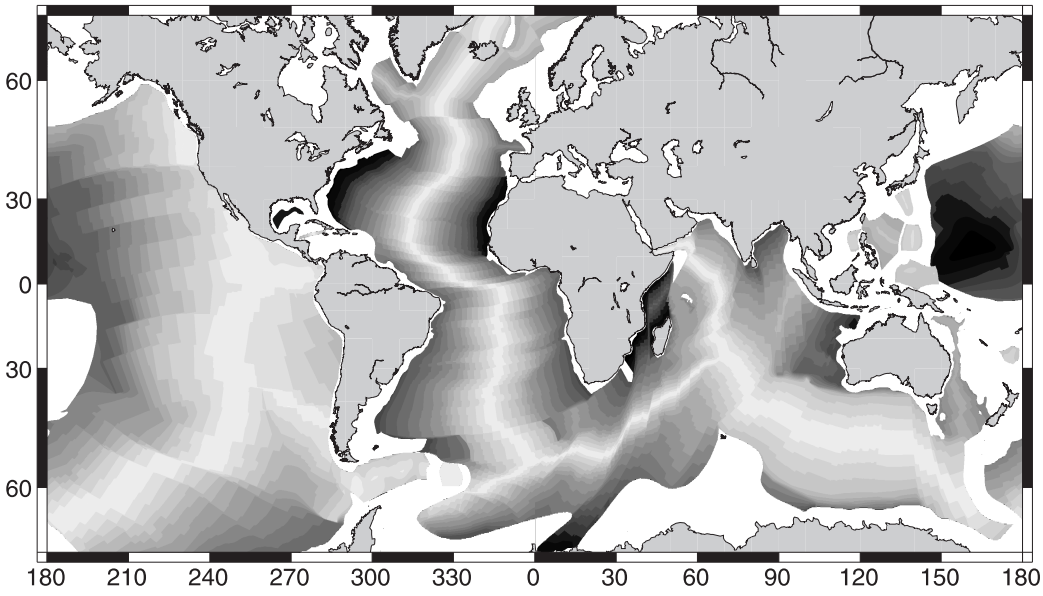

Figure 10: The age of the ocean floor (Müller et al. 1997). Shading intervals are every 10 my from 0 (white) to 160 my (black). Ocean floor older than 160 my is black. Areas with no data ar white. These regions are both on continental and on oceanic lithosphere. Landmasses are grey. Oldest known parts of oceanic lithosphere are around 180 my in the western Pacific just east of the Mariana Trench, between Madagascar and Africa and in the westernmost Atlantic just east of the US. Compare this map also with a topography of the ocean floor and note the similarities.

or it can be calculated with some numerical approximation. Fig. 11 shows the shape of the error function. In many solutions of eq. 6 the variable n from eq. 30 has the form $n = z/\sqrt{4\kappa t}$. There, time t, and distance z are inside the error function and they are in a quadratic relationship to each other. Most solutions that we will use for the description of contact metamorphism contain error functions of this form. The *complementary* error function erfc is defined as:

$$\mathrm{erfc}\,(n) = 1 - \mathrm{erf}\,(n) \quad . \tag{31}$$

Solutions of the time dependent heat conduction equation very often contain error functions or complementary error functions of the term $\mathrm{erf}(l/\sqrt{4\kappa t})$, where l is a spatial coordinate.

3.1.1 Time Scales of Diffusion

We have seen already in the first unit that thermal equilibration is a process that is rapid at first (when the curvature of isotherms is still large) and then slows down more and more and the *complete* equilibrium is only reached after infinite time. This asymptotic form of the equilibration may also be seen in the shape of the error function on Fig. 11. Clearly, it is often useful to define some point in time when we call the equilibration to be "complete". In order to identify such a "time of complete equilibration", we use the fact that solutions of the heat flow equation often contain the term $\mathrm{erf}(l/\sqrt{4\kappa t})$. The

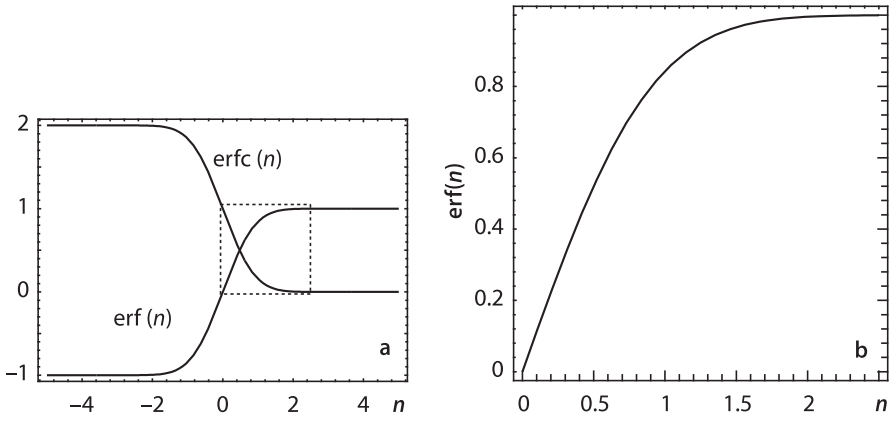

Figure 11: The error function and the complementary error function. The dashed frame in **a** shows the part of erf(n) that is shown enlarged in **b**.

shape of the error function in Fig. 11 shows that it reaches asymptotically 1 as n get very large. Correspondingly, the term $(l/\sqrt{4\kappa t})$ will reach 1 for large l (regardless of t), or for small t (regardless of l). We can also see that – because time is in the denominator inside the error function – *complete* equilibrium is reached only after infinite time (when the term inside the brackets asymptotically approaches zero). In order to define a "duration of equilibration" we may want to arbitrarily choose a point in the equilibration process where the argument of the error function (for which we use n in eq. 30) is 1. This means that:

$$\left(\frac{l}{\sqrt{4\kappa t}}\right) = 1 \qquad \text{or :} \qquad t = \frac{l^2}{4\kappa} \quad . \tag{32}$$

Figure 11 illustrates that for the argument to be 1 (where $t = l^2/(4\kappa)$), the thermal equilibration is 84.3 % complete. This arbitrary value is often chosen as a scaling factor for the equilibration history where it may be said that the diffusive equilibration is "largely complete". In fact, because this is a only a rough measure, the "4" is often left off this relationship and it is written:

$$t_{eq} = t = \frac{l^2}{\kappa} \quad . \tag{33}$$

The value of t_{eq} in eq. 33 is an important measure to estimate the duration of equilibration. It is often called *Thermal Time Constant* or: *Diffusive Time Scale of Equilibration.* In summary, the basic message of this section is:

– During conductive processes the duration of thermal equilibration increases with the square of the length scale of the equilibrating body and inverse proportionally with the diffusivity.

For diffusivities of the order of $\kappa = 10^{-6}\mathrm{m}^2\mathrm{s}^{-1}$ this means that regional metamorphism of nappe piles that are several tens of kilometers thick should last of the order of several tens of my.

Table 3: Different values of the thermal time constant t_{eq} for a series of geologically relevant length scales l.

l	$t_{eq} = l^2/2\kappa$	$t_{eq} = l^2/\pi^2\kappa$
10 m	$5 \cdot 10^7$ s $\approx$ 1.58 y $\approx 10^0$ y	$1.01 \cdot 10^7$ s $\approx$ 16 weeks $\approx 10^{-1}$ y
100 m	$5 \cdot 10^9$ s $\approx$ 158 y $\approx 10^2$ y	$1.01 \cdot 10^9$ s $\approx$ 32 y $\approx 10^1$ y
1 km	$5 \cdot 10^{11}$ s $\approx$ 15 000 y $\approx 10^4$ y	$1.01 \cdot 10^{11}$ s $\approx$ 3 200 y $\approx 10^3$ y
10 km	$5 \cdot 10^{13}$ s $\approx$ 1.5 my $\approx 10^6$ y	$1.01 \cdot 10^{13}$ s $\approx$ 320 000 y $\approx 10^5$ y
100 km	$5 \cdot 10^{15}$ s $\approx$ 158 my $\approx 10^8$ y	$1.01 \cdot 10^{15}$ s $\approx$ 32 my $\approx 10^7$ y

3.2 Aging Oceanic Lithosphere

The oceanic crust that is produced from partial mantle melts at the mid-oceanic ridges is only of the order of 5–8 km thick. That is, it is much thinner than the continental crust. At the mid-oceanic ridge the thickness of the entire oceanic lithosphere is that of the crust (Fig. 12). The high potential energy of the ridges forces this crust to move away from the ridge. As the oceanic crust ages and moves further and further away from the mid-oceanic ridge, the asthenosphere cools and becomes part of the oceanic mantle lithosphere. It is often said that the mantle successively "freezes" onto the base of the oceanic lithosphere as it ages. While this describes the process quite intuitively, it is somewhat incorrect as the asthenosphere itself is not molten. Regardless, the process of the successive cooling of the aging oceanic lithosphere can be described with the diffusion equation using simple initial and boundary conditions. Indeed, the description of oceanic lithosphere with these boundary conditions has become one of the most successful models of plate tectonic theory (s. a. Sclater et al. 1980). It is called the *half space cooling model*.

3.2.1 The Half Space Cooling Model

As any other problem in the theory of heat conduction, the half space cooling model relies on the integration of eq. 6, using a set of boundary and initial conditions. These conditions are provided by geological observation: The temperature at the surface ($T - s$) of mid-oceanic ridges is that of the water temperature. For simplicity, we assume that it is $T_s = 0$. Below the ridge, the mantle temperature is almost constant – convection equalizes all temperature gradients. Thus, we can write a very simple initial condition describing the thermal profile below mid-oceanic ridges:

– $T = T_s$ at the depth $z = 0$ and:

– $T = T_l$ in all depths $z > 0$ at time $t = 0$.

This initial condition is illustrated in T-z-diagram on the bottom right corner of Fig. 12. For the upper boundary condition it is obvious to assume that the temperature at the ocean floor remains constant. As there is effectively no lower boundary, we assume that it lies at infinity and that the temperature there is $T = T_l$ ($T - l$ is the temperature at the base of the lithosphere). We can write this as follows:

– $T = T_s$ at $z = 0$ for all $t > 0$ and:

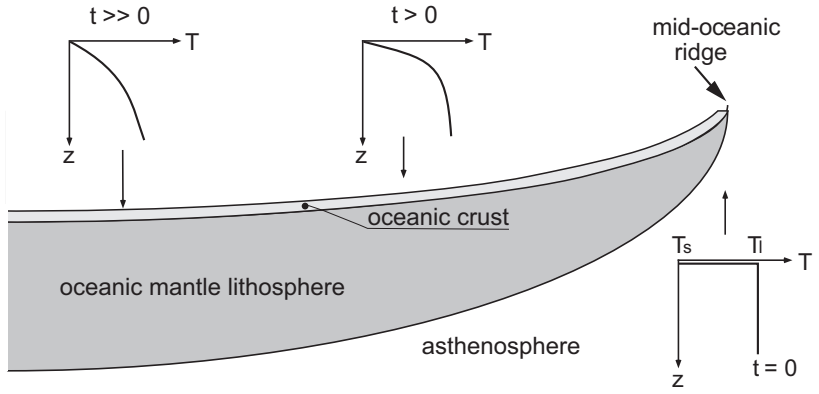

Figure 12: Thickness and thermal profile of oceanic lithosphere at a series of points..

– $T = T_\mathrm{l}$ at $z = \infty$ for all $t > 0$.

(Fig. 12). The solution of the heat conduction equation for these boundary conditions is:

$$T = T_\mathrm{s} + (T_\mathrm{l} - T_\mathrm{s})\mathrm{erf}\left(\frac{z}{\sqrt{4\kappa t}}\right) \quad . \tag{34}$$

This solution is already a bit familiar to us from section 3.1 and we discuss this solution in some more detail in sect. 4.1 (s. a. sect. 3.1). Fig. 13a shows temperature profiles through oceanic lithosphere of different ages, that were calculated with eq. 34. The curves correspond to the two sketches of thermal profiles in the middle and on the left of Fig. 12. Fig. 13b shows the depth of a series of isotherms as a function of age.

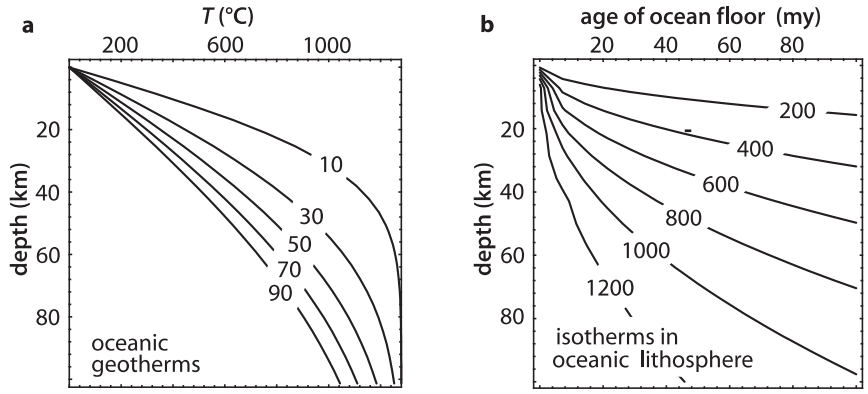

Figure 13: **a** Temperature T versus depth profiles through oceanic lithosphere at a number of different ages labeled in my. **b** The depth of isotherms (in °C) in oceanic lithosphere as a function of age between 0 and 100 my. The curves on both figures were calculated with eq. 34 assuming $T_\mathrm{l} = 1\,280\,°\mathrm{C}$. The age can be converted into distance from the mid-oceanic ridge by using $x = u/t$ where x is the distance from the ridge and u is the rifting rate. Compare the curves also with Fig. 21 where a similar model is used to describe intrusions.

3.2.2 Surface Heat Flow: The Test for the Model

Temperature profiles calculated with this model for the cooling oceanic lithosphere can not be tested directly, as we cannot drill deep enough into the oceanic lithosphere to measure temperature in any representative way. Our observations are confined to parameters which we can measure near the surface. One of these parameters is easy to measure and very useful to infer the thermal profile: the surface heat flow q_s (Pollack et al. 1993) (Fig. 1). The surface heat flow is the product of thermal conductivity and the thermal gradient at $z = 0$. This can be calculated from eq. 34 and can be compared with measured data in the oceans. To obtain surface heat flow we must differentiate eq. 34 with respect to depth and evaluate it at $z = 0$. From eq. 34 this is:

$$q_\mathrm{s} = k(T_\mathrm{l} - T_\mathrm{s}) \frac{\mathrm{d}\left(\mathrm{erf}\left(\frac{z}{\sqrt{4\kappa t}}\right)\right)}{\mathrm{d}z}_{,z=0} \quad . \tag{35}$$

As the error function itself is an integral (see eq. 30), it is easy to differentiate eq. 34 (sect. 3.1). We get:

$$q_\mathrm{s} = k(T_\mathrm{l} - T_\mathrm{s}) \sqrt{\frac{1}{\pi\kappa t}} \quad . \tag{36}$$

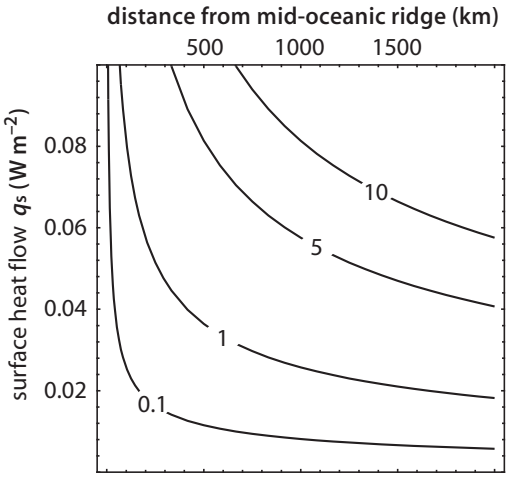

Figure 14: The surface heat flow of oceanic lithosphere as a function of age and therefore as a function of distance from the mid-oceanic ridge as calculated with eq. 37. Contours are for different rifting rate labeled in cm y^{-1}.

This equation can be rewritten for the description of different oceanic plates with different rifting rates. For this, we express the rifting rate u as $u = x/t$. There, x is the distance from the mid-oceanic ridge and t is the age. If we replace t in eq. 36 by x/u, we get:

$$q_\mathrm{s} = k(T_\mathrm{l} - T_\mathrm{s}) \sqrt{\frac{u}{\pi\kappa x}} \quad . \tag{37}$$

Eq. 37 shows us that the surface heat flow as a function of distance from the mid-oceanic ridge is a square root function of distance x from the ridge (as all other parameters in this equation are constants). Fig. 14 shows the surface heat flow in oceanic lithosphere as calculated with eq. 37. The heat flow data of Sclater et al. (1980) show that these curves correspond well with heat flow measured in the deep oceans. We will show later in this course that the half space cooling model is not only a good description for the

temperatures and heat flow in oceanic lithosphere, but can also be used to describe the water depth of the oceans. It can even be used to calculate the magnitude of the ridge push force. The relationship between all these parameters that are described with the half space cooling model is called the *age-depth-heat flow relationship* of oceanic lithosphere. This age-depth-heat flow relationship corresponds fantastically well with our observations up to an age of the oceanic lithosphere of 50 – 80 my. The age-depth-heat flow relationship is generally accepted as one of the greatest successes of plate tectonic theory.

4 Unit: Thermal Effects of Intrusions

Intrusion of magmatic rocks into higher levels in the crust is an important geodynamic process that can be responsible for a large range of thermal, chemical and mechanical changes in the crust. Intrusive rocks, as well as their contact aureoles, are familiar to us from field observations. Thus, their geodynamic interpretations can often be tested directly with structural and petrological data. The process of intrusion itself is a very efficient mechanism for the transport of heat. Thus, most intrusions do not cool very much on their intrusive path and their temperature may be used to infer the temperature of rocks at the depth of their origin. There are two important reasons, why the quantitative description of the thermal evolution of intrusions is quite simple:

- In comparison to the duration of a contact metamorphic event or the duration of an orogenic cycle, the rate of intrusion is very rapid. Thus, for the thermal modeling of intrusions it is possible to assume that their emplacement was *infinitely* rapid, compared to the time of the subsequent thermal equilibration. This is what is called an *instantaneous heating model*. The thermal equilibration of intrusions with their surroundings can therefore be described with the heat conduction equation (eq. 6), neglecting advection.
- Most intrusions are small if compared to the size of their surroundings, for example the distance to the surface or to the base of the lithosphere. Thus, the boundary conditions that are needed to solve the heat conduction equation can often be assumed to lie at infinity in comparison to the scale of the problem.

With these assumptions, it is possible to describe the temperature evolution of intrusions with simple step-shaped temperature distributions akin to the model for oceanic lithosphere:

4.1 Step-shaped Temperature Distributions

The most simple of all model examples describing the cooling of rocks in the direct vicinity of intrusions is given by the thermal equilibration of step-shaped temperature profiles in one dimension. This example is illustrated in Fig. 15 and is one of the most useful examples for the understanding of the cooling history of intrusions. We interpret the temperatures on the two sides of the step as the intrusion- and the host rock temperatures; T_i and T_b, respectively. The step itself is the intrusion contact. If we choose a one-dimensional coordinate system in which the origin $z = 0$ is exactly at the contact of the model intrusion, then the initial and boundary conditions of this equilibration problem may be described by:

- Initial condition: $T = T_\mathrm{i}$ for all $z < 0$ and $T = T_\mathrm{b}$ for all $z > 0$ at $t = 0$.
- Boundary conditions: $T = T_\mathrm{b}$ at $z = \infty$ and $T = T_\mathrm{i}$ at $z = -\infty$ for all $t > 0$.

Integration of eq. 6 using these boundary and initial conditions gives:

$$T = T_\mathrm{b} + \frac{(T_\mathrm{i} - T_\mathrm{b})}{2}\left(1 - \mathrm{erf}\left(\frac{z}{\sqrt{4\kappa t}}\right)\right) = T_\mathrm{b} + \frac{(T_\mathrm{i} - T_\mathrm{b})}{2}\left(\mathrm{erfc}\left(\frac{z}{\sqrt{4\kappa t}}\right)\right) \quad . \tag{38}$$

We will not discuss how eq. 38 was derived (s. sect. 3.1) but when you compare this equation to eq. 34 you will see that it is very similar and differs from the most simple form

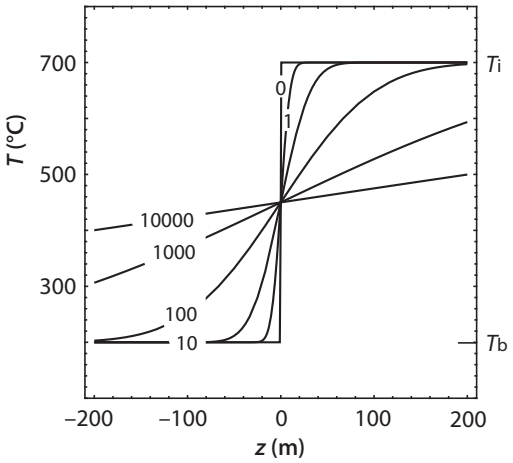

Figure 15: Thermal equilibration of an initially step-shaped temperature distribution. The curves were calculated with eq. 38 for $\kappa = 10^{-6}$ m^2 s^{-1}, $T_\mathrm{i} = 700\,^\circ$C and $T_\mathrm{b} = 200\,^\circ$C. The different curves are temperature profiles at different times (in years) after the intrusion event. (The sign on the z axis is reversed on this figure from the equations in text).

of the half space cooling model only by some shifting and scaling of the error function. In the example of eq. 38, the temperature at $z = 0$ stays constant in time. It has the value $T_\mathrm{b} + (T_\mathrm{i} - T_\mathrm{b})/2$. If we bring all T_i and T_b to the left hand side of the equation we can also write:

$$\theta = 0.5\mathrm{erfc}\left(\frac{z}{\sqrt{4\kappa t}}\right) \quad . \tag{39}$$

in which $\theta = (T - T_\mathrm{b})/(T_\mathrm{i} - T_\mathrm{b})$ is called the *dimensionless temperature*. We begin with some geologically relevant examples that may be described with this solution.

4.2 Thermal Evolution of Dikes

One of the simplest but also most important applications of the equations introduced in the last section is the description of the cooling history of intrusions (Jaeger 1964). As the solutions shown above are one-dimensional, their application is particularly relevant to the description of the thermal evolution of dikes that are narrow compared with their lateral extent. When using the solutions described above to describe the cooling history of dikes, it is implied that the dike extends "infinitely" in the two spatial directions normal to the coordinate described in the cooling problem. In contrast to the previous sections, we only need to be careful to consider both surfaces of the dike. For a coordinate system with its origin in the center of a dike with the thickness l, the initial conditions may be described by: $T = T_\mathrm{i}$ for $-(l/2) < z < (l/2)$ and $T = T_\mathrm{b}$ for $(l/2) < z < -(l/2)$ (Fig. 16). The boundary conditions remain the same as for the step problem. With these conditions, a solution of eq. 6 may be found to be:

$$T = T_\mathrm{b} + \frac{(T_\mathrm{i} - T_\mathrm{b})}{2}\left(\mathrm{erf}\left(\frac{0.5l - z}{\sqrt{4\kappa t}}\right) + \mathrm{erf}\left(\frac{0.5l + z}{\sqrt{4\kappa t}}\right)\right) \quad . \tag{40}$$

It may be easily seen, that the solution is made up of descriptions for two opposing step-shaped temperature profiles at $z = -l/2$ and $z = l/2$. Fig. 17 shows the thermal evolution described by eq. 40. As the diffusion equation is a linear differential equation, the diffusive equilibration of just about any one-dimensional geometry may be described by the summation of solutions for various initial conditions.

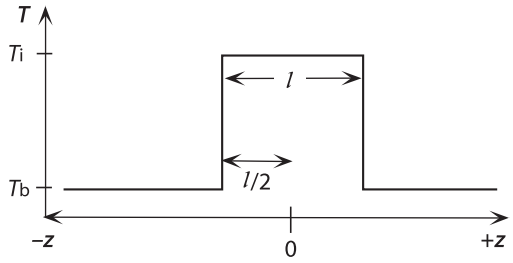

Figure 16: Schematic illustration of the initial condition and the variables of the dike cooling problem of eq. 40.

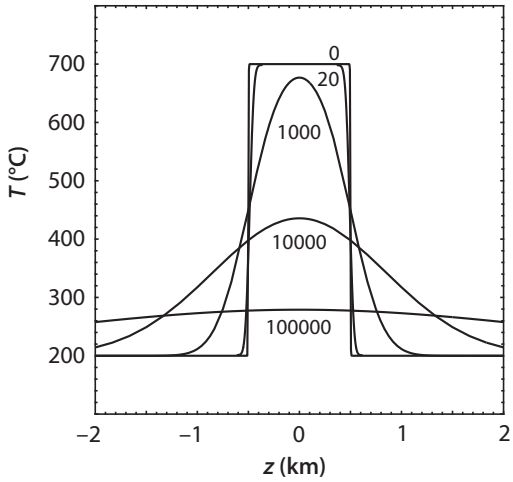

Figure 17: Thermal equilibration of one-dimensional intrusions, for example magmatic dikes of large lateral extent (calculated with eq. 40 and labeled in years after initial intrusion). All parameters are the same as in Fig. 15. Cooling curves of rocks from a range of distance from the dike center are shown in Fig. 18a.

In contrast to Fig. 15, the temperature at the intrusion contact departs from the temperature $(T_\mathrm{i} + T_\mathrm{b})/2$ after some time in Fig. 17. The contact of the dike begins to cool. This is because the dike contact at $z = +l/2$ begins to follow the thermal effects of the temperature step at $z = -l/2$. Correspondingly, the other dike contact at $z = -l/2$ cools, because it "feels" the cooling at $z = +l/2$.

4.2.1 Cooling History of Dike-like Intrusions

In the following paragraphs we will use eq. 40 to infer some characteristic features of contact metamorphism. Firstly, eq. 40 shows us that – in the absence of other thermal processes – the maximum temperature that may be reached by contact metamorphism is much lower than the intrusion temperature: Only at the very contact of the intrusion the contact metamorphic temperatures may reach the half way mark between the initial host rock and intrusion temperature. We can conclude that field observations of contact metamorphic haloes documenting haloes of considerable width and temperature imply that thermal processes other than conductive equilibration have played a role in their formation (s. sect. 4.4.1).

• **Cooling curves** In order to interpret heating and cooling curves of rocks in the contact metamorphic environment, it is useful to plot eq. 40 in a temperature-time diagram (Fig. 18a). This figure illustrates that rocks located at different distances from the intrusion may experience very different cooling curves. For example, it may be seen that some rocks cool, while others heat up, or that rocks cool with different rates. In fact, near the contact of the intrusion, cooling curves have extremely complicated shapes including more

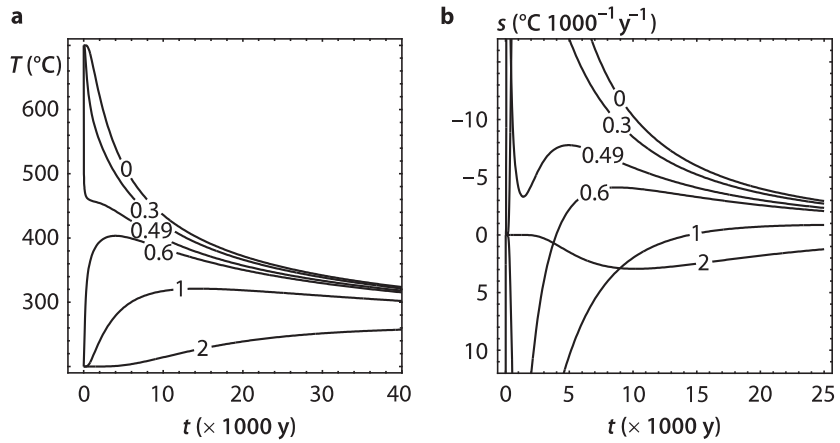

Figure 18: **a** Temperature-time paths (cooling curves) for a series of rocks within and within the contact aureole of a 1 km thick magmatic dike ($l = 1$ km) shown up to 40 000 years after intrusion (all constants are the same as in Fig. 17). The figure was calculated with eq. 40. The curves are labeled for distance from the center of the intrusion in km. As the thickness is $l = 1$ km, the first three curves are within the magma and the others in the country rock. **b** Cooling rates for the same points as shown in **a** plotted against time.

than one maximum in the cooling rate (e. g. the 490-m-curve in Fig. 18a). Spend some time and think through why these different shapes come about.

• **Contact Metamorphic Peak** Aside from cooling curves or cooling rates, there is even more important information on the thermal evolution of intrusions that may be extracted from eq. 40. For example, the *time* of the contact metamorphic thermal peak $t_{T_{\max}}$ for the model of eq. 40 may also be found analytically. At the thermal peak the rate of temperature change is zero: $s|_{t=T_{\max}} = 0$ (read: s at $t = T_{\max}$). From this, we can get the thermal peak temperature and its timing as a function of distance from the intrusion. With the resulting equations and their plots we can make some fundamental predictions about the nature of contact metamorphism:

1. The contact metamorphic peak temperature drops rapidly with *increasing* distance from

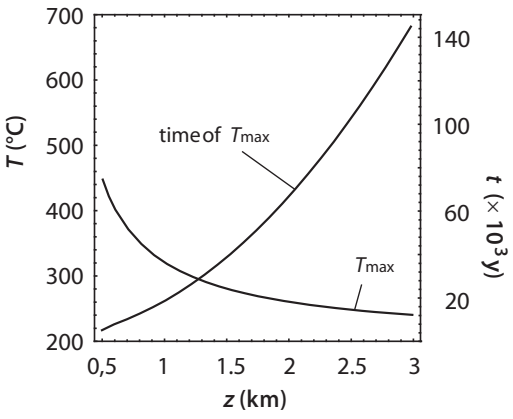

Figure 19: Contact metamorphic peak temperature and the time of the contact metamorphic temperature peak of the simple one-dimensional intrusion from Figs. 16 and Fig. 17. The thickness of the intrusion l is 1 km, $T_i = 700\,^\circ$C, $T_b = 200\,^\circ$C and $\kappa = 10^{-6}$ m^2 s^{-1}.

the heat source.

2. The time of peak contact metamorphism increases rapidly with *increasing* distance from the heat source and with *decreasing* metamorphic grade. This predicts that – if contact metamorphism occurred – low grade metamorphic rocks should experience their metamorphic peak later than high grade metamorphic rocks (Den Tex 1963).

These predictions help to infer heating mechanisms of metamorphic terrains. For example, during regional metamorphism the relationships between grade and timing of metamorphism are reversed. These predictions also have some implications for th einterpretation of Low-pressure high-temperature metamorphic terrains and we make a little excursion into the problems of these terrains.

4.3 Low Pressure - High Temperature Metamorphism

In many regions of this planet, in particular on the Precambrian shields, we can find metamorphic terrains that experienced peak metamorphism at unusually high temperatures, if compared with the depth of metamorphism. In other words, the ratio of peak pressure to peak temperature in these terrains is much higher than that corresponding to a "normal" geothermal gradient or that predicted by models for regional (Barrovian) metamorphism. Such terrains are generally called "low-pressure-high-temperature", or short LPHT- terrains and the metamorphism is often referred to as "Buchan style". LPHT terrains occur at all grades, ranging from greenschist facies metamorphism at less than a kilobar peak pressure (e. g. Xu et al. 1994) to granulite facies metamorphism at less than 3 or 4 kilobars (Greenfield et al. 1998). The heat sources of metamorphism in these terrains are intensely debated. In principal there are two fundamentally different heat sources that might be considered: "external" and "internal" heating.

4.3.1 External Heat Sources

One school of thought argues that the $T - P$ ratio of peak metamorphic conditions in LPHT terrains is much too high to be possibly attainable by a conductive geotherm. Thus, so it is argued, the heat sources must originate from "outside" the terrain under consideration (the heat sources are: "external heat") (e. g. Bohlen 1987; Lux et al. 1986; Sandiford et al. 1991). Examples of external heat sources would be heat sources that are advected from larger depths into the terrain, for example magma or fluids. This process can be considered as "contact metamorphism" in the widest sense. The most important arguments in support of this external heating model are:

– If the terrain was heated by conductive response of the lithosphere to a changed thickness geometry of crust and mantle lithosphere, then this implies that the measured PT ratio corresponds more or less to a geothermal gradient (curve *a* in Fig. 20). Typical PT ratios of LPHT terrains imply that a geotherm would reach the base of the lithosphere ($\approx 1\,200\,^{\circ}\mathrm{C}$) at a depth of about 30 km. Today, we observe such small lithospheric thicknesses only in regions of active extension and intra continental rift zones. In contrast, LPHT terrains are usually characterized by convergent structures and evidence for a plate margin setting are usually absent. Thus, alternative (external) heat sources must be made responsible.

– In many LPHT terrains metamorphism occurred synchronously with deformation. This observation is easily explained if external heat sources are responsible for metamor-

phism. However, it is in contrast with the models that explain regional metamorphism as a function of conductive processes.

– Many LPHT terrains are characterized by isobaric cooling curves. This observation indicates that the rate of cooling was substantially larger than the rate of burial or exhumation. As the duration of conductive cooling of a terrain is proportional to the square of the size of the cooling region, the rates of exhumation or burial may be used to constrain the length scale of the heated terrain. Assuming normal rates of vertical motion of rocks, such estimates indicate that only a region substantially smaller than the entire lithosphere could have been affected by the LPHT event.

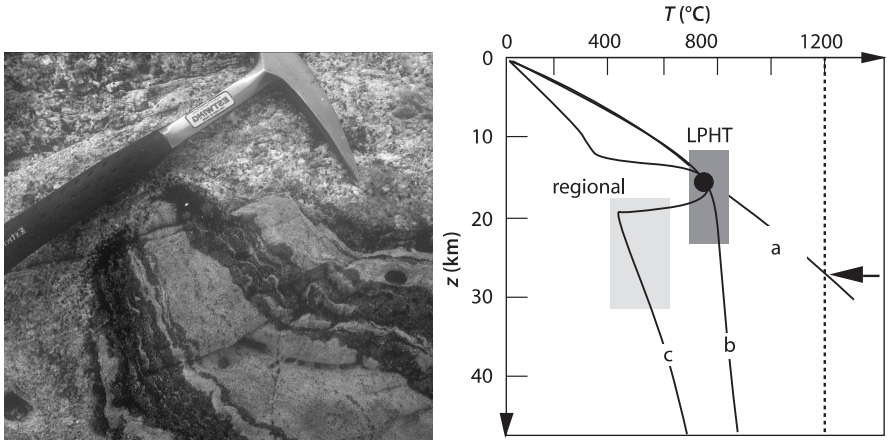

Figure 20: Left: Typical field appearance of LPHT terrains with multiple generations of partial melts (some syndeformational, some post deformational) and garnet – cordierite bearing melanosomes. Right: Three different models for the interpretation of geotherms in LPHT terrains. *a* is a monotonously rising geotherm. Such a geotherm implies that the base of the thermally defined lithosphere at 1 200 °C is located at a depth of only 30 km (arrow). *b* and *c* show two other possibilities for geotherms that are characterized by LPHT metamorphism, but allow normal lithospheric thicknesses.

4.3.2 Internal Heat Sources

In contrast to the arguments presented above, another school of thought argues that neither enough magmatic bodies nor sufficient evidence for fluid infiltration is found in LPHT terrains to justify external heat transfer into the terrains. Thus, so it is argued, LPHT metamorphism must have similar causes as regional Barrovian type metamorphism (s. Harley 1989). In order to explain the exceptional peak metamorphic *PT* ratios a series of models have been invoked that all are based on extremely unusual thickness geometries of crust and mantle lithosphere. For example, extreme thinning of the crust *and* the mantle lithosphere may cause conditions appropriate to LPHT metamorphism. Another possibility that has recently received some attention is unusually high radioactive heat production within the crust (Chamberlain and Sonder 1990; Sandiford and Hand 1998a;b). This might lead to a geotherm of the shape of curve *b* on Fig. 20. Spear and Peacock (1989) discuss models of internal and external heating of metamorphic terrains in some detail.

4.4 Modeling Realistic Intrusions

A series of observations in contact metamorphic aureoles of intrusions show that these are much wider and of a higher temperature than those we have predicted in the last section even as in the two dimensional examples shown. There is two important reasons for this:

– All problems we have discussed so far have been "instantaneous cooling" problems. This means, we have assumed that the cooling history commences at the time of intrusion. This need not be the case. In fact, in dikes through which magma is fed into a pluton, this would be highly unlikely. We need to describe some contact aureoles with a model where the temperature is fixed at the intrusion contact. An example for this is illustrated in Fig. 21.

– So far we have neglected the latent heat of fusion as part of the cooling history. This latent heat of fusion amounts to about 320 kJ per kg of rock or roughly $8.64 \cdot 10^8$ J m^{-3}. During crystallization of intrusions this heat is added to the thermal energy budget available to cause temperature change and causes buffering of the cooling history.

4.4.1 Considering Heat of Fusion: The Stefan Problem

The latent heat of reaction is an important part of the heat budget of high grade metamorphic terrains when partial melting occurs (see sect. 5.2). As we need about 1 000 Joules to heat one kg of rock by one degree (c_p = 1 000 J kg^{-1} K^{-1}), the latent heat of fusion in enough to heat a rock by about 320 °C (because L = 320 kJ kg^{-1}). An intrusion of T_i = 700 °C, that intrudes host rocks of T_b = 200 °C, is ΔT = 500 °C hotter than its surroundings. This corresponds to $\Delta T c_p$ = 500 000 J kg^{-1} additional energy that is brought into the rock by this temperature difference. However, the total *heat content* of the intrusion (including its latent heat) that is brought into the rock is $\Delta T c_p + L$ = 820 000 J kg^{-1}. The excess energy is therefore about 1.64 times as large as the excess temperature. This means that we have underestimated the cooling history in the previous sections substantially (s. p. 34).

If we want to describe the cooling history properly (rather than being satisfied with the ball park estimate above) we need to consider where and when this crystallization heat

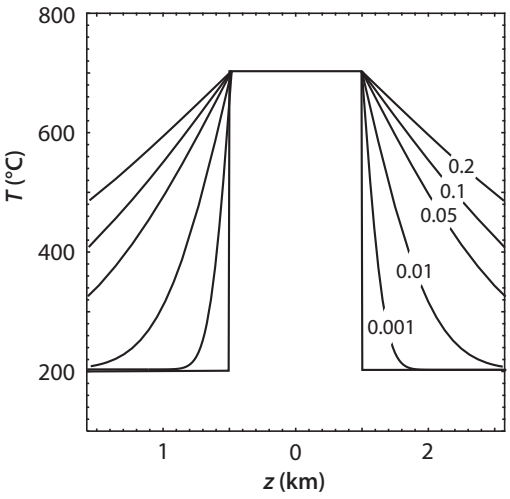

Figure 21: Temperature profiles around a dike which is kept at constant temperature by the flow of magma. Curves are labeled in my. Compare this figure with Fig. 13 and Fig. 15.

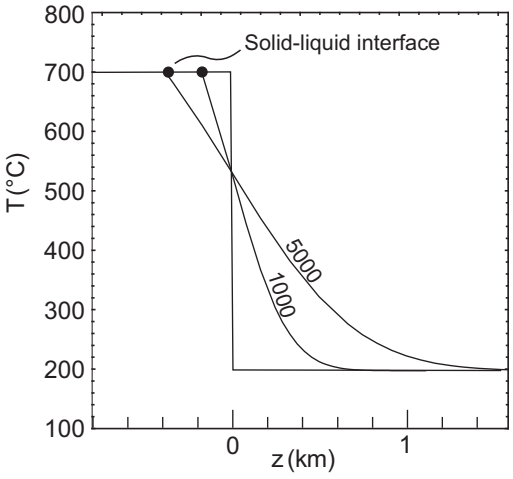

Figure 22: Temperatures in the contact aureole of a crystallizing interface between magma and host rock after 1 000 and 5 000 years. Note that the contact metamorphic aureole is wider and of higher temperature than when only heat conduction is considered (Fig. 17). All parameters assumed here correspond to those used for Fig. 17 with the only difference being that latent heat is considered here.

is added to the energy budget. To illustrate this, it is useful to imagine the processes involved in the freezing of a lake (Fig. 22). During cooling of the air below the freezing point, at first the lakes surface will freeze. The crystallization heat that is freed during this process buffers the further freezing process. During further cooling of the surface, the subsequent thickening of the ice layer will slow down, as the frozen layer insulates the water to the outside and the latent heat of crystallization freed at the ice-water interface remains contained in the water. For this reason it is rare to find pack ice on the polar oceans that is thicker than about 2 m. In fact, it was the observation of ice on the polar oceans that lead Stefan (1891) to describe the problem that now bears his name.

For the one-dimensional case and if the magma of a cooling intrusion crystallizes at a single eutectic temperature, there is an analytical solution that can be used to describe its thermal evolution under consideration of the latent heat of fusion. This is the solution found be Stefan (1891) for the freezing of water. However, most rocks crystallize in divariant reaction over a large temperature interval between a solidus and a liquidus temperature, rather than at a single temperature. Then, numerical solutions of the heat flow equation must be used to consider the effects of latent heat (s. sect. 5.2).

4.4.2 Heat Content of Intrusions and Metamorphic Terrains

If we recall eq. 3, there is a simple relationship between heat and temperature. The relating proportionality constants are the heat capacity c_p and density ρ. In fact, all problems we have described using temperature, could have also been formulated in terms of heat using:

$$\frac{\partial H}{\partial t} = \frac{\partial T}{\partial t} \rho c_p \quad . \tag{41}$$

Instead of going through many calculated examples here, we only want to state that the heat content of an intrusion or a metamorphic terrain can be viewed – in one dimension – as the area underneath a $T - z$ curve. In essence, this is what eq. 3 and eq. 41 state. In other words, the heat content of a dike of thickness l and temperature T_i relative to its surroundings of temperature T_b is given in $\mathrm{J\,m^{-2}}$ by: $(T_\mathrm{i} - T_\mathrm{b}) l \rho c_p$. Using typical values of $\rho = 2\,700\ \mathrm{kg\,m^{-3}}$ and $c_p = 1\,000\ \mathrm{J\,K^{-1}\,kg^{-1}}$, the intrusion of Fig. 17 has a heat content of $H = 1.89 \cdot 10^{12}\ \mathrm{J\,m^{-2}}$. This is the heat content per square meter of dike surface.

In high grade metamorphic terrains containing syn-metamorphic intrusives it is often discussed if the volume of the intrusions is sufficient to contribute significantly to the metamorphism. In other words, it is discussed if the metamorphism is *contact metamorphism* in the widest sense. In order to do this estimate properly, the heat content of the intrusives must be compared with the heat content of the terrain. If the specific heat capacities of the intrusives and the metamorphic host rocks are the same, then the comparison of energy contents can also be made as a comparison of the temperatures. However, we must consider the latent heat of fusion that is part of the heat of the intrusives, but not of the host rocks. As simple calculation shows that:

$$T_{\max} = T_{\mathrm{b}} + \left(T_{\mathrm{i}} - T_{\mathrm{b}} + \frac{L}{c_p} \right) \frac{V_{\mathrm{intrusives}}}{V_{\mathrm{terrain}}} \quad . \tag{42}$$

There, T_{b} and T_{i} are the temperature of the host rock before metamorphism and that of the intrusion, respectively. $V_{\mathrm{intrusives}}$ is the volume of the intrusives and V_{terrain} is the volume of the entire metamorphic terrain. $T_{\max}$ is the maximum temperature that can be reached by contact metamorphism.

If the *aerial* proportion of intrusives to host rock are representative for the *volumetric* proportion of intrusives in the terrain, then the volumes of eq. 42 may be replaced by areas. Using $T_{\mathrm{i}} = 700\,^{\circ}\mathrm{C}$, $T_{\mathrm{b}} = 300\,^{\circ}\mathrm{C}$, $L = 320\,000\ \mathrm{J\,kg^{-1}}$ and $c_p = 1\,000\ \mathrm{J\,kg^{-1}\,K^{-1}}$, eq. 42 shows the following: only about 55 % of the terrain must consist of syn-metamorphic granites in order to heat the entire terrain to 700 °C, even if the intrusion temperature itself was only 700 °C. If the intrusives are 1 200 °C hot mafic magmas, then only 30 % of the terrain must be intrusives in order to heat the terrain to 700 °C.

5 Unit: Production and Advection of Heat

We discern three fundamentally different geological mechanisms that produce heat:

– radioactive heat production,

– chemical heat production,

– mechanical heat production.

In the next sections we discuss the geological relevance of mechanical and chemical heat production. Radiogenic heat production is not mentioned again as we have discussed it already in Unit 2. In general, the rate of temperature change due to heat production may be described by:

$$\frac{\mathrm{d}T}{\mathrm{d}t} = \frac{S}{\rho c_p} \quad . \tag{43}$$

There, T, t, ρ and c_p correspond to temperature, time, density and heat capacity as discussed on p. 5 and S is the volumetric rate of heat production in $\mathrm{J\,s^{-1}\,m^{-3}} = \mathrm{W\,m^{-3}}$. Heat production rate must be divided by density and specific heat to convert the volumetric heat production rate into a rate of temperature change, just as we have done with heat flow in section 1.2. If S is positive, heat is produced, $\mathrm{d}T/\mathrm{d}t$ is positive and rocks heat up. If S is negative, heat is consumed, $\mathrm{d}T/\mathrm{d}t$ is negative and rocks cool. The heat production rate S can be of radioactive, chemical or mechanical origin so that we can write:

$$S = S_{\mathrm{rad}} + S_{\mathrm{chem}} + S_{\mathrm{mec}} \quad . \tag{44}$$

All three of these components may have a significant influence on the thermal evolution of rocks depending on the circumstances.

5.1 Mechanical Heat Production

The forces that deform rocks can be viewed as mechanical energy that is added to the rock. The work done on the system is the product of force applied to the system times the distance over which it is deformed. This energy will be taken up by a variety of *mechanical energy sinks*. A part of this energy will be transformed into potential energy, some into dislocation energy in crystal lattices, some in noise and other forms of energy. However, most authors agree that the majority of this mechanically produced energy will be transformed into friction heat. Frictional heating is also often referred to as *shear heating* (because it is produced when rocks are sheared) or *viscous dissipation*. We abbreviate this mechanical heat production with S_{mec}. The rate of mechanical heat production S_{mec} is given by the product of deviatoric stress τ and strain rate $\dot{\epsilon}$. Stress has the units of Pascal. One Pascal is one Joule per cubic meter ($1\ \mathrm{Pa} = 1\ \mathrm{J\,m^{-3}}$). Thus, stress can be expressed as energy per volume and energy is stress *times* volume. These conversions between the different units should be straight forward, remembering the well-known relationships:

$$\text{force} = \text{mass} \times \text{acceleration} \quad \text{and} \quad \text{stress} = \frac{\text{force}}{\text{area}} \quad .$$

The units of acceleration are $\mathrm{m\,s^{-2}}$ and those of force are therefore: $\mathrm{kg\,m\,s^{-2}}$. Stress and pressure therefore have the units of $\mathrm{kg\,m\,s^{-2}\,m^{-2}}$ or $\mathrm{Pa} = \mathrm{kg\,m^{-1}\,s^{-2}}$ and energy has the

units of $\mathrm{J} = \mathrm{kg\,m^2\,s^{-2}}$. Accordingly, if high deviatoric stresses are required to deform a rock, a lot work is done on the system and the mechanical energy production rate is high, and vice versa. We notice that when we rub our hands together: The harder we press and the faster we rub, the warmer they get. Both deviatoric stress and strain rate are tensors and the rate of mechanical heat production is therefore given by a tensor product. Considering tangential and normal components in three dimensions, friction heat is given by:

$$S_{\mathrm{mec}} = \tau_{xx}\dot{\epsilon}_{xx} + \tau_{yy}\dot{\epsilon}_{yy} + \tau_{zz}\dot{\epsilon}_{zz} + 2\left(\tau_{xy}\dot{\epsilon}_{xy} + \tau_{xz}\dot{\epsilon}_{xz} + \tau_{yz}\dot{\epsilon}_{yz}\right) \tag{45}$$

(see e.g. Burg and Gerya 2005). Here, we consider only the one-dimensional case (and only normal components, i.e. we neglect shear stresses and shear strain rates). Then we can view the mechanical heat production rate as the simple scalar product:

$$S_{\mathrm{mec}} = \tau\dot{\epsilon} \quad . \tag{46}$$

In order to write the temperature change that arises from frictional heating we can write in analogy to eq. 43:

$$\frac{\mathrm{d}T}{\mathrm{d}t} = \frac{\tau\dot{\epsilon}}{\rho c_p} \quad . \tag{47}$$

Note that eq. 47 is independent of the deformation mechanism. Both brittle and ductile deformation mechanisms will produce the same amount of friction heat if they support the same deviatoric stresses. We only may need to be careful with the units: Brittle faults do not have a *strain rate* (in $\mathrm{s^{-1}}$) but a *slip rate* in meters per second. The product of slip rate and deviatoric stress does not have the units of heat production per cubic meter, but the units of heat flow (i.e. $\mathrm{J\,s^{-1}\,m^{-2}}$ normal to the fault surface) which can be converted into a heating rate using the laws of heat conduction discussed in previous sections.

5.1.1 Geological Relevance of Shear Heat Production

A range of authors have discussed the importance of shear heating on a geologically significant scale (e. g. Burg and Gerya 2005; Nabelek and Liu 1999; Brun and Cobbold 1980; Lachenbruch 1980; Scholz 1980; Barton and England 1979; Graham and England 1976). Nevertheless, its importance in many tectonic and metamorphic processes remains contentious. This is because both, deviatoric stresses and strain rates on the scale of the crust are not very well constrained and are among the most discussed geological parameters. We can constrain shear heating to a certain degree using eq. 47 to estimate the temperature increase a rock might experience for some realistic deviatoric stresses and strain rates.

Methods to measure geological strain rates show an upper limit of $\dot{\epsilon} = 10^{-12}$ to 10^{-14} $\mathrm{s^{-1}}$. These numbers imply that deformation doubles the thickness of a rock package (strain of about 100 %) within 1–10 my. The magnitude of deviatoric stresses is much less constrained. Stress determination experiments are performed at strain rates of $\dot{\epsilon} = 10^{-6}$ $\mathrm{s^{-1}}$ and must be extrapolated by six to eight orders of magnitude of strain rate. The relevance of such experimental results remains therefore debated. Moreover, deviatoric stress is strongly temperature dependent. Nevertheless, we know that the order of magnitude of plate tectonic driving forces is between 10^{12} and 10^{13} $\mathrm{N\,m^{-1}}$ and we will show in later units that this implies a rock strength of 50–100 MPa, averaged over the thickness of the lithosphere.

We could also estimate shear heating as follows: If stress and strain rate remain constant over time, then integrating of eq.47 gives:

$$T = t \times \frac{\tau\dot{\epsilon}}{\rho c_p} \quad . \tag{48}$$

The temperature at the end of deformation for a longitudinal strain of 1 is then: $T = \tau/(\rho c_p)$ ($\dot{\epsilon} \cdot t = \epsilon = 1$). Using standard values for the density and specific heat ($\rho = 2\,700$ kg m^{-3} and $c_p = 1\,000$ J kg^{-1} K^{-1}) we can see that a rock that has a shear strength of 100 MPa will be heated by about 37 °C. We conclude that shear heating may be of significant importance to the thermal energy budget of the lithosphere.

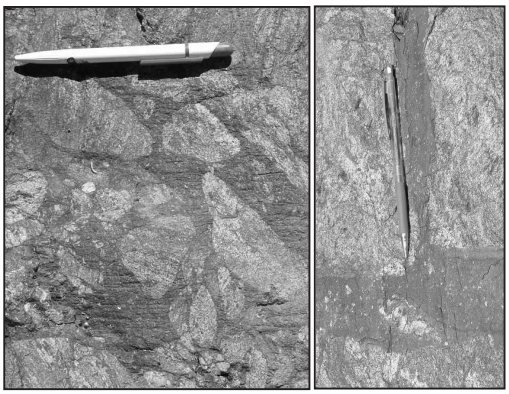

Figure 23: Visible evidence for frictional heating. The left photo shows network typical of many pseudotachylites, the right photo shows a pseudotachylite with chilled margin and recrystallised center.

Examples where friction heat production has a significant influence on the temperature of rocks are well-known to us from pseudotachylites from all crustal levels (Camacho et al. 1995; 2001; Austrheim et al. 1996) (Fig. 23). In those, friction heat was sufficient to even melt the rock. Pseudotachylites form during seismic events where extremely rapid deformation occurred on a very local scale. They are therefore not very appropriate to estimate the influence of friction heat on the thermal evolution of the entire crust where we have to deal with averaged strain rates and averaged stresses (e. g. Kincaid and Silver 1996; Stüwe 1998a). Regardless, even significant amounts of friction heat need not be reflected in significantly increased temperatures. Whether or not shear heating actually becomes geologically significant on a crustal scale depends largely on 2 factors:

- 1. It depends on the relationship between the *length scale* of heat production (which determines how rapidly heat may be conducted away from the site of production) and the *time scale* of heat production. For example, if a 100 m thick shear zone is active for 1 my, then the characteristic time scale of diffusion of this shear zone is of the order of only 1 000 y. Thus, shear heat produced over a time interval of 1 my will be largely conducted away as it is produced. In contrast, if a 15 km nappe pile deforms under the same conditions, then its thermal time constant will be tens of my and all heat produced within 1 my will be largely retained in the pile.
- 2. It depends on the feedback between heating and softening of rocks.

In summary we can say that shear heating *is* a potential candidate for significant heating of rocks.

5.2 Chemical Heat Production

Different rocks are characterized by different internal heat contents defined by the strength of bonding of the atoms in the crystal lattices in the rock-forming minerals. During chemical reaction, the difference in heat content between reactants and products is released or consumed as *latent heat of reaction*. We abbreviate this chemically produced or consumed heat with S_{chem}. By far the largest majority of chemical reactions are *endothermic* when the temperature increases. Because of this, temperature rise of rocks may be buffered by the phase transition. Correspondingly, most reactions are exothermic when crossed down temperature. However, most chemical reactions have a positive slope in a pressure-temperature diagram. Thus exothermal reaction can not only be triggered by a *decrease* in temperature, but also by an *increase* in pressure (at constant temperature). In very general terms, we can chemical reactions that produce heat into three groups. In decreasing order of importance these are:

- **Phase transitions:** The chemically produced heat of reactions involving phase transitions is significant to the thermal budget of rocks.
- **Dehydration reactions:** In the solid state, dehydration reactions are the most important producer of reaction heat (Connolly and Thompson 1989; Peacock 1989). In the greenschist facies they produce of the order of $4 \cdot 10^6$ J per kg of released water. However, rocks contain only of the order of 4 % H_2O and this water is being released over quite a large temperature interval. Thus, the heat of reaction is fairly insignificant during regional metamorphism (about $5\text{–}10 \cdot 10^{-14}$ W cm^{-3}).
- **Solid - solid reactions:** The chemical heat production of solid – solid reaction is negligible for geological problems.

The geologically most important reactions that involve phase transitions are the melting reactions where the *latent heat of fusion* is released or the *latent heat of melting* is consumed. As a consequence, it is important to consider reaction heat when dealing with the thermal energy budget of migmatites and intrusions. A commonly used value for the latent heat of melting of rocks is $L = 320\,000$ J kg^{-1}. Evaporation and condensation reactions are also strongly exothermic and endothermic respectively, but they are not very important in the geodynamics of the lithosphere.

5.2.1 Quantitative Description of Chemical Heat Production

The rate of reaction heat production S_{chem} has the same units as any other heat production rate: W m^{-3}. It can be described by:

$$S_{\text{chem}} = L\rho\frac{\mathrm{d}V}{\mathrm{d}t} \quad . \tag{49}$$

In this equation L is the latent heat of reaction in J kg^{-1}. Since we think of the chemical heat production rate as a *volumetric* heat production rate, it is necessary to multiply L by the density ρ to convert it into a volumetric heat content. The expression $\mathrm{d}V/\mathrm{d}t$ is the volumetric proportion of the reaction that occurs per unit time (in s^{-1}). Note that V has the units of percent and not cubic meters. Thus, the equation determines the part of L that is freed in every time step of the reaction. Substituting eq. 49 into eq. 43 we can

now formulate the temperature change during chemical heat production (and neglecting conduction) to be:

$$\frac{\partial T}{\partial t} = \frac{L}{c_p}\frac{\partial V}{\partial t} \quad . \tag{50}$$

Clearly, we could add a diffusion term to this equation to simultaneously consider chemial heat production and conductive distribution of this heat. However, as most up-temperature reactions are endothermic and most down temperature reactions exothermic, actual heating or cooling by chemical heat production rarely occurs. Instead, this chemical heat is more responsible for buffering the temperature increase or decrease.

Let us illustrate the buffering effects that occur during cooling and crystallisation of a migmatite containing ten percent ($V = 0.1$) eutectic melts (i.e. all melt crystallises at the solidus T_s). If this rock cools with a constant cooling rate s of s =10°C per million years ($s = 10/(3.15 \times 10^{13})$s then it can be seen directly from eq.41 that the heat withdrawal is:

$$\frac{\partial H}{\partial t} = s\rho c_p \tag{51}$$

If s is constant, then this may be integrated so that the heat withdrawn after time t is: $H = s\rho c_p t$ At the solidus this heat withdrawl is used to convert the ten percent melt into rock. Volumetrically this is $LV\rho$ (because L is typically listed per kilogram). Thus, the time of buffering is simply:

$$t = LV/sc_p \tag{52}$$

For a typical value of $L = 300000$ J kg^{-1} this gives $\approx 10^{14}$ s or about 3 million years. After this time interval is over, all melt is crystallises and the rock continues to cool at rate s. (Be careful not to confuse s (cooling rate) with s (SI unit seconds) here).

5.2.2 Thermally Buffered Melting

Melting during prograde metamorphism in the upper amphibolite and granulite facies is a strongly endothermic process. Thus, the rate with which temperature increases during metamorphism at this grade will be buffered by the melting reactions. At univariant melting reactions, the temperature will remain constant until the phase transition from solid reactants to liquid products is complete. It is the very same reason why we have so much snow slush on our roads in spring: ice and water will both have a temperature of 0 °C, until all ice has melted, even if the air temperature has been above freezing for quite some time. For the same reason water will boil at a constant temperature of 100 °C, regardless of the heat added by the stove, until it all has evaporated. In the buffering interval, the amount of heat added to the rock from the outside is exactly balanced by the amount of heat consumed by the phase transition.

Most rocks consist of many chemical components in complicated chemical systems. As a consequence, they do not melt at a single temperature, but over a melting interval between their solidus T_s (where the first melt appear during temperature increase) and liquidus T_l (where the last remaining piece of rock melts) (Fig. 24).

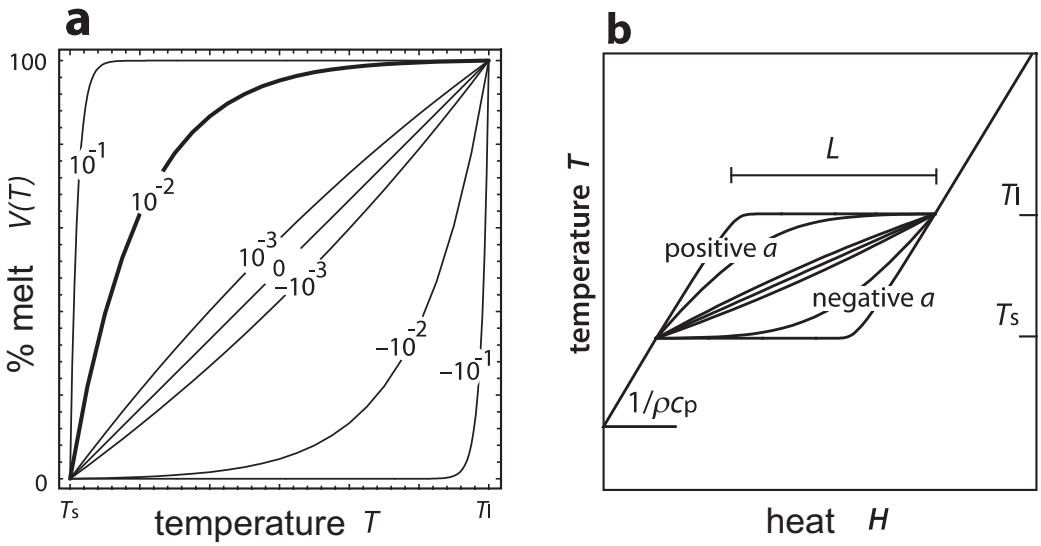

Figure 24: **a** A schematic model for the description of the relationship between melt volume and temperature in the Solidus (T_s) - Liquidus (T_l) interval. The thick drawn line is probably the most realistic curve for the melting of hydrated metapelitic rocks. **b** The relationship between heat content and temperature in the melting interval of a melting rock (shown between solidus temperature T_s and liquidus temperature T_l.

5.3 Advection of Heat in the Lithosphere

Heat can be transported *actively* by the motion of warm rocks. We discern between *advection* and *convection* of heat. *Advection* is generally used if the active transport of heat is only in one direction, for example the transport of heat by an intrusion that moves in the vertical direction. *Convection* is generally used when referring to material transport in a closed loop, for example the convection of mantle material in the asthenosphere, or that of fluids in a hydrothermal system. In this book, we only deal with advection. One-dimensional active transport of heat (for example in the vertical direction z), relative to the z direction may be described by:

$$\frac{\partial T}{\partial t} = u\frac{\partial T}{\partial z} \quad . \tag{53}$$

In eq. 53, u is the transport velocity; the derivative $\partial T/\partial z$ describes the thermal gradient and $\partial T/\partial t$ is the change of temperature with time. For positive u, eq. 53 describes transport *against* the spatial coordinate z: transport is from high z towards lower z. Eq. 53 is also called the transport equation and is equally applicable to the transport of mass, for example during advection of concentration profiles through a crystal lattice. There are three different important mechanisms by which heat is advected in the lithosphere that require different methods of description. These three mechanisms are:

– advection of heat by magmas, e. g. magmatic intrusion;

– advection of heat by solid rock motion, e. g. erosion or deformation;

– advection of heat by fluids, e. g. during infiltration events.

The difference between these three processes in terms of their mathematical description arises mainly from the relative rates of advective and diffusive processes. These three processes will therefore now be discussed separately.

During intrusion of magma from deeper into shallower levels in the crust, the heat of the magma is transported to higher crustal levels by the motion of the magma itself. The process of magmatic intrusion is - in general - much faster than most other geological processes, for example the thermal equilibration during contact metamorphism. It is therefore usually not necessary to describe the intrusion process itself by an advection equation and we have dealt with this in Unit 4.

5.4 Heat Advection by Solid Rock

Any movement and deformation of rocks will carry the heat it contains with it. For example, during exhumation of rocks by erosion, the lithosphere (and its heat) are moved vertically upwards. The column is moved *through* a surface of constant temperature - the surface of Earth. Erosion is therefore a heat advection process. In a similar way, any other motion of rocks, for example during thrusting or folding may be interpreted as an advective process. Here we will only discuss one-dimensional, vertical advection of heat to and from the earth's surface. The time scale of continental denudation processes is comparable to the time scale of thermal equilibration on the scale of the crust and we can therefore not neglect to consider both processes at the same time. If we want to describe advection and diffusion of heat simultaneously, then we must expand eq. 53 by the diffusion term from eq. 6. The equation that must be solved becomes:

$$\frac{\partial T}{\partial t} = \kappa \frac{\partial^2 T}{\partial z^2} + u \frac{\partial T}{\partial z} \quad . \tag{54}$$

A schematic illustration how the two processes interact to shape a geotherm during erosion is shown in Fig. 25. You can see that diffusion and advection interact in shaping the temperature profile until a certain depth length scale), but that advection dominates at larger depths (length scales).

5.5 Heat Advection by Fluids

Heat may also be advected by fluids that circulate through rocks. Heating of rocks due to fluid advection is different from the previous examples, because only part of the rock

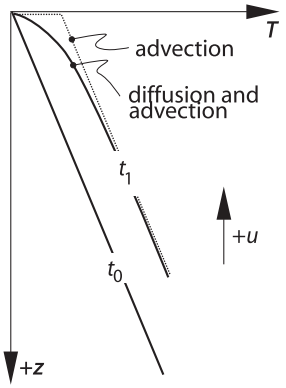

Figure 25: Schematic illustration of one-dimensional advection of heat by erosion. The coordinate system is fixed with $z = 0$ at the earth's surface. Temperature profiles through the crust are shown for two times: at the onset of erosion t_0, at which a linear geotherm is assumed and a later time t_1. The advection rate u is positive upwards. In the shown time interval the erosion process *advects* the geotherm by $u \times t_1$ meters upwards. Simultaneous *diffusion* causes the curvature of the temperature profile.

volume is being advected, namely the fluids that fill the pore volume. Thus, when formulating an advective term in an advection-diffusion equation, we need to take care so that we describe only the advection of a fraction of the total rock volume. In a general one-dimensional form eq. 53 can be written as:

$$\frac{\partial T}{\partial t} = \phi v_{\mathrm{f}} \left(\frac{\rho_{\mathrm{f}} c_{pf}}{\rho c_p} \right) \frac{\partial T}{\partial z} \quad , \tag{55}$$

(McKenzie 1984). There, ϕ is the porosity of the rock and v_{f} is the fluid flux in $\mathrm{m^3 m^{-2} s^{-1}}$. The product ϕv_{f} is the fluid volume that is transported per unit time and per unit area through the rock. This product has the units of $\mathrm{m\,s^{-1}}$, which corresponds to the standard definition of fluxes. It is called the *volumetric fluid flux*. ρ and ρ_{f} are the densities and c_p as well as c_{pf} are the specific heat capacities, both of the rock and the fluid, respectively.

Eq. 55 may be used to describe the thermal effects of fluid advection. However, in many geological processes heat advection by fluids occurs on similar time scales as heat conduction. Thus, it is usually necessary to expand eq. 55 by a term describing diffusion as we did in eq. 55. The importance of the transport of heat by fluids for the thermal evolution of the crust was discussed by Bickle and McKenzie (1987), Connolly and Thompson (1989) as well as Peacock (1989). These authors agree that the fluid flux that may be caused by metamorphic dehydration reactions is less than about 1 kg fluid per square meter and per year. This is not enough to transport heat very efficiently by fluids. Peacock (1989) estimated that the thermal evolution of rocks can only be influenced by fluids if these are focused into narrow zones from regions as wide as 10 km. We can conclude that heat advection by fluids is insignificant at least when we are interested in thermal budgets of the crust as a whole.

5.6 The Peclet Number

In the two sections above we have seen that diffusion and advection interact at some length scale and do not interact on others. It is therefore useful to find a measure that can be used to estimate the relative importance of diffusive and advective processes: the Peclet number. The Peclet number is defined as:

$$Pe = \frac{ul}{\kappa} = \frac{ul\rho c_p}{k} \tag{56}$$

where u is the rate of advection, κ the diffusivity and l the characteristic length scale of the advection process. The second way to write the Peclet number is only inserted above to remind us that the diffusivity is the ratio of conductivity k, density ρ and heat capacity c_p. If Pe is about 1, then diffusion and advection are of similar importance to a process. If Pe is much larger than 1, advection dominates the process. If Pe is much smaller than 1, then diffusion dominates the process. Eq. 56 can be used to derive advection rates. For example, on Fig. 26 isotherms have been displaced by a thrust. Consider the 400°C isotherm. On any length scale that is larger than l_2, this isotherms is simply displaced by the material advection of the hanging wall (i.e. $Pe > 1$). On the length scale of l_1 (dark shaped region) both diffusion and advection have played a role in shaping the curved isotherm (i.e. $Pe = 1$). On the length scale l_1 (light shaded region), diffusion has dominated and the isotherm appears not displaced across the fault (i.e. $Pe < 1$).

Aside from its importance for the description of thermal processes, the Peclet number finds many other application. For example, Bickle and McKenzie (1987) have used the Peclet number for some fundamental interpretations about the relative importance of diffusive and advective processes during fluid infiltration of rocks (Fig. 26).

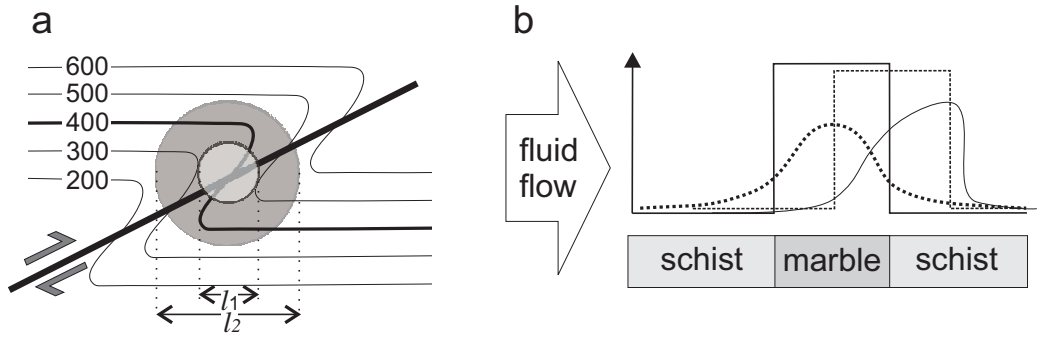

Figure 26: **a** Schematic cartoon showing the displacement of isotherms during thrusting. Note that – within the length scale l_1 – diffusion has eliminated any displacement of isotherms across the fault, while above length scale l_2 only displacement, but no curvature is visible. **b** Diffusion and advection of isotopes from a layered sequence. The vertical axis is isotope concentration, the horizontal axis is a profile across the three rock types shown. The continuous step shaped line shows the concentrations at the time of formation. The dotted line after subsequent diffusion ($Pe < 1$), the dashed line after fluid infiltration ($Pe > 1$), but without diffusion ($Pe = 1$). The asymmetric line during both ($Pe = 1$)

• **Temperatures around Faults** In order to estimate the importance of heat advection due to fault motion we can employ two simple tools which we have discussed in previous sections: The thermal time constant (eq. 33) and the Peclet number (eq. 56). From eq. 56 we can estimate the length scale l where both diffusion and advection influence the thermal structure (i.e. $Pe = 1$) by:

$$l = \frac{\kappa}{u} \quad . \tag{57}$$

on the lengthscale l isotherms will be bent intot the fault zone.

6 Unit: Selected Problems of Heat Transfer

In the past five Units we have seen that hat conduction, heat production and heat advection all can have relevance to the temperatures in the lithosphere. Eq. 8 is the full thermal energy balance considering all these processes. When solving a heat transfer problem it is important to see how this equation can be simplified and then solved (see: Carslaw and Jaeger 1959). In this unit we briefly summarise how this equation can be solved in principle and then present two selected heat transfer examples of topical relevance.

6.0.1 Analytical and Numerical Solutions

In order to make use of a differential equation we must solve it. Only then, they can be used as a tool to extract numbers that describe some process. There are two fundamentally different ways to solve them.

• **1. Analytical solutions** *Analytical* or *closed* solutions of differential equations may be found by integrating them. Let us consider as an example the description of a geotherm by

$$\frac{\mathrm{d}T}{\mathrm{d}z} = \frac{1.5}{\sqrt{z}} \quad . \tag{58}$$

There, T is temperature in °C and z is depth. This differential equation can be integrated without difficulty:

$$T = 3\sqrt{z} + C \quad . \tag{59}$$

The integration constant C must be determined using boundary conditions. Eq. 59 is said to be an "analytical solution of the differential equation eq. 58". If we assume (as our boundary condition) that the temperature at the surface is always zero and we assume a coordinate system where the surface is at $z = 0$, then this constant must be also zero: $C = 0$. Now eq. 59 can be used to calculate temperatures at any depth of our choice by inserting numbers for z. For example, for $z = 100\,000$ m eq. 59 gives $T = 949\,^{\circ}\mathrm{C}$.

• **2. Numerical solutions** Numerical solutions of differential equations are used to extract numbers from differential equations *without* having to solve (integrate) them. With their aid we can arrive at the result that eq. 58 describes a temperature of $T = 949\,^{\circ}\mathrm{C}$ at 100 km depth without having to solve the differential equation, i.e. without having to go from eq. 58 to eq. 59. Great – results without having to solve the problem! However, there is nothing such as a free lunch: numerical solutions are not exact. Numerical approximations are always approximations and they are plagued by stability and accuracy problems. There are two important methods that are in use:

The *finite element method* has the advantage that it is much more elegant to use it for the description of deformation on Lagrangian coordinates. The principal disadvantage of the finite element method is that it is not very intuitive and therefore requires quite an initial effort to learn it.

The *finite difference method* has the enormous advantage that it is quite intuitive, easy to implement on a computer (even by inexperienced mathematicians) and easily adaptable to many different problems. Its principal problems are those of instability, and that they are quite cumbersome when it comes to the treatment of discontinuous boundary conditions and deformed grids.

• **Advantages and disadvantages** Numerical and analytical solutions have both their advantages and disadvantages. The enormous advantage of numerical solutions is that they allow us to arrive at results without having to know enough differential calculus to be able to integrate the equation in question.

Analytical solutions have the advantage that they are much more useful to understand the nature of a geological process. For example, eq. 59 may be used directly to infer that the temperature in the crust rises with the square root of depth. If this model corresponds well with our observations in nature, then we can continue to think about the significance of this quadratic relationship. Such considerations are difficult with numerical solutions as they only deliver numbers.

6.0.2 Initial- and Boundary Conditions

• **Boundary conditions** When solving differential equations, *boundary conditions* are necessary in order to determine the integration constants. This is true for both numerical and analytical solutions. For differential equations of the first order we need one boundary condition, for those of the second order two and so on. The term *boundary condition* is exactly what it implies: it is a condition at the boundary of the model. The most common types of boundary conditions are:

– A prescribed value of the function at the model boundary (e. g. $T = 0$ at $z = 0$; s. eq. 59),

– Neumann boundary condition: A prescribed gradient of the function at the model boundary,

• **Initial conditions** *Initial conditions* are necessary to determine the starting point of a model. For example, if we want to use the diffusion equation (eq. 6) to calculate the evolution of a diffusive zoning profile over time, then we must use a function $T = f(z)$ at the time $t = 0$ from which we can start calculating. The nature of this function $T = f(z)$ must be determined by a known initial condition. Steady state problems usually do not require an initial condition.

6.1 Periodic Temperature Fluctuations

The temperatures at the surface of Earth are subject to the daily or annually periodically changing temperatures of the atmosphere. Problems where this is relevant, range from understanding the thickness of permafrost soils, to the regulation of temperatures in tunnels and insulation of walls of buildings. Many of these problems can be described with a one-dimensional coordinate system with z as the coordinate normal to the surface and with boundary conditions that describe a periodic fluctuation of the temperature at the surface. This may be written as:

– Initial condition: $T = T_0$ at all z at time $t = 0$.

– Boundary condition: $T = T_0 + \Delta T \cos(ft)$ at $z = 0$ for all $t > 0$, and $T = T_0$ at $z = \infty$ for all $t > 0$.

There, ΔT is half the amplitude of the annual fluctuation, t is time and f is the frequency of the periodic temperature cycle (Fig. 27 a). T_0 is the mean temperature over one cycle. The time dependent diffusion equation (eq. 6) can be integrated using these assumptions.

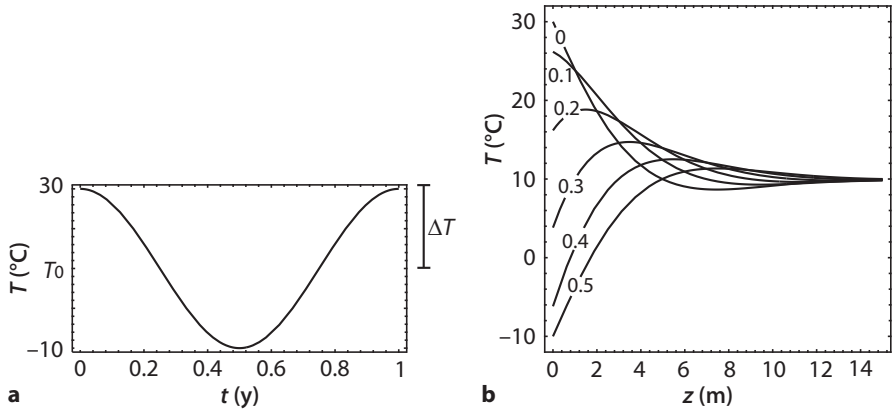

Figure 27: The temperature in the upper few meters of the crust as a function of annually changing surface temperature. **a** shows the upper boundary condition: the temperature T as a function of time t at $z = 0$. The annual mean temperature was assumed to be T_0=10 °C. The variation about this mean was assumed to be $\Delta T = 20\,^{\circ}\mathrm{C}$. **b** shows six thermal profiles in the ground at six different times through the course of half a year. The curves are labeled for time in years. It may be seen that below depths of about 2 m temperatures never sink below the freezing point.

We will not go through this integration here, but the result is amazingly simple. It is given by:

$$T = T_0 + \Delta T \mathrm{e}^{\left(-z\sqrt{\frac{f}{2\kappa}}\right)} \cos\left(ft - z\sqrt{\frac{f}{2\kappa}}\right) \quad . \tag{60}$$

This equation may be used to describe temperature fluctuations at depth as a function of a periodic temperature variation at the surface. It may be seen that this equation contains a trigonometric function and an exponential function. At each time t it describes a cosine function of temperature which decays in amplitude exponentially with depth.

6.2 Isotherms and Surface Topography

An important example of a heat conduction - advection problem concerns the influence of the surface topography on isotherms at depth. Rocks inside mountains are thermally insulated, while rocks nearer the surface of an incising valley are cooled by the surface. As a consequence, isotherms follow the Earth's surface it in a damped form. Just how the distance of a given isotherm from the surface varies with amplitude and wavelength of the topography is of large importance for the interpretation of low temperature geochronological data in mountainous regions, for the design of ventilation systems in tunnels and more (Fig. 28) (Braun 2002; 2006). In this section we discuss some models that can be used to estimate the magnitude of this effect.

6.2.1 The Upper Boundary: The Topography

For simplicity we assume that the surface topography may be described by a sine-function with the wavelength λ and the amplitude $h_0/2$ where we interpret the wavelength λ as

the distance between two parallel valleys and h_0 as the maximum elevation of the peaks above the valleys. Using the coordinate system illustrated in Fig. 29a,b, the elevation h at any point of the topography is described by:

$$z_{(T=0)} = -h = -h_0 \frac{1}{2}\left(1 + \cos\left(\frac{2\pi x}{\lambda}\right)\right) \tag{61}$$

Using such a simple function to describe topography allows us to evaluate the magnitude of the thermal effects as a function of two simple parameters of topography: the wavelength and the amplitude.

We also assume that the temperature along the curve described by eq. 61 is the surface temperature $T_s = 0$ and neglect any atmospheric temperature gradient or seasonal variation. However, even for these simplified assumptions, integration of the two-dimensional diffusion- or diffusion-advection equation (eq. 6 or 54) under this boundary condition is very difficult. A common way to surround this problem is by substituting this boundary condition of *constant* temperature at a *variable* spatial position, by a boundary condition of *variable* temperature at a *constant* elevation, for example at $z = 0$. This would be described by:

$$T(x)_{(z=0)} = \Delta T \frac{1}{2}\left(1 + \cos\left(\frac{2\pi x}{\lambda}\right)\right) \tag{62}$$

where $\Delta T = h_0 g$ and g is the geothermal gradient in the absence of topography. This assumption implies that the thermal gradient inside the mountains is linear. ΔT corresponds to h_0 in the proper formulation (s. Fig. 29). This approximation is good if the wavelength of the topography is large compared to the amplitude because then the lateral cooling through the sides of the valley can be neglected. Note that this approximation of the topography is actually quite a correct description if the surface temperature on a flat shield *does* vary laterally, for example because of the presence of lakes. Using these assumptions, we can discern different types of scenarios described by different solutions of the diffusion – advection equation:

6.2.2 Topography Without Erosion

If there is no erosion, there is no advection towards the surface. As a consequence, the topographic perturbation effect on isotherms is substantially smaller than it would be

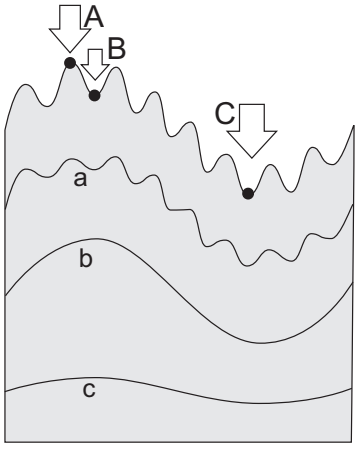

Figure 28: Schematic illustration of isotherms underneath topography. (a), (b) and (c) show three different isotherms at depth. Note that the topographic perturbation of isotherms decreases with depth in proportion to the wavelength of the topography. Using age elevation relationships at A and B with an isotopic system that closes at isotherm (a) would result in an overestimate of the erosion rate.

in an eroding terrain. To estimate it we need to solve a two dimensional version of the diffusion equation, subject to the boundary conditions of eq. 62. The solution is:

$$T_{(x,z)} = T(x)_{(z=0)} \times \mathrm{e}^{-2\pi z/\lambda} \quad . \tag{63}$$

We can see from this solution a fundamental result (shown in Figs. 29b): The perturbation of isotherms decreases exponentially with depth and in proportion to the wavelength of the topography. The solution is a beautiful example of the elegance of analytical solutions. Lets use the Alps and an isotherm relevant for fission track analysis ($\approx 100°$C corresponding to a depth of ≈ 3 km) as an example: The Alps have a topographic amplitude of about 3 km and a series of topographic wavelengths from about $\lambda \approx 2$ km in the most rugged regions to $\lambda \approx 200$ km from the northern to the southern Molasse basin. Inserting these numbers into the exponential term of eq. 63 shows that the narrow wavelengths are just about invisible for the 100°C isotherm, while 90% of the longest wavelength is preserved at 3 km depth. This caused Brown (1991) to conclude the interpretation of age – elevation profiles from apatite fission tack data may be done without topographic correction.

6.2.3 Eroding Topography

During erosion material is advected towards the surface, isotherms are compressed into the topography and the amplitude of a given isotherm is substantially larger than when no erosion occurs. To estimate the perturbation effect quantitatively we need to solve a two dimensional form of the diffusion – advection equation (eq. 54). This equation may be expanded into two dimensions and modified to account for the variable boundary at the top surface. Solutions typically show the same fundamental relationship discussed in connection with eq. 63, namely that the effect decreases exponentially with depth and in proportion to the wavelength of the topography. However, depending on the erosion

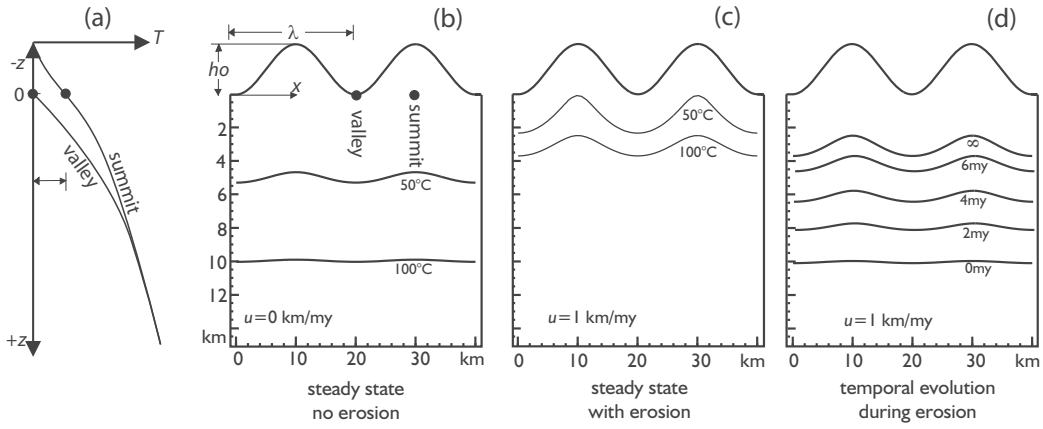

Figure 29: Isotherms underneath regions of high topographic relief. **b**, **c** and **d** show two-dimensional profiles through a mountainous topography. The two isotherms in **b** are for a non-eroding topography calculated with eq. 62 and adding a linear thermal gradient to the solution to place the different isotherms at the correct depths. **c** shows a thermal steady state case for an eroding topography. In **d** the time dependent evolution underneath an eroding topography is shown for a single isotherm, in this case 100 °C. The two black dots in **a** and **b** are at equal depth, but they have a different temperature.

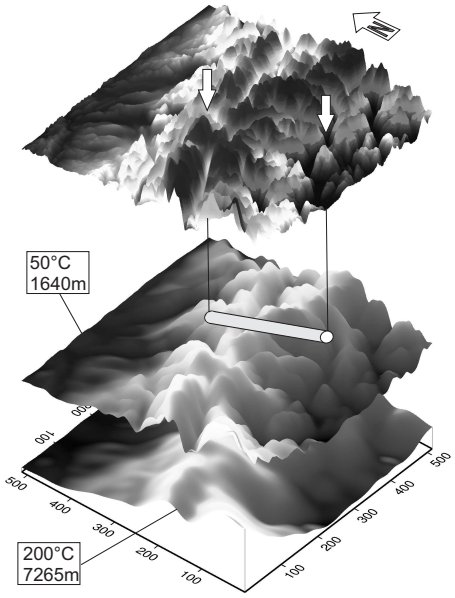

Figure 30: Example of a three dimensional conduction-advection model to consider topographic perturbation effects on topography (Hergarten and Stüwe in prep). For this example, the digital elevation model of the Gotthard region was interpolated onto a three dimensional grid to consider thermal effects important for ventilation in the longest road tunnel on earth: the Gotthard base tunnel.

rate, the advection processes may be strong enough to perturb isotherms of geological relevance. Stüwe et al. (1994) found a semi-analytical solution of the two-dimensional diffusion-advection equation to describe this problem (Fig. 29c and 28). They concluded that at erosion rates above 500 m my^{-1} it becomes important to consider the topographic effects on the interpretation of apatite fission track results.

7 Unit: The Elevation of Mountains

Isostasy is a stress balance. Isostasy relates the vertical distribution of mass to elevation in a state of equilibrium in which the lithosphere is considered to be floating on the underlying relatively weak asthenosphere. Isostasy does a good job of explaining the first-order variation of elevation over most of the Earth's surface. When we consider isostatic equilibrium it is useful to discern:

– hydrostatic isostasy and

– flexural isostasy.

Hydrostatic isostasy is a stress balance in the vertical direction only. Thus, hydrostatic isostasy is a model that should really only be applied to regions that are large compared to the elastic thickness of the lithosphere. In other words, to geological features that are of at least several hundreds of kilometers in extent, i.e. areas like the Tibetan Plateau or the Canadian Shield. *Flexural isostasy* describes a stress balance in two or even three dimensions (s. Fig. 31). As a consequence, flexural isostatic considerations can be used to interpret the shape of much smaller scale features, for example foreland basins or subduction zones.

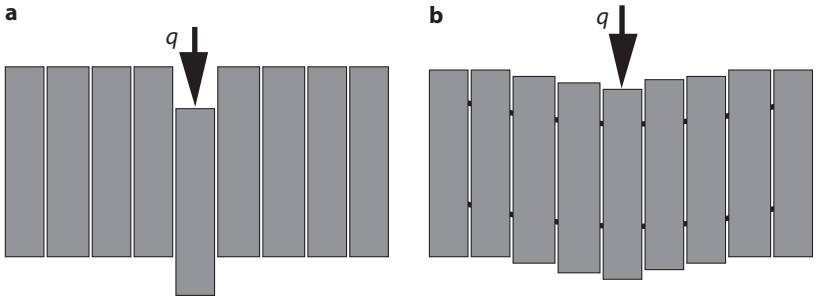

Figure 31: Illustration of the difference between **a** hydrostatic isostasy and **b** flexural isostasy. In **a** all vertical columns are considered independently of each other. In **b** the shear stresses between vertical columns are akso considered. q is the load.

7.0.4 Isostatic Equilibration Rates

Isostasy describes an equilibrium state and is therefore independent of time. Nevertheless, many geologists misinterpret the temporal evolution of isostatic rebound as a feature inherent to isostasy. For example, we observe that isostatic equilibrium of Scandinavia in response to its deglaciation in the last ice age, occurs on a time scale of 10^4 years (e. g. Sabodini et al. 1991). Such isostatic compensation rates can be measured, for example by dating raised beaches (Fig. 32). However, this observation does *not* tell us that isostasy itself is time-dependent. Isostasy is a stress balance and as such *independent* of time. If a plate tries to rise or sink to reach its isostatic equilibrium state in response to a changed load, it has to displace the underlying asthenosphere. Thus, the rate of isostatic compensation can be used to estimate the viscosity of the asthenosphere (e. g. Lambeck 1993).

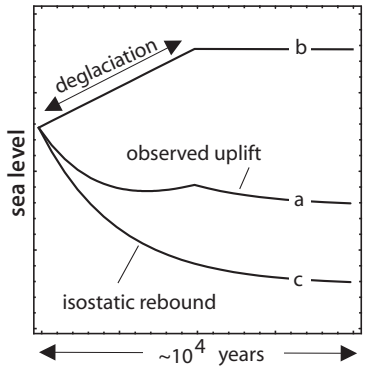

Figure 32: Observed and interpreted sea level changes. *a* Typical evolution of surface uplift relative to sea level in regions of recent deglaciation, for example Scandinavia (e. g. Lambeck 1991). Such curves typically contain two distinct parts and may be interpreted as the sum of sea level *rise* due to deglaciation (curve b) (because of increased water mass in the oceans) and sea level *drop* because of isostatic rebound (curve c). From such curves, mantle viscosities of the order of 10^{20} Poise have been calculated.

7.1 Hydrostatic Isostasy

The hydrostatic isostatic model is based on the assumption that all vertical profiles through the lithosphere may be considered independently of each other. That is, shear stresses on vertical planes are neglected (Fig. 31a). Then, there will be a depth at which the vertical stresses of all vertical profiles are equal. This depth is called the *isostatic compensation depth*. At this depth, the weight of all columns are equal. If you dive underneath a boat you dive beneath this isostatic compensation depth: Regardless if the boat is above you or not, the water pressure is the same. If we consider two profiles A and B, the *isostasy condition* may be formulated in terms of an equation (s. Fig. 33):

$$\sigma_{zz}^{\mathrm{A}}|_{z=z_{\mathrm{K}}} = \sigma_{zz}^{\mathrm{B}}|_{z=z_{\mathrm{K}}} \quad . \tag{64}$$

In this equation σ_{zz}^{A} and σ_{zz}^{B} are the vertical normal stresses of the two columns A and B and the depth z_{K} is the isostatic compensation depth. The vertical dash stands for "at the location". For most geological purposes we want to compare the elevation of two neighboring lithospheric columns in isostatic equilibrium. For this, it is useful to assume as isostatic compensation depth the shallowest possible depth below which there is no density differences between two neighboring columns. For most examples this can be assumed to be the base of the lithosphere of the column which reaches deepest into the asthenosphere.

The downward force that is exerted by one cubic meter of rock is given by the product of its mass $\times$ gravitational acceleration. The downward force that is exerted by an entire vertical column per square meter (the vertical normal stress) is thus the product of density and acceleration integrated over the thickness of the column:

$$\sigma_{zz}\Big|_{z=z_{\mathrm{K}}} = \int_0^{z_{\mathrm{K}}} \rho g \mathrm{d}z \quad . \tag{65}$$

Inserting eq. 65 into eq. 64 gives:

$$\int_0^{z_{\mathrm{K}}} \rho_{\mathrm{A}}(z) g \mathrm{d}z = \int_0^{z_{\mathrm{K}}} \rho_{\mathrm{B}}(z) g \mathrm{d}z \quad , \tag{66}$$

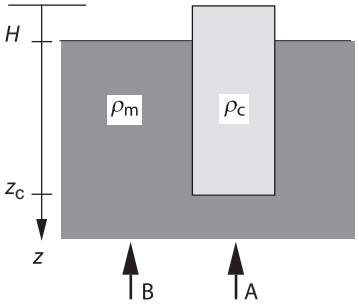

Figure 33: Illustration of isostatic equilibrium. Note that the z-axis is defined positively downwards and has its origin at the surface of the light shaded block (e.g. an iceberg or the lithosphere) that is assumed to float in a dark shaded region of higher density (e.g. water or the asthenosphere).

where $\rho_A(z)$ and $\rho_B(z)$ are the densities of the two columns that are to be compared, both as a function of depth, z. Within the coordinate system shown in Fig. 33, the lower limit of integration 0 corresponds to the upper surface of the higher of two columns that are to be compared. The upper limit of integration is the isostatic compensation depth z_K. g is the gravitational acceleration. Eq. 66 is the basis of all calculations of isostasy. When considering the isostatically supported elevation of a mountain belt, it is useful to divide the density variations in the lithosphere into two parts (a) density variations that are due to material differences and (b) density variations that are caused by thermal expansion.

7.1.1 Isostasy due to Material Differences

We begin by solving the balance written out in eq. 66 for the elevation of a single lithospheric column above the asthenosphere. For simplicity we forget in the first instance about the mantle part of the lithosphere and consider the crust only so that $z_K = z_c$ (Fig. 33). The block in Fig. 33 has a constant density ρ_c (e.g. density of the crust) and floats in a denser medium of the constant density ρ_m (e.g. density of the mantle). We call its elevation above the surface of the denser medium H_{mat}, although it is just labeled as H in Fig. 33. We use the subscript $_{mat}$ to emphasize that – for now – we consider only the *material* contribution to density differences between the profiles A and B. The densities and the acceleration are independent of z. Thus, they can be drawn out of the integrals on both sides of eq. 66 and integration is easy. By integrating the left half of the equation and splitting up the right half of eq. 66 we get according to Fig. 33:

$$\rho_c g z\Big|_0^{z_c} = g\int_0^{H_{mat}} \rho_{air}\mathrm{d}z + g\int_{H_{mat}}^{z_c} \rho_m \mathrm{d}z \quad . \tag{67}$$

The density of air is negligible in comparison with ρ_m or ρ_c. Thus, the first integral on the right hand side of eq. 67 is also negligible. After finishing the integration, canceling out g and inserting the integration limits we get:

$$\rho_c z_c = \rho_m z_c - \rho_m H_{mat} \quad . \tag{68}$$

Solving for elevation H gives:

$$H = H_{mat} = z_c\left(\frac{\rho_m - \rho_c}{\rho_m}\right) \quad . \tag{69}$$

This relationship describes the hydrostatically balanced elevation of the surface of a floating body above the medium it floats in. Remember that $H = H_{mat}$ emphasizes the fact that this elevation difference is only based on the material difference between the block

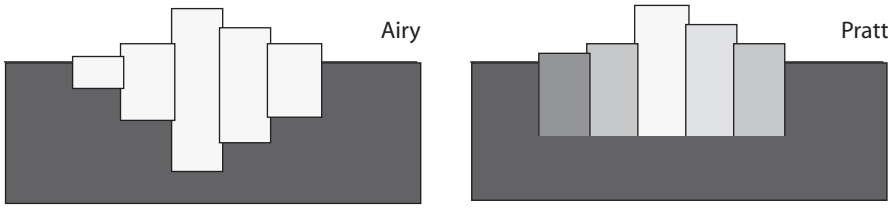

Figure 34: Comparison of the interpretations of the isostatic model according to Airy and Pratt. The shading indicates density. Darker shading means higher density.

and the liquid. We can control this equation for some end member scenarios: If ρ_c is zero, then this equation states that $H = z_l$: the entire column floats on top of the liquid. This is the scenario given by a kids balloon floating on a lake. Alternatively if the two densities approach each other ($\rho_m = \rho_c$), then the entire body is submerged ($H = 0$). This is the scenario we observe with water soaked logs that float almost completely submerged in water. We can conclude that our observations confirm the simple model.

7.1.2 Isostasy According to Airy and Pratt

Two centuries ago, different models were developed to explain elevation differences observed in the mountain belts of the world in terms of the isostasy model. The two most notable models are those of *Airy* and *Pratt* (Fig. 34). Both earth scientists recognized that mountain belts are likely to rest in isostatic equilibrium and that their elevation is proportional to the density contrast between crust and mantle, as expressed by eq. 69. Pratt observed that many low lying Proterozoic shields are made up of high grade metamorphic rocks of high density, while mountain belts are often made up of hydrated, low grade metasediments and carbonates. He concluded that most continental crusts extend to roughly similar depths and that the observed differences in surface elevation are the consequence of horizontal density variations in the crust.

In contrast, Airy estimated that the density of the crust is largely the same in all continental regions and therefore concluded that topographically higher regions, must be compensated by crustal roots at depth. Seismic studies in many mountain belts show that most regions of high surface elevation are indeed compensated by significant roots at depth.

7.1.3 Isostasy Due to Thermal Expansion

In order to calculate the contribution of thermal expansion to surface elevation we need to introduce α: the *coefficient of thermal expansion*. α has the units of strain per temperature increment, which is K^{-1}. For most rocks the coefficient of thermal expansion is of the order $\alpha = 3 \cdot 10^{-5} K^{-1}$. Using α and the density of the mantle ρ_m (at the temperature of the asthenosphere), the density of colder rocks of the same material as a function of temperature may be calculated with:

$$\rho(T) = \rho_m(1 + \alpha(T_l - T)) \quad . \tag{70}$$

There, T_l is the temperature at the base of the lithosphere at $z = z_l$. According to eq. 70: $\rho = \rho_m$, where $T = T_l$. At lower temperatures, the density increases linearly. At the

surface, where we can assume that the temperature is T_s =0 °C, eq. 70 becomes:

$$\rho_{(T=T_s)} = \rho_0 = \rho_m (1 + \alpha T_l) \quad . \tag{71}$$

If the density of the mantle is about ρ_m=3 200 kg m^{-3} at T_l, then the density at the surface is: ρ_0=3 300 kg m^{-3}. Assuming a linear geotherm in the lithosphere, we can describe the mean density of the lithosphere with:

$$\overline{\rho} = \rho_m \left(1 + \alpha \frac{T_l + T_s}{2}\right) \quad . \tag{72}$$

In order to estimate which proportion of the elevation of a mountain belt is due to thermal expansion (H_{therm}), we insert eq. 72 into the left hand side of eq. 66. The following algebra remains the same as in eq. 67 and eq. 68 except that the upper limit of integration is not the base of the crust, but the base of the lithosphere, because thermal expansion and contraction affects the entire lithospheric column. After integration according to the same principles as we did before we get here:

$$H_{therm} = -z_l \alpha (T_l + T_s)/2 \quad . \tag{73}$$

The negative sign arises because $\overline{\rho}$ is larger than ρ_m.

7.1.4 The Elevation of Mountain Belts

First off a warning: Gravimetric data tell us that many active orogens are *not* in isostatic equilibrium, but that their topography is dynamically supported. This means the surface elevation is actively held up or pushed down and is *out* of isostatic equilibrium. Dynamically supported topography may generally be found on length scales that are comparable to the elastic thickness of the lithosphere and will be discussed there (e. g. Forsyth 1985; Lyon-Caen and Molnar 1983; Molnar and Lyon-Caen 1989). It is therefore emphasized that the model of hydrostatic isostasy should only be used for topographic features that are at least some hundreds of kilometers in lateral extent. For example, the European Alps are barely 200 kilometers across and are only partly compensated isostatically (Karner and Watts 1983). This limitation of the hydrostatic model should be kept in mind when we interpret the simple considerations below.

Nevertheless, let us now consider the elevation of a lithosphere with the thickness z_l and a crustal thickness of z_c above its surroundings considering both the influence of the different materials and the influence of thermal expansion. The higher density of the cold lithosphere provides a *negative* contribution to the overall buoyancy (eq. 73). The *material* contribution of the crust to the elevation, on the other hand, is positive and was derived in eq. 69. Density variations within the mantle part of the lithosphere are neglected here. Then, the isostatically supported surface elevation relative to the surroundings is given be the sum of the thermal and the material contributions:

$$H = H_{mat} + H_{therm} = z_c \left(\frac{\rho_m - \rho_c}{\rho_m}\right) - z_l \alpha (T_l + T_s)/2 \quad . \tag{74}$$

If we summarize all the material parameters into the constants:

$$\delta = (\rho_m - \rho_c)/\rho_m \qquad \text{and :} \qquad \xi = \alpha (T_l + T_s)/2 \quad , \tag{75}$$

then this eq. 74 simplifies to:

$$H = \delta z_c - \xi z_l \quad . \tag{76}$$

If we insert meaningful numbers into eq. 74 (e. g. $\rho_m = 3\,200$ kg m^{-3}, $\rho_c = 2\,700$ kg m^{-3}), we get:

$$\delta \approx 0.15 \qquad \text{and:} \qquad \xi \approx 0.018 \quad . \tag{77}$$

This implies that the influence of material difference between crust and mantle, per meter of lithospheric column, is about ten times more important to the isostatically supported surface elevation than the influence of the thermal expansion. However, because the crust constitutes only about one third of the lithosphere, the crustal material contribution to the elevation is in total only about 3 times larger than the contribution of thermal contraction, which applies to the whole lithosphere. In total, H is about 3 600 m.

This is the elevation of the upper surface (of a lithosphere with z_c and z_l as above) above the hypothetical surface of a liquid mantle, as we illustrated in Fig. 33. Mid-oceanic ridges are the only place on the globe where we can measure the depth of this reference level. It turns out that mid-oceanic ridges lie indeed about 3 600 m below the average elevation of the continents and lie at a very constant depth below sea level (Turcotte et al. 1977; Cochran 1982).

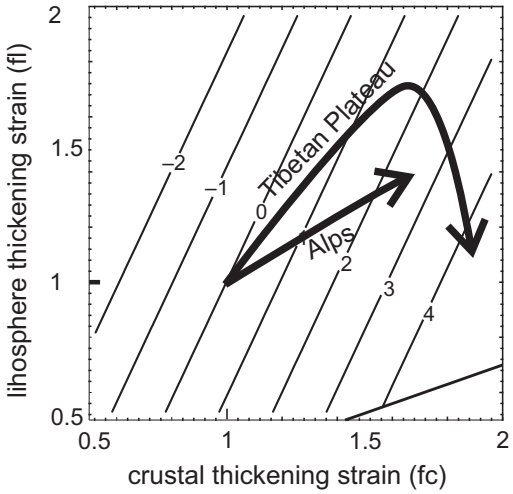

Figure 35: Isostatically supported surface elevation of mountain belts in the f_c-f_l-plane (in km with eq. 78). Following assumptions were used: $\rho_m = 3\,200$, $\rho_c = 2\,750$, $\alpha = 3 \cdot 10^{-5}$, $z_c = 35$ km, $z_l = 100$ km. Using these values, the two constants are: $\delta \approx 0.14$ and $\xi = 0.018$. Typical orogenic evolutions are superposed.

In most geological problems it is much more interesting to know the elevation of a mountain belt above its surroundings, rather than above the mid-oceanic ridges. For this purpose, it is useful to reformulate eq. 74, so that the elevation is given as the elevation difference between a thickened (or thinned) lithosphere and an undeformed reference lithosphere:

$$H = (\delta f_c z_c - \xi f_l z_l) - (\delta z_c - \xi z_l) = \delta z_c (f_c - 1) - \xi z_l (f_l - 1) \quad . \tag{78}$$

The parameters f_c and f_l describe the thickening strains of the crust and the mantle lithosphere. The elevation of isostatically supported mountain belts above the undeformed reference lithosphere is shown in Fig. 35 (for the concept of an undeformed reference lithosphere see: Le Pichon et al. 1982). More detailed assumptions about the thermal

expansion have no influence on the surface elevation (e. g. Zhou and Sandiford 1992). Fig. 35 shows clearly that homogeneous thickening of the entire lithosphere (a diagonal line from bottom left to top right in this diagram) causes relatively small changes of the surface elevation, because the two contributions in eq. 76 and eq. 78 have opposite signs. Accordingly, the negative buoyancy caused by the thickening of the mantle part of the lithosphere is largely compensated by the positive buoyancy of the thickened crust. It may also be read from this figures, that doubling of the crust, without thickening of the lithosphere would imply an isostatic uplift of about 3–4 km.

8 Unit: The Depth of the Oceans

The water depth of the oceans In isostatic equilibrium) is a direct function of the distance to the mid-oceanic ridges. The functional relationship between water depth and distance from the mid-oceanic ridge was described with a fantastically simple model by Parsons and Sclater (1977). Their model is one of *the* largest successes of the theory of heat conduction and we have discussed it already in unit 3.

Oceanic lithosphere consists (except for a thin 7 km thick crust) largely of asthenosphere material that has cooled to form lithospheric mantle. Because of the small and constant thickness of the crust, material contributions to density variations may be neglected and thermal expansion (contraction) is the governing factor for variations in the density structure. In order to use this density variation to estimate the isostatically supported elevation of the ocean floor, we use the model sketched in Fig. 36. According to eq. 66 the vertical normal stresses of the columns A and B must be the same in the compensation depth $z = z_\mathrm{l}$. For column A the vertical normal stress at depth $z = z_\mathrm{l}$ is given by:

$$\sigma^\mathrm{A}_{zz}|_{z=z_\mathrm{l}} = \rho_\mathrm{w} g w + \int_0^{z_\mathrm{l}} \rho_{(z)} g \mathrm{d}z \quad . \tag{79}$$

There, w is the water depth in column A, ρ_w is the water density, g is the gravitational acceleration and $\rho_{(z)}$ is the density of the lithosphere as a function of depth. For column B we can formulate:

$$\sigma^\mathrm{B}_{zz}|_{z=z_\mathrm{l}} = \rho_\mathrm{w} g w + \rho_\mathrm{m} g z_\mathrm{l} \quad . \tag{80}$$

(see Fig. 36). After inserting eqs. 79 and 80 into eq. 66, the isostasy condition of gets the following form:

$$\rho_\mathrm{m} z_\mathrm{l} + w(\rho_\mathrm{m} - \rho_\mathrm{w}) = \int_0^{z_\mathrm{l}} \rho_{(z)} \mathrm{d}z \quad . \tag{81}$$

With foresight to the following steps, we bring the first term of this equation to the right hand side, find its derivative with respect to z and write it therefore into the integral. Eq. 81 gets the form:

$$w(\rho_\mathrm{m} - \rho_\mathrm{w}) = \int_0^{z_\mathrm{l}} (\rho_{(z)} - \rho_\mathrm{m}) \mathrm{d}z \quad . \tag{82}$$

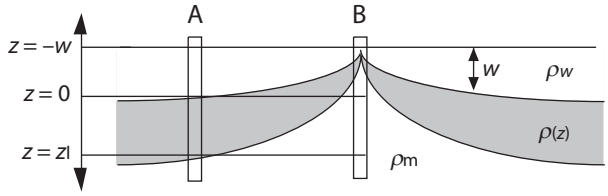

Figure 36: Schematic profile through a mid-oceanic ridge and the oceanic lithosphere as used for the calculation of water depth. The oceanic crust is neglected because it is everywhere of the same thickness.

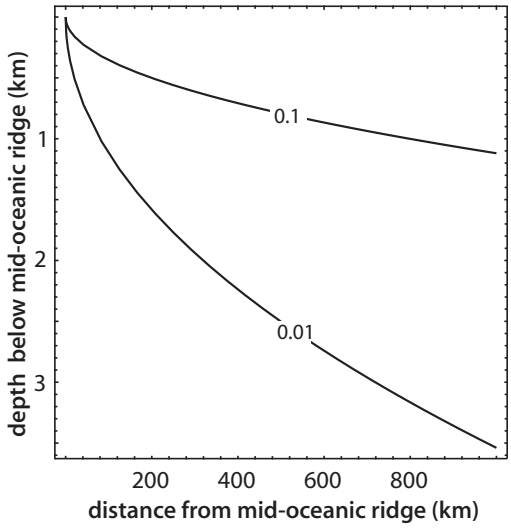

Figure 37: Profiles of water depth as a function of distance from the mid-oceanic ridge as calculated with eq. 86. The curves are shown for different rifting rates in $\mathrm{m\,y^{-1}}$. Following constants were used: $\rho_\mathrm{m} = 3\,200\ \mathrm{kg\,m^{-3}}$, $\rho_\mathrm{w} = 1\,000\ \mathrm{kg\,m^{-3}}$, $\alpha = 3 \cdot 10^{-5}\ \mathrm{K^{-1}}$, $T_\mathrm{l} = 1\,280\,^\circ\mathrm{C}$, $T_\mathrm{s} = 0\,^\circ\mathrm{C}$ and $\kappa = 10^{-6}\mathrm{m^2 s^{-1}}$

This equations states that the water depth is dependent on the density structure as a function of depth $\rho_{(z)}$. In oceanic lithosphere this density function is a direct function of the temperature profile. Thus, if we know the temperature as a function of depth, then $\rho_{(z)}$ in eq. 82 is known, because we know already the relationship between density and temperature from eq. 70. Thus we can begin by inserting eq. 70 into eq. 82:

$$w(\rho_\mathrm{m} - \rho_\mathrm{w}) = \int_0^{z_\mathrm{l}} \rho_\mathrm{m}\alpha(T_\mathrm{l} - T(z))\mathrm{d}z \quad . \tag{83}$$

The variable $T(z)$ is the only unknown in this equation, but it is well-described by the half-space cooling model and we determined it in sect. 3.2. . Thus, the temperature profile of eq. 34 may be directly inserted into eq. 83. We get:

$$w(\rho_\mathrm{m} - \rho_\mathrm{w}) = \int_0^{z_\mathrm{l}} \rho_\mathrm{m}\alpha(T_\mathrm{l} - T_\mathrm{s})\mathrm{erfc}\left(\frac{z}{\sqrt{4\kappa t}}\right)\mathrm{d}z \tag{84}$$

or, after taking the constants out of the integral and solving for w:

$$w = \frac{\rho_\mathrm{m}\alpha(T_\mathrm{l} - T_\mathrm{s})}{(\rho_\mathrm{m} - \rho_\mathrm{w})} \int_0^{z_\mathrm{l}} \mathrm{erfc}\left(\frac{z}{\sqrt{4\kappa t}}\right)\mathrm{d}z \quad . \tag{85}$$

This is not too difficult to solve and results in:

$$w = \frac{2\rho_\mathrm{m}\alpha(T_\mathrm{l} - T_\mathrm{s})}{(\rho_\mathrm{m} - \rho_\mathrm{w})}\sqrt{\frac{\kappa t}{\pi}} \quad . \tag{86}$$

If we insert standard values for all the constants in this equation we get:

$$w \approx 5.91 \cdot 10^{-5}\sqrt{t} \quad . \tag{87}$$

In words, the depth of the water is proportional to the square root of age of the oceanic lithosphere. Note that this water depth is only the *additional* water depth on top of the water depth *at* the mid-oceanic ridge (Fig. 36). We can convert this into water depth as a function of distance from the mid-oceanic ridge if we substitute age by the ratio of distance to rifting rate: x/u, (which is also age). Fig. 37 shows some water depth profiles calculated with this equation. The fantastic coincidence of these curves with bathymetric measurements in the oceans of the world confirm the model.

8.1 Flexural Isostasy

Most topographic features of our planet that are less than many hundreds of kilometers across are *not* completely in hydrostatic isostatic equilibrium. This includes whole mountain ranges like the European Alps (Karner and Watts 1983; Lyon-Caen and Molnar 1989) and can be measured gravimetrically: Gravimetry measures mass and in isostatic disequilibrium the total mass above the isostatic compensation depth is not everywhere the same. Thus, gravity anomalies may be interpreted in terms of the degree of isostatic disequilibrium. Isostatic disequilibria may form in response to a large range of processes. For example, a continental plate may be *actively* pushed downwards by the load of another plate, or it may be *actively* held up by mantle convection exerting an upwards force to the bottom of a plate. Topographic features that are created by non-isostatic processes are called: *dynamically supported*. Flexural isostasy is a stress balance that also considers *horizontal* elastic stresses (Fig. 31b). Flexural isostasy is therefore at least a *two-dimensional* stress balance. It may be used to interpret surface topography in terms of both, hydrostatic balance and elastic flexure.

8.1.1 Examples of Elastic Deformation

Although it may not be intuitive that rocks can be elastic, there are quite a few observations that show us that they are! For example, regular spacing between joints and other cracks is a function of the elastic behavior of rocks and the continuous versus discontinuous displacement across seismically active structures is an elastic deformation that can be measured even with GPS measurements. Elastic strains are of the order of about one per mil at the most.

• **Examples in oceanic lithosphere** Oceanic lithosphere is rheologically stronger than continental lithosphere and is therefore little internally deformed. It has a very uniform thickness and a largely flat surface. As a consequence, plate scale elastic features that develop in response to vertical loads may spectacularly be seen without much disturbance by features created by other deformation mechanisms. The best known example for elastic deformation of the oceanic lithosphere are the valleys around *sea mounts*, for example around the Hawaii-Emperor chain. They were created by *hot spots* that have their origin deep inside the mantle (Fig. 38). The volcano may be considered as an external load to a plate of more or less constant thickness that bends it downwards. Another example of elastic deformation of oceanic lithosphere is the bending of the plates at subduction zones. The shape of trenches and the fore bulge on the seaward side of the trench are also the consequence of elastic bending of the plate.

• **Examples in continental lithosphere** The elastic bending of *continental* plates may be observed in the foreland of many collisional orogens, where molasse basins form as the consequence of the elastic deflection of the plate in response to the load of the mountain belt. One of the best know examples is the northern molasse of the European Alps. There, the European Plate is bent downwards under the load of the alpine mountain chain. The deepest point of the deflection is the valley of the river Donau. However, in collisional orogens the *external* load applied by the weight of the mountain belt is partly compensated by an *internal* loads: the root of the mountain belt.

Passive continental margins also show often evidence for elastic bending of continental lithosphere (Fig. 42). The best known examples for this are the great escarpments along

the coasts of southern Africa and Australia (Tucker and Slingerland 1994; Kooi and Beaumont 1994). There, the unloading of the plate that is caused by the asymmetric erosion of the continental margin is compensated by elastic updoming of the coastal foreland. The Australian Great Barrier Reef, for example, may be interpreted as an elastic fore bulge similar to those observed in the vicinity of subduction zones (Stüwe 1991).

8.1.2 The Flexure Equation

Elastic deformation describes an empirically derived *constitutive relationship* in which stress and strain are proportional to each other. The proportionality constant between stress and strain is called the modulus of elasticity or *Young's modulus* E. How much a plate bends under an applied stress depends on E and its compressibility, which is described by the *Poisson ratio* ν.

Let us now consider the bending of a simple, ideal elastic plate like the one sketched in Fig. 39. We also neglect buoyancy forces for now. When integrating the horizontal normal stresses σ_{xx}, over the thickness of the elastic plate h, then it may be shown (or even intuitively seen) that the bending moment M is proportional to the curvature of the plate (s. Fig. 39):

$$M = -D\frac{\mathrm{d}^2 w}{\mathrm{d}x^2} \quad . \tag{88}$$

In this equation, w is the vertical deflection of the plate and the constant of proportionality D is called the *flexural rigidity* of the plate. The bending moment M is the integrated torques on both sides of the load.

Eq. 88 may be coupled with a force balance equation that relates bending moments, the vertical load q, any applied horizontal forces F and the shear forces (s. Fig. 39) to each other (s. Turcotte and Schubert 1982; Ranalli 1987). This is called the one-dimensional flexure equation and is:

$$D\frac{\mathrm{d}^4 w}{\mathrm{d}x^4} = q_x - F\frac{\mathrm{d}^2 w}{\mathrm{d}x^2} \quad . \tag{89}$$

There, q_x is the vertical load as a function of horizontal distance x and has the units of force per area: stress. Thus, if the distribution of loads is known, this equation may be

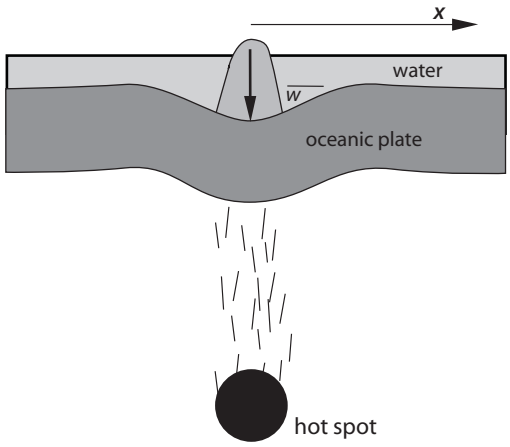

Figure 38: Flexure of oceanic lithosphere due to the loading of a sea mount.

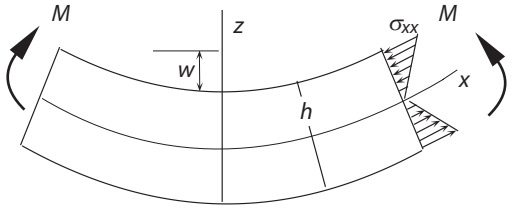

Figure 39: Bending of an ideal elastic plate in a simplified model view which is useful for the description of bending lithospheric plates.

solved for either the deflection of the plate w or for its flexural rigidity D (in N $\times$ m). Usually, the deflection is well known from bathymetric or topographic observation and eq. 89 is used to derive the rigidity or "stiffness" of the plate. This flexural rigidity is a direct function of the elastic material properties of an ideal elastic plate of thickness h and is related to these by:

$$D = \frac{Eh^3}{12(1-\nu^2)} \quad . \tag{90}$$

Thus, if the material constants E and ν are known and the flexural rigidity of a plate was derived from modeling its shape using eq. 89, then this may be converted directly into an elastic thickness of the lithosphere using eq. 90. All descriptions of the bending of elastic plates are based on the integration of eq. 89, or its two-dimensional equivalent.

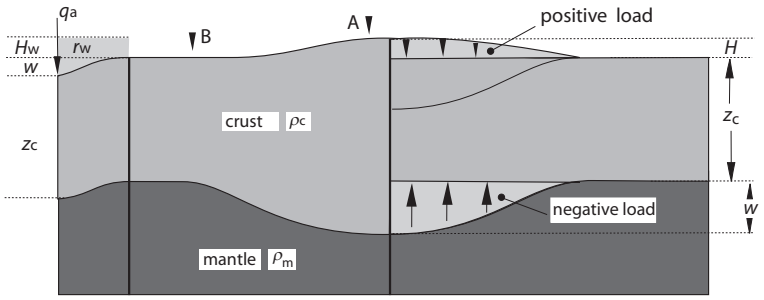

Figure 40: Distribution of loads during the elastic bending of lithospheric plates.

8.1.3 Application to the Lithosphere

Eq. 89 may be directly applied to describe flexural isostatic equilibrium, i.e. the elastic bending of lithospheric plates under external and internal loads. When we do this, we need to be aware of some important points:

1. The flexural rigidity D must be interpreted correctly. Field observations tell us that the rigidity of lithospheric plates is of the order of $D \approx 10^{23}$ Nm ($\pm$ about one order of magnitude) and laboratory experiments show that the material constants are about $E \approx 10^{11}$ Pa and $\nu \approx 0.25$. According to eq. 90 these parameters imply that the elastic thickness of the lithosphere h is only some tens of kilometers. Thus, the elastic thickness of the lithosphere is much thinner than the lithosphere according to thermal or mechanical definitions. The elastic thickness must be considered as the theoretical thickness of a plate with homogeneous elastic properties. Considering that the brittle strength of the upper crust as well as the ductile strength of the lower most lithosphere are likely to be very small, it is only the central part of the lithosphere that is dominated by elastic behavior.

2. The distribution of loads on the plate must be thought through. The load as a function of distance q_x as used in eq. 89 is the sum of a series of *internal* and *external* loads that act upwards and downwards onto a plate. In order to clarify *which* different forces act on the plate, it is useful to divide the plate under consideration according to the scheme illustrated in the right hand part of Fig. 40. There, it may be seen that the downward force exerted by the mountain range on the plate is given by the vertical normal stress $q_{\rm ext} = \rho_{\rm c} g H$. This is the *external* or the *positive* load. This load is opposed by a buoyancy force in the region of the displaced mantle. This is the *internal* or *negative* load shown on Fig. 40 with the upwards arrows. This internal load has the magnitude $q_{\rm int} = (\rho_{\rm m} - \rho_{\rm c}) g w$, where w is the deflection of the plate. The net load that is applied to the plate is therefore:

$$q(x) = q_{\rm ext} - q_{\rm int} = \rho_{\rm c} g H(x) - (\rho_{\rm m} - \rho_{\rm c}) g w \quad . \tag{91}$$

Note that the load is here already expressed as a function of horizontal distance x. If eq. 91 is inserted into eq. 89, this may be solved for w numerically or – for some simple boundary conditions - also analytically.

8.1.4 Applications to the Oceanic Lithosphere

A series of elastic bending problem in the oceanic lithosphere may be well-described with eq. 89 if two simplifying assumptions are made:

– 1. We assume that there are no horizontal forces applied to the plate. Then, the entire last term of eq. 89 is zero.

– 2. We assume that the vertical load is only applied at a single location at the end of the plate; i.e. there is no dependence of the load on x.

Based on the second assumption, and assuming that the downwards deflected region is filled with water, eq. 91 simplifies to:

$$q = q_{\rm a} - (\rho_{\rm m} - \rho_{\rm w}) g w \quad . \tag{92}$$

as illustrated on the very left hand edge of Fig. 40 ($\rho_{\rm w}$ is the water density). Eq. 89 simplifies to:

$$D \frac{{\rm d}^4 w}{{\rm d}x^4} = -(\rho_{\rm m} - \rho_{\rm w}) g w \quad . \tag{93}$$

Eq. 93 describes a range of geological features surprisingly well and has the great advantage that it may be integrated analytically for a range of geologically relevant boundary conditions. After integration, the constants D, g, $\rho_{\rm m}$ and $\rho_{\rm c}$ often occur in the following relationship:

$$\alpha = \left(\frac{4D}{g(\rho_{\rm m} - \rho_{\rm w})} \right)^{1/4} \quad . \tag{94}$$

α is called the *flexure parameter* of the lithosphere.

• **Seamount chains** The first example we want to discuss is that of a line-shaped load of islands on a continuous plate of constant thickness. For appropriately formulated boundary and initial conditions (e.g. the load applies only at $x = 0$, symmetry of the deflection so that $\mathrm{d}w/\mathrm{d}x{=}0$ at $x = 0$ and others) a solution of eq. 93 is:

$$w = w_0 \mathrm{e}^{-x/\alpha} \left(\cos(x/\alpha) + \sin(x/\alpha)\right) \quad . \tag{95}$$

There, w_0 is the maximum deflection of the plate directly underneath the load and w is normalized to this value (we can see from eq. 95 that $w \to w_0$ for $x \to 0$). Interestingly, the maximum deflection w_0 is given by:

$$w_0 = \frac{q\alpha^3}{8D} \quad . \tag{96}$$

Eq. 95 is a good approximation for the description of the water depth around the Hawaii and Emperor Island chains (s. Fig. 41a). The equation is also historically important, as is was one of the first models used to estimate the elastic thickness of the lithosphere using the bathymetric surveys around Hawaii.

• **Trench morphology** The second example that may be described with the approximation of eq. 93 is the shape of oceanic lithosphere near trenches. There, the loading of the subducting oceanic plate may be viewed as a line-loading by the margin of the upper plate. For this case, boundary conditions must be assumed that describe a broken half plate which is subjected to a load at its end. For appropriately formulated boundary conditions a solution of eq. 93 is:

$$w = w_0 \mathrm{e}^{-x/\alpha} \left(\cos(x/\alpha)\right) \quad . \tag{97}$$

The shape of plates as described by eq. 97 is illustrated in Fig. 41b. Note how similar this solution is to eq. 60: They both describe sine-functions that decay exponentially with

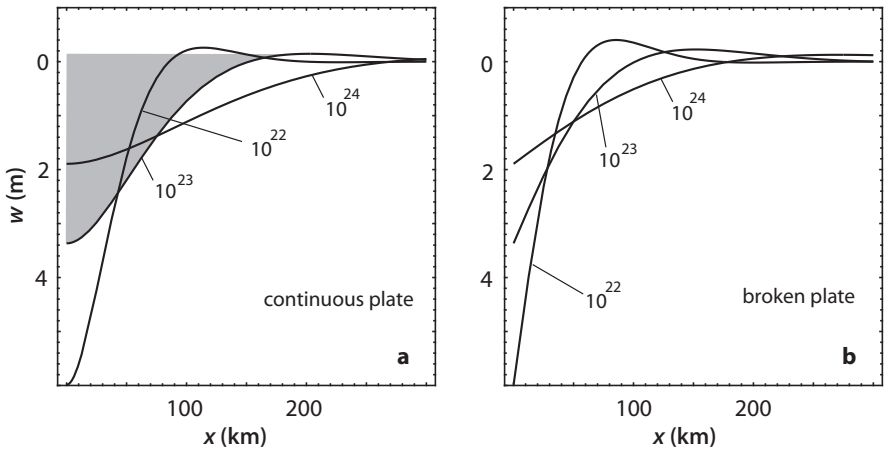

Figure 41: Shape of elastically bent plates. **a** Continuous plate loaded only at $x = 0$: the left margin of the diagram (eq. 95). Only half of the plate is shown. **b** Broken plate, also loaded only at $x = 0$ (eq. 97). The curves are labeled with the flexural rigidity of the plates in Nm.

distance. A comparison of the curves shown on Fig. 41b with bathymetric measurements shows that most subduction zones are steeper near the trench than what is described by the curves at the left margin of Fig. 41b. It is interpreted that this indicates that subducted plates are not only loaded by the upper plate but that convection in the mantle wedge and other forces exert a additional torques on subducting plates.

8.1.5 Applications to the Continental Lithosphere

Continental lithosphere deforms internally much easier than oceanic lithosphere by pervasive ductile mechanisms. Thus, elastic features are often not so clearly exposed and loads of mountain ranges and the like are distributed over large parts of the plates. Nevertheless, it should be said that the load of long mountain chains on homogeneous continental plates is analogous to the problem of long island chains on oceanic lithosphere. Thus, eq. 95 can – in principle – also be used to describe foreland basins, but care must be taken by accounting for sedimentary fill of foreland basins, compensating crustal roots etc (s. Turcotte and Schubert 1982). For example, ρ_w must be replaced by ρ_c in the formulation of the flexural parameter (s. eq. 91). The topography of *passive continental margins* is probably the example in the continental lithosphere that is most obviously described by elastic flexure (Fig. 42).

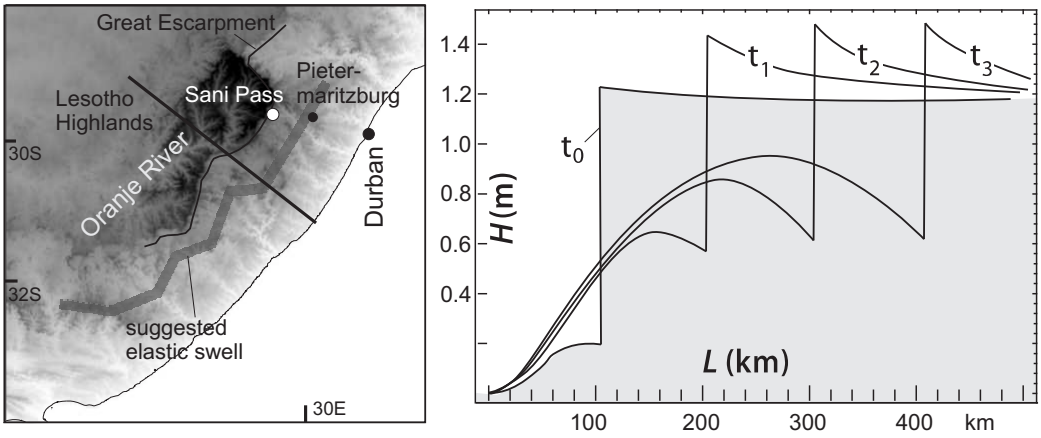

Figure 42: Elastic flexure at passive continental margins. The map shows the Great Escarpment of southern Africa. The model at right is a cross section through an idealized passive margin showing surface elevation H as a function of distance from the continental shelf L at four different time steps.

9 Unit: Deformation Mechanisms

For a mechanical description of deformation we need a mathematical rule that relates stress (or force) to strain (or strain rate). Such a relationship is called a *flow law*, *deformation law* or *deformation mechanism*. In order to understand these fully, it is mandatory to understand the basic principles of the stress tensor. That is, the meaning (and the differences) of terms like *normal stress*, *shear stress*, *deviatoric stress*, *pressure*, *differential stress* or *mean stress*. These definitions are repeated in Unit 13. If you do not know what the differences between these terms are it is recommended that you read up on them before proceeding.

On a microscopic scale, structural geologists discriminate between a large number of deformation laws. However, on geological time scales and lithospheric length scales, most geologists use only one of five terms to describe deformation mechanisms:

– brittle deformation

– plastic deformation

– ductile deformation

– elastic deformation

– viscous deformation.

These five terms have very different meanings and some of them are very rigorously defined and others are not. We will deal with these five terms at length over the next sections (s. also: Weijermars 1997; Twiss and Moores 1992; Jaeger and Cook 1979). Here we summarize some of the most important information on these five terms and how they relate stress to strain in general terms.

• *Brittle deformation* is no really a deformation mechanism at all. We will see below that the laws of brittle deformation only describe a stress state and not a relationship between stress and strain. The deformation law usually used to describe rocks in a brittle fashion is plastic deformation.

• *Plastic deformation* law states that a constant stress is required to deform the rock. Irregardless how much or how fast we deform, the required force is all the same. Deforming sand is a good example.

• *Ductile deformation* is a wonderful term that has no specified meaning other than that we want to say that the deformation is not elastic and not brittle. It is therefore an extremely useful term if you are a field geologist and do not want to commit yourself to any of the well-defined terms like “viscous”, “plastic” or “dislocation creep” - all of which have very rigorously defined meanings.

• *Elastic deformation* is the law that states that the *strain* of a rock is proportional to the applied *total stress*. As such, it is the only deformation mechanism which is not permanent: As soon as the stress is released, the strain is gone as well.

• *Viscous deformation* is the law that is most commonly used to describe ductile deformation on the crustal scale. Viscous means that the strain *rate* of a rock is proportional to the applied *deviatoric stress*.

We all have every day encounters with elastic and viscous deformation mechanisms, namely with rubber bands (elastic) and mixing cake dough (viscous). When stretching a rubber band, the amount of stretch depends on how hard we pull. The more pull, the more stretch. The applied stress and the resulting strain are proportional. On the other

hand it does not matter at all whether we pull fast or slow. The stretch is always the same for the same applied force, independent on the speed (strain rate) with which we do the experiment. With mixing dough its exactly opposite: It does not matter at all whether we mix it only a bit or very thoroughly (little or much strain in the dough), the needed force is always the same. However, how much force we need depends very strongly on the mixing rate. If we mix it rapidly, we need much more force than if we mix slowly.

9.0.6 Elastic Deformation

Elastic deformation is characterized by a proportionality between stress and strain. Both these parameters are described by tensors which each include 6 independent values. However, if this proportionality is ideally linear, and we only consider uniaxial (one-dimensional) loading then this relationship is called *Hooke's law* and may be simply written as:

$$\sigma_{xx} = E\epsilon_{xx} \tag{98}$$

where the subscripts emphasize that this equation is meant to be one dimensional (and not a full tensor equation). When the deformation is uni-axial, then ϵ is the (dimensionless) longitudinal normal strain and is defined as the change in length during deformation relative to the original length. The proportionality constant E is called the *Young's modulus* and has the units of stress ($\mathrm{N\,m^{-2}}$). For rocks, the Young's modulus is of the order of 10^{10} to 10^{11} Pa. Young's modulus is a kind of a summary of the Lame elastic constants which are the elastic coefficients that occur when eq. 98 is written as a full tensor equation.

If more than one of the three principal stresses is larger than zero, then it is also important to consider that rocks are compressible. This is described by the Poisson constant ν. For the largest principal stress we can write:

$$\sigma_1 = \epsilon_1 E + \nu\sigma_2 + \nu\sigma_3 \tag{99}$$

or, if strain is written as a function of stress:

$$\epsilon_1 = \frac{1}{E}\sigma_1 - \frac{\nu}{E}\sigma_2 - \frac{\nu}{E}\sigma_3 \quad . \tag{100}$$

For the other two spatial directions equivalent equations may be formulated. The Poisson constant is given by the ratio of two stretches, namely the infinitesimal strain normal to the applied stress and the stretch *in* direction of the applied stress.

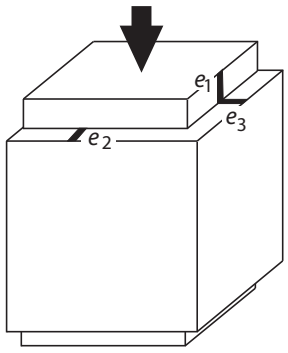

Figure 43: Stretch of a cube as the consequence of compression in the vertical direction. The Poisson constant is defined as $\nu = -e_3/e_1$.

During compressive deformation, a rock will shorten in the direction of the applied stress. Thus, the incremental stretch e_1 in Fig. 43 is negative. If the rock is isotropic, then this shortening is distributed evenly between expansion in the other two spatial directions. Thus, $\nu = +0.5$ for incompressible materials. For example, rubber is almost incompressible and has a Poisson constant of almost $\nu = +0.5$. In contrast, the Poisson constant of rocks is of the order of 0.1–0.3. We can see that rocks are quite compressible in the elastic regime. However, the total strains of rocks in the elastic regime are quite small, because the Young's modulus of rocks is very large. Thus it is no obvious to us that rocks are actually quite compressible.

9.0.7 Brittle Fracture

When the stresses applied to rocks cannot be compensated elastically, permanent deformation will occur. This may occur by ductile or brittle processes. Among brittle processes, two different modes of brittle deformation may be discerned: rocks deform either by creating new cracks, or by friction along existing fractures. In both cases the friction along the failure planes plays a critical role. Brittle failure is commonly described with the *Mohr-Coulomb-criterion*. However, it should be said here that – strictly speaking – the Mohr-Coulomb-criterion describes only a state of stress, namely the critical state at which failure occurs. It does not place stress and strain in a relationship to each other and is therefore not a constitutive relationship or flow law.

• **Mohr-Coulomb-criterion** Coulomb (1773) was the first to recognize that the brittle strength of materials is largely a linear function of the applied normal stress $\sigma_{\rm n}$ and that it depends only to the second order on a material constant called cohesion σ_0. At geological stresses cohesion is largely negligible. According to the Coulomb criterion, failure occurs when the shear stress on a given plane reaches a critical value $\sigma_{\rm s}^{\rm c}$ that is a function of the normal stress acting on that plane σ_n, as:

$$\sigma_{\rm s}^{\rm c} = \sigma_0 + \mu\sigma_{\rm n} \quad . \tag{101}$$

The coefficient μ that relates shear stress and normal stress on a failure plane is called the *internal coefficient of friction*. This coefficient is dimensionless. In the literature, the critical failure stress is often abbreviated with τ. However, it is probably clearer if we reserve τ exclusively for deviatoric stresses and we therefore choose a different notation in this edition: We use the subscript $_{\rm s}$ for all shear stresses (for both stress: $\sigma_{\rm s}$ and deviatoric shear stress: $\tau_{\rm s}$) and apply additional superscripts if necessary. According to the Coulomb criterion (eq. 101) brittle deformation is a nearly linear function of total stress. It is independent of temperature or strain rate $\dot{\epsilon}$ and almost independent of the material as the cohesion is almost negligible and the internal coefficients of friction are very similar for most rocks (Byerlee's law).

Mohr (1900) then discovered that the failure criterion of Coulomb may be elegantly portrayed graphically. His graphical analysis is called the Mohr diagram. In the Mohr diagram shear stresses are plotted against normal stresses and the stress state in a rock is plotted as a circle (Fig. 44. From this figure we can see that $\sigma_{\rm s}$ is the largest on planes that lie at an angle of 45° to the principal stress direction (i.e. $2\theta = 90°$ and $\sin(2\theta) = 1$):

$$\sigma_{\rm s}^{\rm max} = \frac{\sigma_1 - \sigma_3}{2} \quad . \tag{102}$$

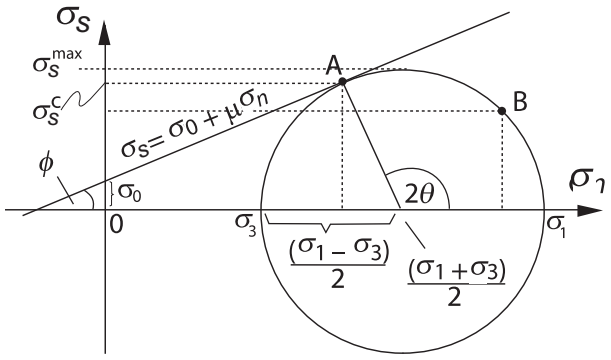

Figure 44: The relationship between normal stress (horizontal axis) and shear stress (vertical axis) in the Mohr circle. The normal stresses are compressive (positive) to the right of the origin and tensional (negative) to the left. Eq. 101 describes the tangent to the Mohr circles drawn around centers at $(\sigma_1 + \sigma_3)/2$ with the radius $(\sigma_1 - \sigma_3)/2$. In the ductile regime shear stresses do not increase linearly with normal stresses anymore. However, for many rocks the curve is even in the brittle regime not completely linear, but slightly concave against the normal stress axis. For failure planes in a rock it is true that: $\sigma_s^{\rm c} = \sin 2\theta(\sigma_1 - \sigma_3)/2$ and $\sigma_{\rm n} = (\sigma_1 + \sigma_3)/2 - \cos(2\theta)(\sigma_1 - \sigma_3)/2$.

Thus, the maximum shear stress a rock can support is half as large as the applied differential stress. However, it is important to note that the *largest* shear stress is *not* where failure occurs. From Fig. 44 we can see that the normal stress at $\sigma_{\rm s}^{\rm max}$ is just a little bit larger (it is: $\sigma_{\rm n} = -(\sigma_1 + \sigma_3)/2$ than the normal stress at the critical failure stress $\sigma_{\rm s}^{c}$ (at point A, for which the normal stress is explained in Figure caption Fig. 44.

The slope of the tangent to the Mohr circles in Fig. 44 is given by the internal *angle of friction*. This angle of friction ϕ and coefficient of friction μ are related by:

$$\tan\phi = \mu \quad . \tag{103}$$

For most rocks this angle is about 30–40°, which is equivalent to an internal coefficient of friction between roughly 0.6 and 0.85. This relationship is called Byerlee's law as he was the first to measure μ on a crustal scale and derived ϕ from μ.

• **Byerlee's and Amonton's laws** If preexisting cracks occur in a rock then there is no cohesion. To be more precise: the remaining cohesion is negligible compared to the cohesion of an intact rock. The shear stresses needed to deform a rock only need to overcome the coefficient of friction and the normal stresses applied to the rock. Eq. 101 simplifies to:

$$\sigma_{\rm s}^{\rm c} = \mu\sigma_{\rm n} \quad . \tag{104}$$

This equation is usually called *Amonton's law*. Byerlee (1968; 1970) showed empirically that, at pressures below 200 MPa, (roughly less than 8 km) the crust may be characterized by an internal coefficient of friction around 0.85:

$$\sigma_{\rm s}^{\rm c} = 0.85\sigma_{\rm n} \quad . \tag{105}$$

However, depending on rocks deforming brittle in compression, extension, or under a strike slip regime, the best coefficient of fricition may change (Fig. 45). At larger depths, but

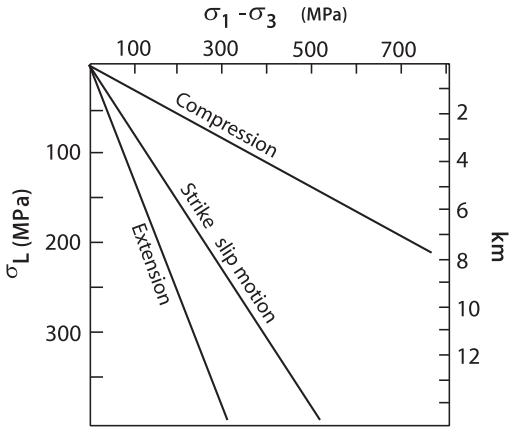

Figure 45: Brittle failure as a function of depth and normal stress or "lithostatic pressure".

above the brittle ductile transition brittle failure in the crust appears to be best described by:

$$\sigma_{\rm s}^{\rm c} = 60\,{\rm MPa} + 0.6\sigma_{\rm n} \quad . \tag{106}$$

These empirical relationships are called *Byerlee's laws* (Fig. 45). Because of the fact that $\mu \approx 0.85$, most faults occur at 30 degrees angle to the maximum principle stress. Byerlee's laws state that rocks at 5 km depth will fail at roughly 110 MPa, in 10 km depth at roughly 230 MPa and in 15 km depth at about 300 MPa.

9.0.8 Viscous Deformation

On the scale of a thin section, rocks behave not viscously but according to a large range of deformation mechanisms (e.g. grain boundary migration, diffusion creep and many others). The dependence of deformation mechanism on the physical conditions may be portrayed in *deformation mechanism maps* (Frost and Ashby 1982). In such maps parameters like temperature, grain size, stress and viscosity are plotted against each other and the diagrams a divided into different fields where different mechanisms apply. However, on a larger scale, it is useful to average different deformation mechanisms and assume that rocks behave like viscous fluids. Viscous deformation of ideal fluids is described by a proportionality between deviatoric stress and strain rate. If we make a simple shear experiment in which we compare the scalar quantities of the shear strain rate $\dot{\gamma}$ and the shear force (per area) we require to shear it τ_s, then we can write:

$$\tau_s = \eta\dot{\gamma} \quad . \tag{107}$$

If we use the full deviatoric stress tensor τ and the full strain rate tensor $\dot{\epsilon}$, then this is given by:

$$\tau = 2\eta\dot{\epsilon} \quad . \tag{108}$$

where the factor 2 arises from the definition of strain rate (see Unit 13). Both equations are used in the literature (Ranalli 1987). In both the proportionality constant η is called the *dynamic viscosity*. There is also a parameter called the *kinematic viscosity* which is the ratio of dynamic viscosity and density and has the units of diffusivity, namely: $\mathrm{m}^2\,\mathrm{s}^{-1}$. The dynamic viscosity has the units of Pascal times second (Pa s) or $\mathrm{kg\,m}^{-1}\,\mathrm{s}^{-1}$. For air

it is roughly 10^{-5} Pa s, the viscosity of water is roughly 10^{-3} Pa s, the viscosity of ice roughly 10^{10} Pa s, of salt 10^{17} Pa s and of granite it is roughly 10^{20} Pa s. If η is constant with respect to strain rate then eq. 108 is linear. A fluid that behaves according to such a linear relationship is called a *Newtonian fluid*. Eq. 108 states that the larger the deviatoric stress that is applied, the faster the rock will deform. Note that, in the orientation of the *maximum* shear strain rate, the stress in eq. 108 will be $\tau_{\max}$, which is equivalent to half of the differential stress $\sigma_{\mathrm{d}}/2 = (\sigma_1 - \sigma_3)/2$, (s. eq. 102). There are two reasons why rocks typically don't deform according to the simple form of eq. 107 with a constant viscosity:

• **1. The Arrhenius relationship** Viscosity is extremely strongly temperature dependent. This temperature dependence is described by the *Arrhenius relationship*:

$$\eta = A_0 \mathrm{e}^{Q/RT} \quad . \tag{109}$$

In this relationship the constants A_0 and Q are material-specific constants called the *pre exponent constant* and the *activation energy* (in J mol^{-1}), respectively. The parameter R is the universal gas constant and T is the absolute temperature. If we try to read eq. 109 we can see that it states that the viscosity of any material will trend towards infinity at absolute zero and will decrease exponentially from there to approach the value A_0 asymptotically at high temperatures. (Do not forget to always use absolute temperature when performing calculations with eq. 109).

• **2. Non linearity** Rocks rarely deform as a Newtonian fluid (i. e. there is rarely a linear relationship between the applied deviatoric stress and strain rate). In fact, many rocks deform roughly 8 times as rapid if the applied stress is doubled. More generally, this may be written in terms of a power law relationship:

$$\tau_s^n = A_{\mathrm{eff}} \dot{\gamma} \quad . \tag{110}$$

There, the exponent n is called the *power law exponent*. It is a material constant and is between 2 and 4 for many rock types. The parameter A_{eff} is a material constant. It is analogous to η in eq. 108, but does not have the units of viscosity and we therefore use a different symbol. A_{eff} has the units Pa^n s. However, in analogy to a Newtonian fluid, it is possible to derive an *effective viscosity* from eq. 110 which is given by the ratio of deviatoric stress and strain rate. This is:

$$\eta_{\mathrm{eff}} = \frac{\tau_s}{\dot{\gamma}} = A_{\mathrm{eff}}^{1/n} \times \dot{\gamma}^{(1/n)-1} \quad . \tag{111}$$

• **General viscous flow law for the lithosphere** If we want to apply a non-linear viscous relationship like eq. 110 to rocks, it is useful to couple it with the Arrhenius relationship. However, because of the parameter A_{eff} does not really have the units of viscosity, and because experiments are typically not performed as shear experiments (where $\dot{\gamma}$ is measured), viscous flow laws are usually formulated somewhat differently. Typically, they are formulated as a relationship between differential stress $(\sigma_1 - \sigma_3)$ and longitudinal strain rate $\dot{\epsilon}_l$, as it is measured in uniaxial shortening experiments. Such an empirical relationship is called *Dorn's law* and is typically written as:

$$(\sigma_1 - \sigma_3) = \left(\frac{\dot{\epsilon}_l}{A}\right)^{(1/n)} \mathrm{e}^{\left(\frac{Q}{nRT}\right)} \qquad \text{or :} \qquad \dot{\epsilon}_l = \sigma_{\mathrm{d}}^n A \mathrm{e}^{-\frac{Q}{RT}}, \tag{112}$$

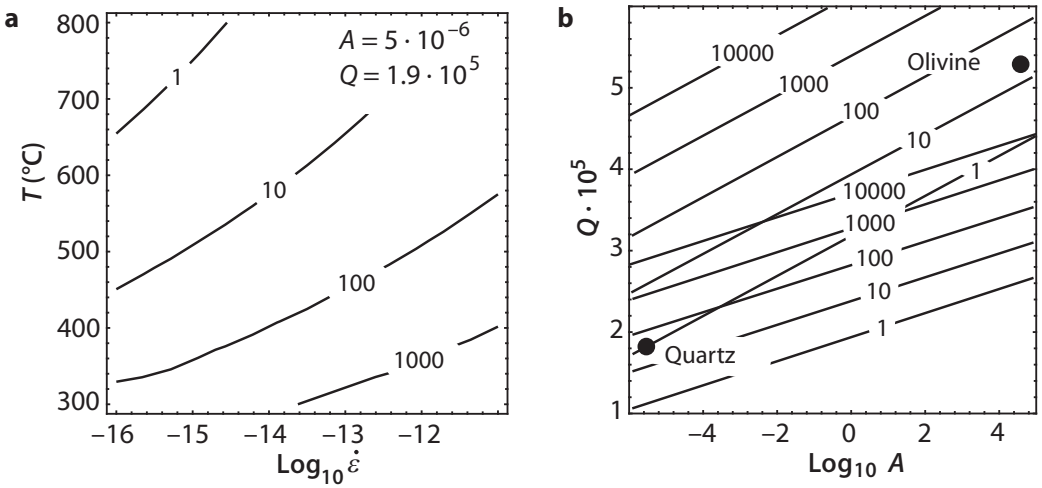

Figure 46: Differential stress (in MPa) during viscous deformation as a function of a range of parameters as calculated with eq. 112. A power law exponent of $n = 3$ was assumed. **a** Differential stress as a function of temperature and strain rate for the material constants of quartz. **b** Differential stress as a function of activation energy Q (in $\mathrm{J\,mol^{-1}}$) and pre exponential constant A (in $\mathrm{MPa^{-3}\,s^{-1}}$). *Continuous lines* are for 500 °C, *dashed lines* are for 1 000 °C. The assumed strain rate is $\dot{\epsilon} = 10^{-13}$ $\mathrm{s^{-1}}$. The rheological data for quartz and olivine from sect. 10.1.1 are plotted.

(e.g. Sonder and England 1989 or Houseman and England 1986). The three material constants A, Q and n are constrained by series of experiments performed at constant strain rate and temperature (e.g. Gleason and Tullis 1995). For exponents larger than 1, Dorn's law is also called simply *power law*. Note that the constant A has (in contrast to A_{eff}), the units of $\mathrm{Pa^{-n}\,s^{-1}}$ and incorporates the factor 2 we encountered in eq. 108. Also note again that – if you want to use eq. 112 to estimate the lithospheric strength or non lithostatic contributions to pressure – only half of the differential stress contributes to pressure.

For mechanical models in which temperature is not considered explicitly, it is useful to summarize the temperature dependent terms of eq. 112. Fig. 46a shows the differential stress as a function of temperature and strain rate for the material constants of quartz. Fig. 46b shows differential stress as a function of activation energy and pre exponent constant at fixed temperatures and strain rates.

Dorn's law is an empirical deformation law and in some cases it is necessary to modify it empirically. One example where this is necessary is the deformational behavior of olivine. Fig. 46b shows that olivine deforms at 500 °C (which may be a realistic assumption for the Moho-temperature) only at unrealistically high stresses around 10^7 MPa if it were described with eq. 112. Thus, Goetze (1978) and Goetze and Evans (1979) suggested that a better description of the behavior of olivine above 200 MPa is given by the relationship:

$$(\sigma_1 - \sigma_3) = \sigma_{\mathrm{D}} \left(1 - \sqrt{\frac{RT}{Q_{\mathrm{D}}} \ln \left(\frac{\dot{\epsilon_{\mathrm{D}}}}{\dot{\epsilon}_l} \right)} \right) \quad . \tag{113}$$

There, Q_{D} is again an activation energy, σ_{D} a critical stress that must be exceeded and $\dot{\epsilon_{\mathrm{D}}}$ is the critical strain rate (s. Table 5). Comparing eq. 113 with eq. 112 shows that this

Table 4: Dependence of brittle and viscous deformation on some physical parameters.

dependent on	**brittle**	**viscous**
total pressure (depth)	yes (linear)	no
material	no	yes ($\approx$ power of 3)
strain rate	no	yes
temperature	no	yes (exponential)

law is by far not as temperature dependent as the power law. Combinations of eqs. 112, 113 and Byerlee's laws form the basics of many simple quantitative models describing the rheology of the lithosphere as a whole (Brace and Kohlstedt 1980).

Eq. 112 shows that the stresses during viscous deformation are strongly dependent on *temperature*, *strain rate* and *material constants*, but are independent of the confining pressure. Thus, ductile deformation is subject to completely different laws than brittle deformation (Table 4).

10 Unit: Rheology and Force Balance of the Lithosphere

In the previous section we showed that the deformation of the lithoshere is predominantly controlled by brittle and viscous deformation, and that these two mechanisms depend on very different physical parameters (Table 4). In this unit we assemble this information to a rheological profile through the lithosphere and interpret such profiles.

10.1 Rheology of the Continental Lithosphere

In the late seventies of last century Brace, Goetze and others summarized much of the information from the previous sections to formulate a simple rheological model for the lithosphere. This rheological model is sketched in Fig. 47 and the following figures and will be the basis for our discussion. Note that in these strength profiles (e.g. Figs. 47, 48 and 49) differential stress rather than deviatoric stress is usually plotted on the horizontal axis, because σ_d is a single scalar value that may be used to characterize the stress state. It is important to note throughout this chapter that $\sigma_\mathrm{d}/2$ corresponds to the maximum deviatoric stress (s. discussion around eqs. 102 and 108 and Unit 13).

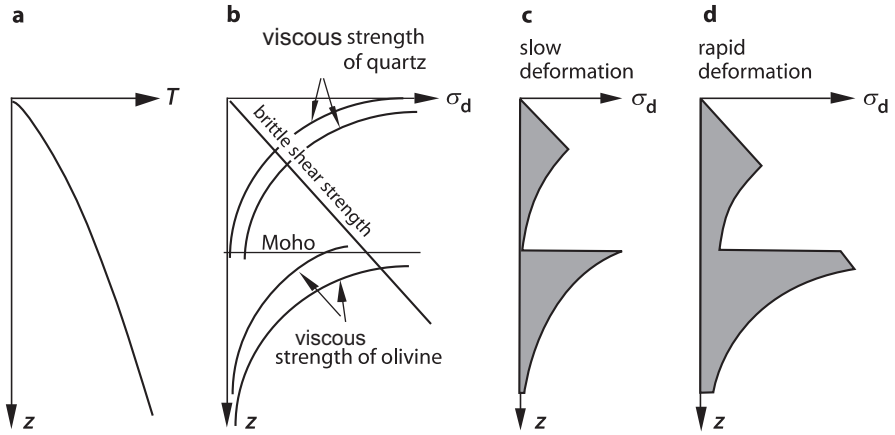

Figure 47: Schematic illustration of a *Brace-Goetze lithosphere*. The shaded area in **c** and **d** yield the vertically integrated strength. The units of this integrated strength are $\mathrm{N\,m^{-1}}$. This integrated strength may be interpreted as the force per meter length of orogen applied to the orogen in direction normal to the orogen (assuming the orogen is everywhere deforming).

The strength profiles in Fig. 47 consist of two different types of curves. The straight lines are for brittle fracture. They show increasing rock strength with increasing depth as the normal stresses in the crust increase with depth as shown in eq. 101 (Fig. 47b, s. sect. 9.0.7). The curved lines describe viscous deformation. The strength they describe decreases exponentially downwards, because temperature *increases* with depth roughly *linearly* (s. sect. 9.0.8) and viscosity for a given mineral decreases exponentially with temperature. Each curve is for a given strain rate that is assumed to be constant over the entire lithosphere. A higher strain rate will yield a curve that has a higher strength at a given depth. Fig. 47b shows that, for a given strain rate, two different failure strengths may be associated with each depth. A rock at a given depth will always deform according to the

deformation mechanism that requires *less* stress. Using this logic, we can draw strength profiles like those illustrated in Fig. 47c and 47d. The depth at which brittle strength and viscous strength have the same magnitude is called the *brittle-ductile transition*. Note that the depth of this transition is strain rate dependent in this model.

In first approximation it is fair to assume that a rock will begin to deform when the rheologically weakest phase fails. As quartz is one of the softer minerals and most crustal rocks contain quartz, the ductile deformation of the crust may well be described with the rheological data for quartz. Rocks in the mantle part of the lithosphere are quartz absent and dominated by olivine. Therefore, Fig. 47 shows two pairs of curves for power law creep; one pair for the creep stresses of quartz at low and high strain rates, the other for the creep behavior of olivine at low and high stain rates. Together, all these curves result in a strength profile for the continental lithosphere that contains two strength maxima, one at mid crustal levels, the other in the uppermost portions of the mantle part of the lithosphere. This extremely simple model for the rheological stratification of the lithosphere is called a *Brace-Goetze lithosphere* (after a suggestion by Molnar 1992).

10.1.1 Qualitative Features of the Brace-Goetze Lithosphere

The model of the Brace-Goetze lithosphere has a large number of features that are in phenomenal correspondence with observations in nature. Some of these are discussed here (see also: Jackson 2002).

• **Brittle failure in the mantle** A comparison of Figs. 47c and d shows an interesting qualitative difference between the two strength profiles. At *low* strain rates the entire lithosphere below the brittle ductile transition deforms viscously. However, at *large* strain rates, the viscous strength of the upper mantle is larger than its brittle strength and the uppermost mantle will fracture. Of course, the occurrence of brittle fracture in the upper mantle depends on a large number of other factors as well. However, we want to note

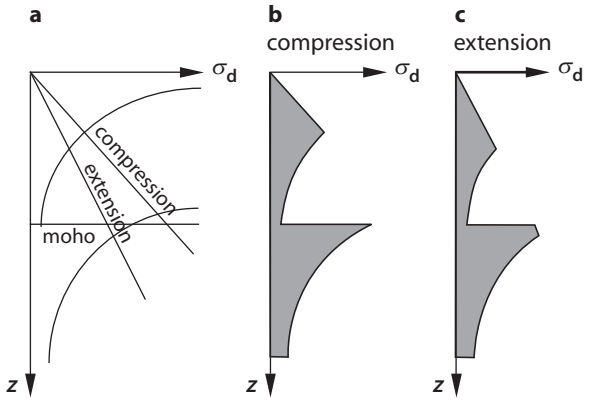

Figure 48: Schematic diagram showing the changes in mechanical strength of a Brace-Goetze lithosphere when changing the deformation regime qualitatively, i.e. from compression to extension. **a** The change from compression to extension decreases the brittle failure strength, while the viscous strength remains unaffected by this change, if the absolute value of the strain rate remains constant. Potentially, this may be reflected in brittle failure of the upper mantle (**b** and **c**).

that the brittle strength of the upper mantle is comparable to its viscous strength at geologically realistic strain rates. Should it be true that the upper most mantle deforms brittle under some circumstances, then this process might have important consequences for the accumulation of mafic material (underplating) at the Moho (Huppert and Sparks 1988). The transition from viscous flow to brittle failure in the upper most mantle may not only occur due to a change in strain rate (*increase* of viscous strength), but may also occur due to a *decrease* of the brittle strength. This may occur if there is a transition from compression to extension.

• **Changes in the rheological stratification** Changes in the strain rate of an orogen can also change the rheological stratification of the lithosphere. This is illustrated in Fig. 49 using a simple model lithosphere made up of three lithological layers. The figure shows that a change in the strain rate may change the rheological layering. At low strain rates there are three strength maxima, while at high strain rate there are only two (Fig. 49b,c). Such weak points may be the nucleus for the formation of a tectonic nappe boundary. Thus, it is possible that the thickness of nappes in a lithologically stratified crust is a function of the strain rate (Kuznir and Park 1986).

• **Changes in the geotherm** During viscous deformation it is not only changes in the strain rate that can change the strength of the lithosphere. Changing the geotherm may have the same influence. Other mechanisms that can cause changes in the strength of the lithosphere are, for example, strain hardening, or metamorphism.

• **Strength change due to metamorphism** During metamorphism and deformation, both mineralogy and grain size change. It is therefore conceivable that a rock has a higher shear strength after metamorphism than before. For example, a garnet mica schist has a larger shear strength than its precursor: a clay. This is an interesting aspect which may be crucial in the consideration of postorogenic extension of mountain belts. In general it is thought that the stresses required for the late extension of an orogen are smaller than those required for its shortening. This is based on the fact that brittle deformation requires smaller stresses in tension than in compression. However, this is contrasted by the fact that the crust may have increased its strength by metamorphism.

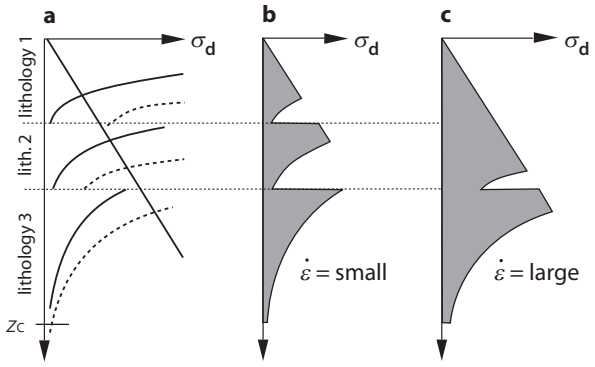

Figure 49: Schematic diagram showing how changes of the deformation rate can cause changes in the rheological stratification of the lithosphere.

• **Quantitative description of a Brace-Goetze lithosphere** In order to describe the Brace-Goetze lithosphere quantitatively we require quantitative information on 1. the depth dependence of temperature, i.e. a description of a geotherm; 2. the material constants (both 1 and 2 we need in order to calculate viscous stresses); 3. we need density and thickness of the crust and mantle part of the lithosphere in order to calculate vertical stresses and therefore the brittle strength. Table 5 lists typical numerical values for these parameters (Brace and Kohlstedt 1980). For the thermal structure of the lithosphere we will assume in the following that the radiogenic heat production decreases exponentially with depth according to eq. 18 with the characteristic drop off depth $h_r = 10$ km. We also assume that the thermal conductivity is $k = 2\ \mathrm{J\,s^{-1}\,m^{-1}\,K^{-1}}$, and that the temperature at the base of the lithosphere is $T_l = 1\,280\,^\circ\mathrm{C}$. Assumption on thickness and density are also listed in Table 6.

Table 5: Rheological parameters of the continental lithosphere relevant for its viscous behavior. These data are largely after Sonder and England (1986).

parameter	**value/unit**	**definition**
power law	*(eq. 112)*	
A_q	$5 \cdot 10^{-6}\ \mathrm{MPa^{-3}\,s^{-1}}$	pre exponent constant for quartz
Q_q	$1.9 \cdot 10^5\ \mathrm{J\,mol^{-1}}$	activation energy for quartz
n_q	3	power law exponent for quartz
A_o	$7 \cdot\ 10^4\ \mathrm{MPa^{-3}\,s^{-1}}$	pre exponent constant for olivine
Q_o	$5.2 \cdot 10^5\ \mathrm{J\,mol^{-1}}$	activation energy for olivine creep
n_o	3	power law exponent for olivine
Dorn's law	*(eq. 113)*	
Q_D	$5.4 \cdot 10^5\ \mathrm{J\,mol^{-1}}$	activation energy for olivine creep
$\dot{\epsilon}_D$	$5.7 \cdot 10^{11}\ \mathrm{s^{-1}}$	strain rate
σ_D	8 500 MPa	critical stress

We also make the assumption that the viscous behavior of olivine is described by eq. 112 below stresses of 200 MPa and by eq. 113 for stresses above 200 MPa. Brittle failure is described with Byerlee's law. That is, below 500 MPa brittle failure is assumed to occur without cohesion and an internal coefficient of friction of 0.8 and above 500 MPa the cohesion is 60 MPa and the internal coefficient of friction is 0.6. Some strength profiles calculated with these assumptions are dawn in Fig. 50.

10.1.2 Strength of the Lithosphere

When considering the distribution of stresses in the continental lithosphere, we have so far always only considered the stresses at a given depth. However, if we want to consider the deformation of entire continental plates, we need to know the mean stresses averaged over the entire lithosphere, or we need to know the total force that it needed to deform the entire lithosphere from top to base. Within the model of a Brace-Goetze lithosphere, this force is given by the vertically integrated stresses. This integrated strength is abbreviated with F_l and corresponds to the shaded region in Figs. 47, 48 and 49). If we make the thin

Table 6: Rheological parameters of relevance for the brittle deformation of a Brace-Goetze lithosphere.

parameter	**value/unit**	**definition**
$\mu_{(<500\text{MPa})}$	0.8	coefficient of friction in the crust
$\mu_{(>500\text{MPa})}$	0.6	coefficient of friction in the mantle
$\sigma_{0(<500\text{MPa})}$	0	cohesion of the crust
$\sigma_{0(>500\text{MPa})}$	60 MPa	cohesion of the mantle
λ	0.4 and 0.8	pore fluid/lithostatic pressure ratio
z_c	35 km	thickness of the crust
z_l	125 km	thickness of the lithosphere
ρ_c	2 750 kg m^{-3}	density of the crust
ρ_m	3 300 kg m^{-3}	density of the mantle lithosphere

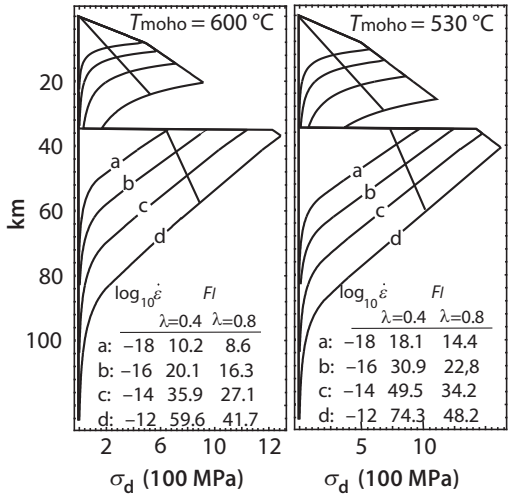

Figure 50: Strength profiles for the continental lithosphere as calculated with the model for a Brace-Goetze lithosphere and the data from Table 5 and 6). *a*, *b*, *c* and *d* are profiles for four different geologically relevant strain rates. The two diagrams show the strength profiles for two different Moho-temperatures that result from assumptions for the radiogenic surface heat production of $S_0 = 5 \cdot 10^{-6}$ W m^{-3} and $S_0 = 7 \cdot 10^{-6}$ W m^{-3}. In each diagram two linear curves for brittle failure for $\lambda = 0.4$ and $\lambda = 0.8$ are plotted. The stress curve with the higher stresses is for the lower value of λ. It was assumed that $\lambda_\text{c} = \lambda_\text{l}$. The vertically integrated stresses F_l are given in 10^{12} N m^{-1}.

sheet approximation, then the integrated strength of the lithosphere may be calculated as:

$$F_\text{l} = \int_0^{z_\text{l}} (\sigma_1 - \sigma_3)\,\mathrm{d}z \quad . \tag{114}$$

It has the units of force per meter or Pa m = N m^{-1}. F_l may be interpreted as the force acting in the direction normal to the orogen *per* meter length of orogen (i.e. in

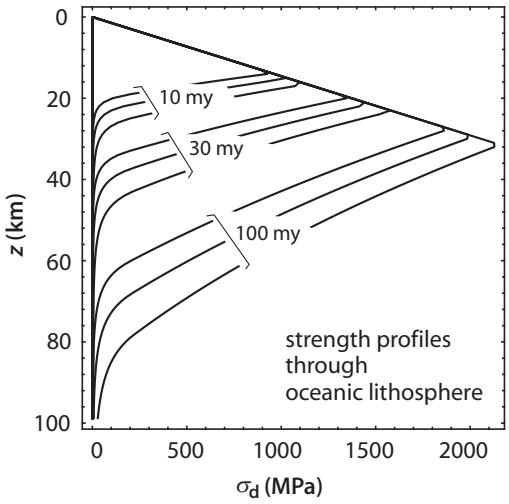

Figure 51: Strength profile through the oceanic lithosphere at ages of 10, 30 and 100 my. For each of these ages, stresses were calculated for three strain rates of $\dot{\epsilon} = 10^{-16}$, 10^{-14} and 10^{-12} s^{-1}. For each age, the curve for the highest strain rate has the largest strength. The temperature profiles needed to calculate the stresses were calculated using eq. 34.

direction parallel to the orogen), that is required to deform the orogen with a given stain rate (Fig. 47, 48, 49). In the literature, the terms "strength" is often used very loosely. Strength (in Pa), *integrated* strength (in N m^{-1}), sometimes *stress* and occasionally even *force* are all often confused. We want to remember that *strength* has the units of stress (it is the stress that leads to brittle failure or viscous flow) and that *integrated strength* is a force per meter (which is equal to stress $\times$ meter). In the viscous regime strength is only defined for a given strain rate. This should be clear from eq. 112, where it is shown that the viscous stresses (strength) are strongly dependent on strain rate.

10.2 Rheology of the Oceanic Lithosphere

The fundamental assumptions which we have made for the calculation of stresses and strength profiles for the continental lithosphere are also valid for the oceanic lithosphere. However, there are two important differences: 1. In contrast to the continental lithosphere, oceanic geotherms are time dependent and there is no radiogenic heat production in the oceanic lithosphere. As a consequence, different relationships must be used to calculate the temperature profile with depth and ultimately the rheology. 2. There is practically no quartz bearing crust in the oceanic lithosphere and the rheology of oceanic lithosphere is therefore largely governed by the rheology of olivine. As a consequence, there is only one maximum in the strength profile (Fig. 51). On the other hand, the strength profiles of oceanic lithosphere are highly dependent on its age (sect. 3.2). The depth dependent temperature profile of oceanic lithosphere may be calculated with eq. 34. A strength profile for the oceanic lithosphere may then be calculated (Fig. 51).

10.2.1 Strength of the Oceanic Lithosphere

Eq. 114 may be used to calculate the integrated strength of the oceanic lithosphere just like we used it above to calculate the integrated strength for the continental lithosphere. In fact, it is possible to calculate the integrated strength of the oceanic lithosphere with much higher accuracy than of the continental lithosphere, because oceanic geotherms are much better known than continental geotherms. A comparison of Fig. 50 with Fig. 51 shows that only very young oceanic plates are likely to have a smaller integrated strength

than continental lithosphere. This result corresponds to our observations: We know that most intra plate seismicity occurs in the continents and not in the oceans. There is practically no deformation inside the oceanic plates of Earth. An oceanic plate acts - because of its high integrated strength - like a passive transmitter of stresses from the mid oceanic ridges to the continents.

10.2.2 Force Balances in Orogens

Proper force balance equations are briefly discussed in Unit 13. Here, we want to introduce a more intuitive way to formulate a force balance for orgens that we can use without too much algebra. For this we divide (very loosely and not very precisely) the forces that keep orogens in mechanical equilibrium into three groups:

1. *Driving forces*: Driving forces are forces applied from the outside to an orogen, for example ridge push or slab pull. In the following we abbreviate these forces with F_d. Some of these forces were already discussed in sect. 11.1.1.

2. *Internal forces*: These are the forces internal to the lithosphere which resist the driving forces and are limited by the inherent strength of the rocks in the lithosphere. These are the forces discussed in detail in sect. 10.1. It is the vertically *integrated* strength of the lithosphere, which has the units of force/meter and was explained on p. 76. We represent this in the following with F_l.

3. *Potential energy*: Forces resulting from the potential energy difference of an orogen relative to its surroundings are also called *gravitational stresses* or: *horizontal buoyancy forces*. We denote those in the following with F_b.

This division is not completely sound, as many of the plate tectonic driving forces themselves are also caused by potential energy differences and many of the other forces are also coupled. However, it helps us to understand the balance of forces in orogens which we can write as:

$$F_\mathrm{l} = F_\mathrm{d} - F_\mathrm{b} \quad . \tag{115}$$

Basically this equation states that the strength of the lithosphere balances the effective force applied to the orogen, with the "effective force" being the difference between the external driving force causing convergence and the buoyancy force causing extension. We will discuss this equation in some detail in a few pages. However, first we want to discuss the process of building up potential energy in an orogen in some more detail. Note also that all orogenic forces are usually not given in the units of force (N), but that they are discussed in terms of force *per* meter (Nm^{-1}) and that the unit of "force per meter" is equivalent to the units of "potential energy per area" or the units of "stress $\times$ distance".

• **Evolution of orogens in the equilibrium of forces** The force balance we have discussed in the last paragraphs may be summarized in the following equation:

$$F_\mathrm{eff} = F_\mathrm{d} - F_\mathrm{b} \quad . \tag{116}$$

which we already introduced in eq. 115. There, F_d is the tectonic driving force *per* meter length of orogen, F_b is the gravitational stress *times* the thickness of the lithosphere. F_b is also called *horizontal buoyancy force*, or: *extensional force* or: *potential energy per area*.

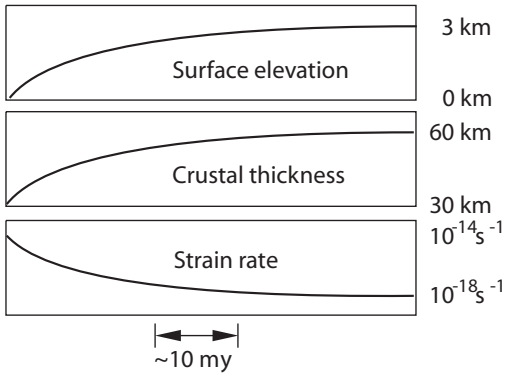

Figure 52: Schematic illustration of the evolution of a collisional orogen subject to the force balance of eq. 117. Surface elevation and crustal thickness converge to a steady state when the magnitude of the horizontal buoyancy force approaches the tectonic driving force

The difference between the driving force and the horizontal buoyancy force is the effective driving force applied to a continent F_{eff}. Equation 116 is often referred to as the "orogenic force balance". Note that – although this equation is called a "force balance" – it *really* balances parameters that have the units of force per meter or stress $\times$ meter. Eq. 116 is often also written as:

$$F_{\text{eff}} = F_{\text{d}} - F_{\text{b}} = F_{\text{l}} \quad . \tag{117}$$

There, F_{l} is the vertically integrated strength of the lithosphere in Nm^{-1} and corresponds to the area under the failure envelope discussed in Figs. 47, 48 and several others. Note that F_{l} can only equal the left hand side of the equation if the orogen is deforming (i.e. at the point of failure). When $F_{\text{eff}} < F_{\text{l}}$, there is no deformation. However, we assume that active orogens are always on the point of failure so that $F_{\text{eff}} = F_{\text{l}}$ (sect. 10.1.2, eq. 114). The bulk of the lithosphere is dominated by viscous deformation mechanisms where deviatoric stress and strain rate are proportional. Thus, an orogen will always deform with a strain rate that is just large enough so that the vertically integrated flow stresses balance exactly the effective driving force (per meter). If the strain rate would be *lower* than this, the integrated strength of the lithosphere would be smaller than the effective driving force (per meter) and the deformation rate would increase. Conversely, if the strain rate would be *larger* than the effective driving force, then the strength would be too large for any deformation to occur. Note also that, within eq. 117, the integrated failure strength of the lithosphere is zero when the effective driving force is zero.

Because of the balance described by eq. 116 it is possible to solve this equation for strain rate of an orogen, if a relationship is assumed that relates stress to strain rate (e.g. a viscous flow law). Such an analysis has been done by a number of authors and provides insights into the basic principles of the mechanical evolution of collisional orogens. If the tectonic driving force is assumed to be constant, then such orogenic evolutions track towards an equilibrium where $F_{\text{b}} = F_{\text{d}}$ and $F_{\text{eff}} = F_{\text{l}} = 0$ (Fig. 52). Thus, collisional orogens are self limiting. As such, collisional orogens are fundamentally different from extensional orogens, which are not necessarily self limiting.

• **The mean strength of the lithosphere** Differences in surface elevation of the continental lithosphere can only be created if the lithosphere has a finite strength. That is: if the horizontal and vertical principle stresses are of different magnitude (McKenzie 1972; Molnar and Lyon-Caen 1988). If the were no stress differences, then the surface of a plate subjected to lateral forces from the outside would lift everywhere by the same

amount; like water between two converging sides of an aquarium. There would be no mountain ranges and the surface of the continents would look rather boring. Conversely, it is possible to use the thickness and surface elevation of a mountain belt to estimate the mean strength of the lithosphere (Molnar and Lyon-Caen 1989) (see Unit 11).

Consider a mountain range which collapses under its own weight and to which there is no forces applied externally. then, there is no external driving force and We can reformulate eq. 117 to:

$$F_{\mathrm{b}} = -F_{\mathrm{l}} \quad . \tag{118}$$

The left hand side of eq. 118 is the potential energy difference between mountains and foreland per unit area and was evaluated in eq. 126 or, somewhat more precisely, with eq. 128 (s. also Fig. 57). The right hand side of eq. 118 is the integrated strength of the lithosphere (s. eq. 114). It is the product of the mean differential stress of the extending mountain range and its thickness. Thus, the elevation contrast between mountain belts and their foreland may directly be used to provide an upper bound on the mean strength of the lithosphere.

According to the estimates of Molnar and Lyon-Caen (1988), the surface elevation contrast between the Tibetan Plateau and the Indian foreland indicates a mean strength of the Asian lithosphere of $\sigma_{\mathrm{d}} = 69$ MPa (see eq. 126). For the Altiplano in the Andes similar estimates indicate a mean strength of $\sigma_{\mathrm{d}} = 52$ MPa. This mean strength is estimated purely on the basis of topography differences and is therefore quite a sound estimate. If we acknowledge that some parts of the lithosphere will be significantly "softer" than this value (e. g. the uppermost and lowermost parts of the crust as shown in Fig. 47), then there *must* be other parts of the lithosphere that are significantly "stronger" than this value to maintain the mean value given by these estimates. These considerations provide a strong argument for the existence of a significant shear strength of parts of the lithosphere.

11 Unit: Plate Driving Forces: Potential Energy

Plate tectonic driving forces may be divided into two fundamental groups according to the way they are transmitted:

– transmission by shear stresses,

– transmission by normal stresses.

Because plate tectonic driving forces act horizontally, *shear stresses* must be applied to horizontal surfaces and *normal stresses* to vertical surfaces. If the transmission occurs by shear stresses, this is often called *basal traction*. If the transmission occurs by normal stresses, we speak of *end loading* or *side forcing* (Fig. 53).

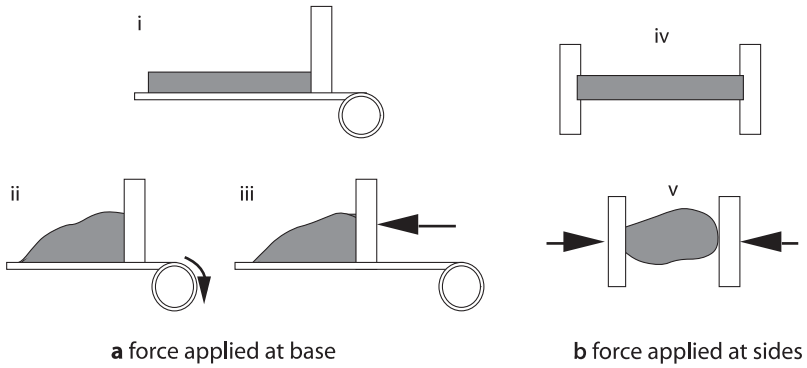

Figure 53: Illustration of the two fundamental mechanisms for the transmission of plate tectonic driving forces. **a** illustrates transmission by *basal friction*. In *ii* basal friction is shown in a *Eulerian* reference frame ("conveyer belt" model). In *iii* basal friction is shown in a *Lagrangian* reference frame ("bulldozer" model). **b** illustrates transmission by lateral normal stresses ("side forcing").

11.0.3 Transmission of Stresses by Shear- or Normal Stresses

One model for the explanation of plate motions is that the friction between the base of the lithosphere and the convective motion in the asthenosphere is the principal driving mechanism (Ziegler 1992; 1993). The most important argument *for* this model comes from the reconstruction of past plate motions. These do not correspond very well with the global geometry of mid oceanic ridges and subduction zones. Thus, it is thought that these plate motions reflect the geometry of convection cells in the mantle instead. The most important argument *against* this model is implicit in Fig. 47. This figure shows that differential stresses at the base of the lithosphere are much too small to be able to transmit forces from the mantle into the lithosphere. It is therefore hard to imagine that this softest part of the lithosphere can transmit stresses large enough to build the mountain ranges of our planet (s. mechanical definition of the lithosphere). The tractions at the base of the lithosphere are not likely to be larger than 10^{-2} MPa (Richardson 1992).

The other - and by far more accepted - model for the explanation of plate motions is that *plate boundary* forces drive plate tectonics by lateral normal stresses (e. g. Forsyth and Uyenda 1975). These forces are predominantly caused by *potential energy variations*. Such

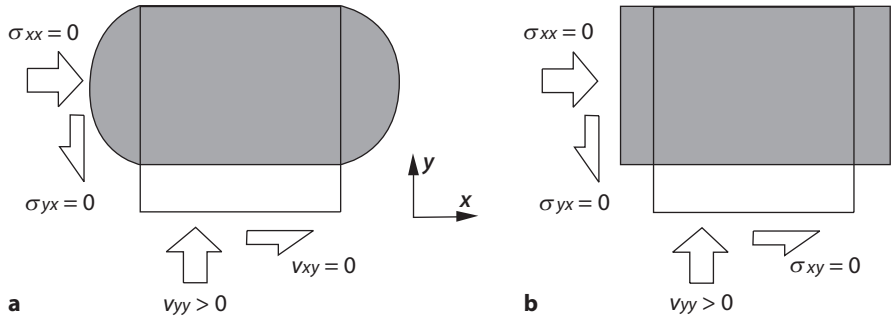

Figure 54: Illustration showing how apparently small differences in the boundary conditions can cause very different deformation geometries.

variations occur inside the continents and along the boundaries of oceanic lithosphere and will be discussed on the following pages. Despite the two different models for the origin of plate tectonic driving forces we should not forget that, ultimately, *all* plate tectonic forces find their origin in the thermal energy of Earth.

11.0.4 Boundary Conditions of Deformation

In the last section we have discussed normal and shear *stresses* that cause the deformation of plates. However, it is not clear that it is stresses that are the appropriate boundary conditions for plate deformation. For example, the India-Asia collision keeps going at constant convergence rate irregardless the stresses that arise as a consequence of the build up of the Himalaya. Thus, this may be an example where *velocities* rather than stresses form an appropriate boundary condition. We therefore discriminate between:

– Orogenic boundary conditions given by velocities,

– Orogenic boundary conditions given by stresses.

Both types of boundary conditions may have a *normal* and a *tangential* component. Thus, for a two-dimensional mechanical model with the two spatial coordinates x and y, we require a tangential and a normal boundary condition on each boundary. A total of four variables must be defined by the boundary conditions (Fig. 54).

11.0.5 Potential Energy

Practically all important plate tectonic driving forces find their origin in differences of the potential energy of different parts of the earth (Turcotte 1983). In this section we explain what we understand with the term *potential energy* in a plate tectonic context. We will return to this concept again in the sections 11.1, 11.2 and 10.2.2.

In sect. 7.1 we have shown that the vertical normal stress at a given depth in the crust z is given by the product of density, gravitational acceleration and the height, or thickness of the vertical rock column above it. This vertical normal stress is the vertically acting *force per area*. It may be calculated by integrating ρg between 0 and z, as we did in eq. 65. If the density over the thickness z remains constant, then this is simply $\rho g z$. This term has the units of Pa or $\mathrm{kg\,s^{-2}\,m^{-1}}$ or $\mathrm{J\,m^{-3}}$. We can see that *stress* has the same units as *energy per volume*.

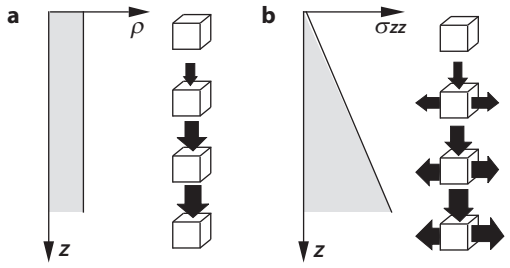

Figure 55: Density ρ and vertical normal stress σ_{zz} as a function of depth z. The value σ_{zz} is the vertically integrated density, times acceleration. Thus, the curve in **b** corresponds to the gray shaded region in **a**. The row of little unity cubes next to **a** illustrates how the vertical stress increases with depth. The column of cubes next to **b** illustrates that the horizontal force exerted by the column on its surroundings is given by the sum of all vertical stresses. This corresponds to the gray shaded area in **b**.

This quantity can also be interpreted as the potential energy of a cubic meter of rock at depth z. If we want to know the potential energy not of a single cubic meter, but that of a whole body, for example that of a mountain range, then we need to integrate this *potential energy per cubic meter* over the lateral and vertical extent of the range. Fortunately, it is usually sufficient to know the potential energy *per area*, i.e. that of a complete vertical column, but only for one square meter of area. Using this *potential energy per area* we can compare different regions on the globe, for example two neighboring lithospheric columns of different thickness and density distribution. In the following we will represent the potential energy *per area* with E_{p}. In order to determine E_{p} at depth z we simply need to sum up (i.e. integrate) the vertical stresses in the lithospheric column of interest between the surface (which usually is $z=0$ in the reference frame we use) and the depth of interest z:

$$E_{\mathrm{p}} = \int_0^z \sigma_{zz}\mathrm{d}z = \int_0^z \int_0^z \rho_{(z)} g \mathrm{d}z\mathrm{d}z \quad . \tag{119}$$

Very often the "depth of interest" is the isostatic compensation depth. If the density is independent of depth, then eq. 119 may be simplified to give:

$$E_{\mathrm{p}} = \int_0^z \sigma_{zz}\mathrm{d}z = \int_0^z \rho g z \mathrm{d}z = \frac{\rho g z^2}{2} \quad . \tag{120}$$

This integral corresponds to the gray shaded region in Fig. 55b. We want to remember that E_{p} has the units of energy *per* area and is, therefore, strictly speaking, no energy as such.

11.0.6 Horizontal Forces Arising from Potential Energy Variations

In a static, non-deforming lithosphere the horizontal and vertical normal stresses have the same magnitude (see Fig. 55). It is true that:

$$\sigma_{zz} = \sigma_{xx} = \sigma_{yy} \quad . \tag{121}$$

This is also stated in eq. 108, which says that there is no deviatoric stress if the strain rate is zero. The sum of all vertical stresses integrated over the thickness of a plate is

the potential energy of the plate per area. Since horizontal and vertical stresses are the same, this potential energy per area is equivalent to the force exerted by the lithosphere onto its surroundings, per meter length of orogen. If two neighboring vertical lithospheric columns have the same potential energy per unit area, then they also exert equally large horizontal forces onto each other and there is no "net force" between them. However, if they have different potential energies per area, then this potential energy difference between the two plates may be interpreted as the net force F_b that is exerted by one column onto the other in the horizontal direction and per meter length of orogen. This net force arising from potential energy differences is also called *horizontal buoyancy force* (somewhat cumbersome) or *gravitational stress* and it is important to remember that it has the units of force per meter length of orogen. This potential energy difference may be written as (s. Fig. 56):

$$\Delta E_\mathrm{p} = F_\mathrm{b} = \int_0^{z_\mathrm{K}} \int_0^{z_\mathrm{K}} \rho^\mathrm{A}(z) g \mathrm{d}z \mathrm{d}z - \int_0^{z_\mathrm{K}} \int_0^{z_\mathrm{K}} \rho^\mathrm{B}(z) g \mathrm{d}z \mathrm{d}z \quad . \tag{122}$$

There, z_K could be any depth, but for many purposes it is useful to assume that it is the same isostatic compensation depth we used on p. 51. Below this depth there is no density differences between the vertical columns A and B (s. eq. 64). $\rho^\mathrm{A}(z)$ is the density of profile A as a function of depth z.

If density is a continuous function of depth, then eq. 122 may be usually integrated without too much trouble. However, in the lithosphere, the density distribution has (a the least) a discontinuity at the Moho so that it may be necessary to split the integral in eq. 122, even for very simple assumptions on the density distribution in the lithosphere.

The importance of the density *distribution* in the lithosphere for the potential energy may be illustrated nicely with an interesting example. Fig. 56 shows two columns in isostatic equilibrium. The two columns have the same isostatically supported surface elevation, because they are made up of sections of the same densities and thicknesses. However, they have different potential energies because in column B the dense part lies up high. Potential energy does not only depend on thickness and density, but also on the *distribution* of density with depth. Thus, there is a net buoyancy force between the two columns shown in Fig. 56. This net force is exerted by column B towards column A.

We can conclude that it is dangerous to infer lateral forces from topography on the surface of earth (England and Molnar 1991). In fact, it is even possible, that topographically *lower* regions exert a gravitational stress on topographically *higher regions*, averaged over the thickness of the lithosphere (Stüwe and Barr 2000).

11.0.7 Force Balance Between Mountains and Foreland

In this section we estimate the forces exerted by a mountain range onto its foreland (Fig. 57). For this, we will follow the logic of Molnar and Lyon-Caen (1988) and also use their choice for the vertical axis of the cross section. We assume an origin at the Moho and measure the vertical direction positively upwards as illustrated in Fig. 57b. This choice for the vertical axis helps the intuitive understanding if the integration of eq. 122, as one of the integration limits is always zero. However, note that the results are independent of the chosen reference frame as we do not calculate *absolute* potential energies, but only potential energy differences between two neighboring columns. Thus, as long as we choose the same coordinate system for the two columns that are to be compared, it does not matter which reference frame we pick.

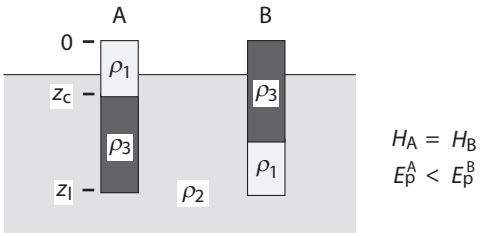

Figure 56: Schematic cartoon showing two columns in isostatic equilibrium ($\rho_1 < \rho_2 < \rho_3$). The surface of both columns has the same elevation above the liquid of density ρ_2, because both bodies consist of equally thick sections of the densities ρ_1 and ρ_3, i.e. they have the same weight. However, column B has a much higher potential energy per unit area than column A, because the distribution of density is different. In column B the high density part of the section lies higher. As a consequence, B exerts a net force towards A.

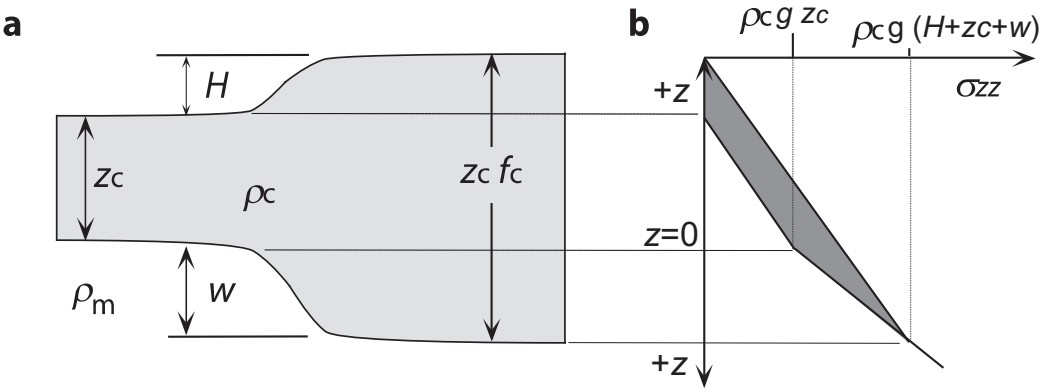

Figure 57: Cartoon contrasting the distribution of vertical stresses in mountain ranges relative to their foreland. **a** The thickness of the crustal root is w, the surface elevation relative to the reference lithosphere in the foreland H. In isostatic equilibrium it is true that: $H\rho_c = w(\rho_m - \rho_c) = w\Delta\rho$. In **b** the vertical stresses are drawn for the mountain range and the foreland. The dark shaded area between the two stress curves has the units of stress $\times$ meters or force per meter length of orogen exerted by the range onto the foreland. It corresponds to the potential energy difference between the mountain range and the foreland.

We begin by calculating the potential energy per unit area of the foreland following the logic of Molnar and Lyon-Caen (1988) and the geometry shown in Fig. 57. We can find this by integrating eq. 119. For the undeformed lithosphere in the foreland the potential energy above the Moho is simply:

$$E_p^{\text{foreland}} = \rho_c g z_c^2/2 \quad . \tag{123}$$

Correspondingly, the potential energy of the thickened crust relative to the Moho is:

$$E_p^{\text{range}} = \rho_c g(H + z_c)^2/2 + \Delta\rho g w^2/2 \quad . \tag{124}$$

where $\Delta\rho = (\rho_m - \rho_c)$ and the thicknesses H, Z_c and w are as labeled on Fig. 57. The first term in the equation above is simply the potential energy of the thickened crust above

the chosen origin at the Moho of the undeformed lithosphere. the second term is in the negative z direction, but the density contrast is also negative (as it acts as a buoyant force) providing in total a positive contribution to the potential energy. The potential energy difference per unit area is given by the difference of eq. 123 and eq. 124 (s. eq. 122). It is:

$$\begin{aligned}\Delta E_\mathrm{p} &= F_\mathrm{b} = E_\mathrm{p}^\mathrm{range} - E_\mathrm{p}^\mathrm{foreland} \\ &= \rho_\mathrm{c} g H^2/2 + \rho_\mathrm{c} g H z_\mathrm{c} + \Delta\rho g w^2/2 \quad . \end{aligned} \tag{125}$$

Eq. 125 may be simplified because we assume that both, mountain range and foreland are in isostatic equilibrium. The isostasy condition states that: $\Delta\rho w = H\rho_\mathrm{c}$. Using this we can simplify eq. 125 to:

$$\Delta E_\mathrm{p} = F_\mathrm{b} = \rho_\mathrm{c} g H \left(H/2 + z_\mathrm{c} + w/2\right) \quad . \tag{126}$$

The force F_b corresponds to the dark shaded region in Fig. 57b. It is the difference between the vertically integrated vertical stresses σ_{zz} of two vertical columns in the mountain range and in the foreland, respectively (Tapponier and Molnar 1976). For a 3 km high mountain range with a 30 km root, eq. 126 gives a force F_b of the order of $3\text{–}4 \cdot 10^{12}$ N m^{-1}. We will see that this number is comparable with the forces applied to and exerted by mid ocean ridges.

Despite its simplicity, eq. 125 may be used to draw some very fundamental conclusions. For one, we can see that the third term is significantly larger than the first term. Thus, the potential energy difference between two mountain ranges of the same elevation becomes larger if the compensating root is thicker. For example, a 100 km thick root of a mountain range made up of low density mantle material contributes significantly more to the potential energy of a range than a 60 km thick root of crustal material. We can also see from eq. 125 that the potential energy of a mountain range grows with the square of both the surface elevation *and* the thickness of its root. The work that must be done to increase the surface elevation of a mountain range by one meter increases therefore as the mountain range gets higher (Molnar and Tapponier 1978; s. sect. 10.2.2). This is the reason why mountain ranges do not grow infinitely on this planet and have a limiting elevation. As potential energy variations are some of the most important driving forces in the lithosphere we will continue with more details in the following sections 11.1 and 11.2.

11.1 Forces in Oceanic Lithosphere

The forces exerted by oceanic lithosphere onto the continents around them are considered to be the fundamental driving mechanism for plate tectonic motion (McKenzie 1969b). There are two important driving forces in oceanic lithosphere: 1. the potential energy of the mid-oceanic ridges and 2. the forces that occur in subduction zones.

11.1.1 Ridge Push

Mid-oceanic ridges have a high topography and a high potential energy relative to the average oceanic lithosphere. This potential energy is one of the more important (and certainly best known) plate tectonic driving forces. While strictly speaking the mid-oceanic ridge applies a torque to the plate, we will neglect here the curvature of Earth and continue using the term "ridge push". It is important to understand that ridge push finds its origin in the high potential energy of the ridge, rather than in the frictional stresses between an outward welling mantle plume and the oceanic plate as drawn in Fig. 58a.

The ridge push force per meter length of ridge (equivalent to the potential energy of the ridge per unit area) may be calculated with eq. 122, using similar assumptions to those we have made when designing a model to explain the water depth of the oceans (s. Fig. 36). The density of oceanic lithosphere must be expressed in terms of temperature (eq. 70) and temperature as a function of depth (eq. 34; s. Turcotte and Schubert 1982; Parsons and Richter 1980). Then - using the half space cooling model - it may be shown that the ridge push force is a function of the thermal profile through the oceanic lithosphere and therefore of age. Without reiteration the derivation of the ridge push force here, we simply state that it is given within this model by the equation:

$$F_\mathrm{b} = g\rho_\mathrm{m}\alpha T_\mathrm{l}\kappa t \left(1 + \left(\frac{\rho_\mathrm{m}}{\rho_\mathrm{m} - \rho_\mathrm{w}}\right)\frac{2\alpha T_\mathrm{l}}{\pi}\right) \approx 1.19 \cdot 10^{-3} t \quad . \tag{127}$$

All parameters of this equation are explained in sect. 7.1. From eq. 127 we can see that the ridge push force is a *linear* function of age of the oceanic lithosphere (Fig. 59). As such it is different from water depth which - within this model is described by a square root function of age (Fig. 37). The numerical value of the proportionality constant between age and force in eq. 127 ($1.19 \cdot 10^{-3}$) is derived using the following constants: $T_\mathrm{l} = 1\,200°\mathrm{C}$; $\rho_\mathrm{m} = 3\,200\ \mathrm{kg\,m^{-3}}$; $\rho_\mathrm{w} = 1\,000\ \mathrm{kg\,m^{-3}}$; $\alpha = 3 \cdot 10^{-5}\ \mathrm{K^{-1}}$ and $\kappa = 10^{-6}\ \mathrm{m^2\,s^{-1}}$. Fig. 59 shows that ridge push is about an order of magnitude *smaller* than the integrated strength of continents at normal orogenic strain rates. Thus, we may conclude that ridge push alone is insufficient as the principal plate tectonic driving force.

• **Asthenospheric flow at mid-oceanic ridges** In the past, ridge push has been interpreted to be related to frictional stresses of upwelling asthenosphere that "pushes" the ridge apart as illustrated in Fig. 58a. However, several observations speak against this model. For example, if upwelling material causes ridges, then it would be expected that different ridges have different elevations above the abyssal planes - dependent on the force exerted by the upwelling materials. In contrast, practically all mid ocean ridges lie at a constant water depth. Today we know that there are only very few places where mid-oceanic ridges coincide with diapirically upwelling mantle material. Rather, the asthenospheric flow at most mid-oceanic ridges is of the geometry shown in Fig. 58b. Among other arguments, this was recognized by McKenzie and Bickle (1988) using on geochemical arguments. These authors showed that partial melting that would occur due to adiabatic

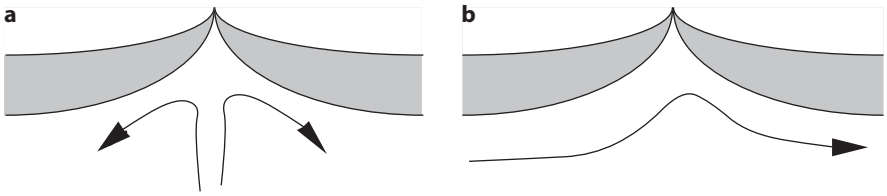

Figure 58: Cartoon showing two possible motions of the asthenosphere below mid oceanic ridges. **a** Asthenospheric material wells up below the mid ocean ridge in form of a *mantle plume*. During this process, adiabatic decompression of asthenosphere material will cause massive partial melting. It is thought that this situation pertains to regions where these melts are now present as large igneous provinces like the Karoo Basalts in southern Africa or the Deccan Traps in India and may be Iceland. **b** shows the mantle motion that is thought to be representative for most mid oceanic ridges.

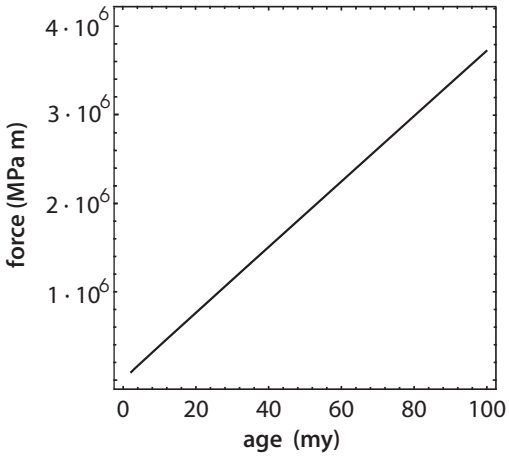

Figure 59: The force exerted by mid-oceanic ridges onto the surrounding plate per meter length of ridge, shown as a function of age of the oceanic lithosphere. Calculated with eq. 127.

decompression of upwelling melt in a mantle plume would be enough to form a 15 km thick oceanic crust. In contrast, normal oceanic crust is measured to be only about 5–7 km thick. This thickness can be produced by adiabatic melting of only the upper most asthenospheric regions. Asthenospheric flow as sketched in Fig. 58b is sufficient to produce a 5–7 km thick oceanic crust. Thus, it is thought that the flow directions of asthenospheric convection have little to do with the position of the mid-oceanic ridges. There are only very few places where mid-oceanic ridges coincide with diapirically upwelling mantle material. One of these places is Iceland.

11.1.2 Slab Pull and Trench Suction

Old oceanic lithosphere is denser that the underlying asthenosphere and it has therefore a negative buoyancy and it wants to sink. However, because oceanic lithosphere is very strong and stiff, it cannot immediately do this as soon as it reaches this critical age where its density becomes large compared to that of the underlying asthenosphere. Rather, the oceanic plate "glides" along the surface of the asthenosphere until this gravitationally unstable configuration is brought out of balance and a subduction zone forms. Once the edge of such an old oceanic plate has begun to subduct, it drags the remainder of the plate behind it. This is what is called *slab pull*. Such subduction processes may cause, or may be caused by, small scale convection in the upper mantle. This convection occurs predominantly in the wedge shaped region between the subducting and the upper plate. Once such a convection system is set up, it may actually drag both the upper plate and the subducting plate into the subduction zone. This is what is called *trench suction*. Slab pull is gravitationally induced, simply because the dense oceanic lithosphere wants to sink into the less dense upper mantle. In fact, the slab pull force is reinforced by the fact that the density of the down-pulling slab increases significantly once it has passed the olivine-spinel-transition at roughly 400 km depth. The magnitude of slab pull is roughly 10^{13} N m^{-1} (s. Turcotte and Schubert 1982). Thus, slab pull is about an order of magnitude larger than ridge push. However, it is likely that slab pull is being counteracted by frictional stresses of about the same magnitude between the sinking plate and the surrounding asthenospheric mantle. Thus, the net force exerted by subduction zones onto the foreland need not be very large.

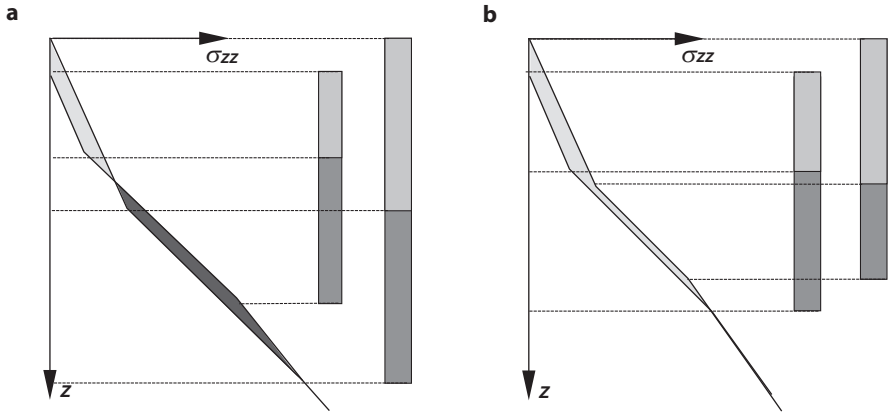

Figure 60: Illustration of vertical stresses and potential energy differences between two neighboring lithospheric columns. Vertical normal stress is plotted as a function of depth. The shaded region between the two curves is the potential energy difference per area between the two adjacent columns. In **a** this difference is positive in the upper part of the lithosphere (light shading) but negative in the lower part (dark shading). This means, that there is a net force acting from the right hand column towards the left hand column, while this net force is directed towards the right in the lower part. Because both shaded regions are roughly of the same area, there is practically no net force between the two columns, averaged over the thickness of the lithosphere. In **b** the entire right hand lithospheric column exerts a net force onto the left hand column.

11.2 Forces in Continental Plates

Inside the continents, plate tectonic driving forces arise predominantly from lateral variations in the density structure, which cause lateral variations in *potential energy*. When we discussed Fig. 57 we have already estimated the magnitude of these forces for a plate of constant density but variable thickness (eq. 125). In this section we want to refine these estimates. Fig. 60 illustrates two examples of potential energy differences between two lithospheric columns. Similar to Fig. 57 this potential energy difference is given by the shaded region between the two curves for vertical normal stress as a function of depth. This area corresponds to F_b in eq. 122 and may be interpreted as the net force exerted by one column onto the other per meter length of orogen and averaged over the thickness of the lithosphere (horizontal buoyancy force).

The considerations of Fig. 60 may be quantified by integrating eq. 122 and using simple descriptions for density as a function of depth. If we assume a simple lithosphere of two layers (a crust and a mantle lithosphere) and assume a linear thermal profile in the lithosphere so that the density due to thermal expansion may be described with eq. 72, then the lateral buoyancy force is described by:

$$\frac{F_\mathrm{b}}{\rho_\mathrm{m} g z_\mathrm{c}^2} = \frac{\delta(1-\delta)}{2}(f_\mathrm{c}^2 - 1) - \frac{\alpha T_\mathrm{l}}{6(z_\mathrm{c}/z_\mathrm{l})^2}\left(f_\mathrm{l}^2 - 1 - 3\delta(f_\mathrm{c} f_\mathrm{l} - 1)\right) + \frac{\alpha^2 T_\mathrm{l}^2}{8(z_\mathrm{c}/z_\mathrm{l})^2}(1 - f_\mathrm{l}^2) \tag{128}$$

(Turcotte 1983; Sandiford and Powell 1990). All parameters in this equation are the same as those we used in eq. 78 to calculate the elevation of mountain belts in isostatic

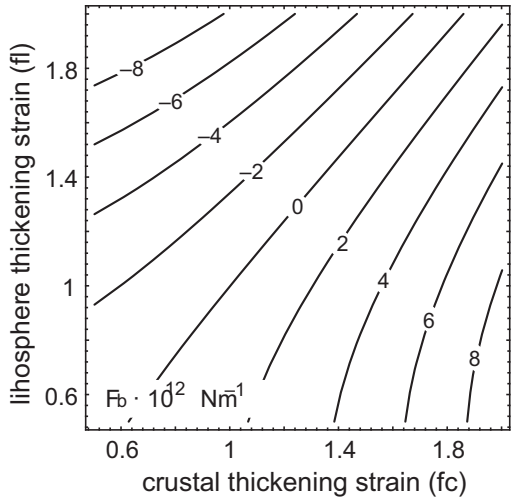

Figure 61: Diagram of lithospheric thickening strain f_l plotted against crustal thickening strain f_c and contoured for potential energy difference per area (equivalent to: "horizontal buoyancy force per meter" or: "lateral force"). The potential energy difference is always that between any point in f_c-f_l space and the reference lithosphere at f_c=$f_\mathrm{l} = 1$. The diagram was calculated with eq. 128 and is contoured for F_b in 10^{12} $\mathrm{N\,m^{-1}}$. Other assumptions are: $\rho_\mathrm{m} = 3\,200$ $\mathrm{kg\,m^{-3}}$; $\rho_\mathrm{c} = 2\,750$ $\mathrm{kg\,m^{-3}}$; $\alpha = 3 \cdot 10^{-5}$; $z_\mathrm{c} = 35\,000$ m; $z_\mathrm{l} = 125\,000$ m; $T_\mathrm{l} = 1\,200\,^\circ$C. The curvature of the contours arises because of the quadratic dependence of potential energy on thickness.

equilibrium but the definition of δ differs from that of Sandiford and Powell (1990) and the way eq. 128 is written here differs therefore slightly from theirs as well. Here δ is the density ratio of crust and mantle lithosphere $\delta = (\rho_\mathrm{m} - \rho_\mathrm{c})/\rho_\mathrm{m}$, g is the gravitational acceleration, T_l the temperature at the base of the lithosphere and α is the coefficient of thermal expansion and f_c and f_l are the vertical thickening strains of the crust and the lithosphere, respectively. Lateral forces calculated with eq. 128 are shown in Fig. 61.

12 Unit: Dynamic Evolution of Orogens

At the end of Unit 10 we ahve already discussed the force balance of orogens in a qualitative way and have seen how the orogen will converge to a staeady state as the buoyancy forces that oppose the driving forves get larger. With our now-gained knowledge on potential energy we will quantify these considerations in this section.

• **Building up potential energy** In sect. 11.0.5 we showed that the potential energy of orogens grows with the square of the surface elevation *and* with the square of the thickness of the orogenic root (eq.124). Thus, it takes significantly more energy to increase the surface elevation of a high mountain range by one meter than it takes to increase the elevation of a low range by the same amount (Molnar and Tapponier 1978). As a consequence, the height of a mountain range and the thickness of an orogenic root are limited, if the driving force is a constant. This limiting elevation is reached when the potential energy of the range per square meter area is exactly as large as the tectonic driving force per meter length of orogen. Then, a steady state equilibrium of the forces is reached.

In order to understand how this equilibrium is reached, consider Fig. 62a, which illustrates a very simple model orogen. The left of this diagram shows normal thick crust of the thickness z_c and the density ρ_c. On the right, this diagram shows an elevated mountain range in isostatic equilibrium of the elevation H. The diagram is equivalent to Fig. 57. The difference in potential energy between the two mountain range and the foreland per square meter of area is given by eq. 125 and 126. Let us also recall that ΔE_p is a potential energy *per* area and has the units of $\mathrm{J\,m^{-2}}$ and may also be interpreted as the mean net horizontal force exerted by the mountain range onto the foreland per meter length of orogen.

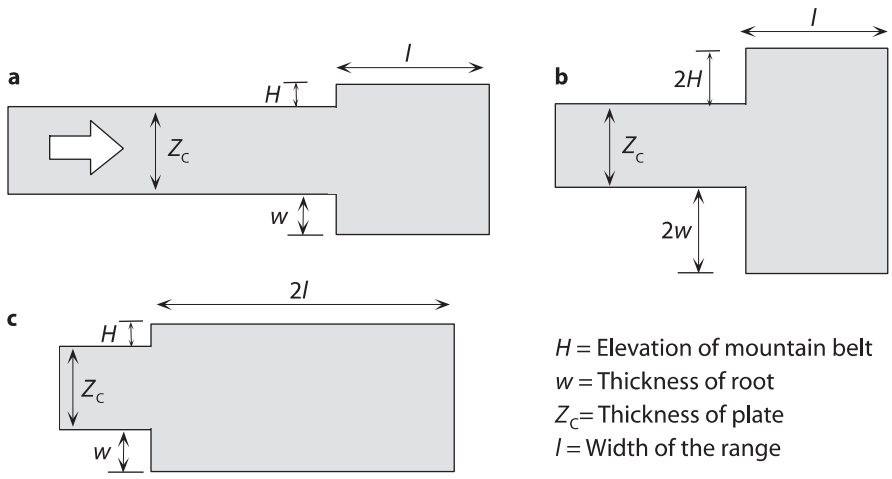

Figure 62: **a** Cartoon of a collisional orogen showing crust of normal thickness on the left and a mountain range on the right. Further displacement of the crust from left to right is compensated in **b** by further thickening and in **c** by lateral growth of the range. The difference in deformation style between b and c causes a significant difference of the potential energy of the mountain range (see eqs. 129 to 132) (s. also Fig. 57; after Molnar and Lyon-Caen 1988).

By analogy, the potential energy *per meter length of orogen* may also be interpreted as the product of the potential energy per area times the width of the mountain range l. From eq. 126 we can derive directly that:

$$\Delta E_{p,m^{-1}} = \rho_c g H l \left(H/2 + z_c + w/2\right) \quad . \tag{129}$$

The subscripts are used to emphasize that we are dealing with the units of potential energy difference *per meter* , while the ΔE_p that we used in eq. 125 and eq. 126 has the units of potential energy difference *per area*. Further growth of the mountain range may now proceed either in the vertical direction (Fig. 62b) *or* in the horizontal direction (Fig. 62c). If the crust inside the orogen is doubled in *thickness*, then the potential energy of the range per meter grows to the following value:

$$\Delta E^{\text{high}}_{p,m^{-1}} = 2\rho_c g H l \left(H + z_c + w\right) \quad . \tag{130}$$

If the growth of the mountain range is by doubling its width (at constant thickness, as shown in Fig. 62c), then the potential energy per meter growth to the following value:

$$\Delta E^{\text{wide}}_{p,m^{-1}} = 2\rho_c g H l \left(H/2 + z_c + w/2\right) \quad . \tag{131}$$

The difference of the potential energy increases between the two deformation styles is given by the difference between eq. 130 and eq. 131:

$$\Delta E^{\text{high}}_{p,m^{-1}} - \Delta E^{\text{wide}}_{p,m^{-1}} = \rho_c g H l \left(H + w\right) = \left(\frac{\rho_c \rho_m}{\rho_m - \rho_c}\right) g l H^2 \quad . \tag{132}$$

The last simplification in the equation above was performed using the isostasy condition $\Delta\rho w = H\rho_c$ that we also used in eq. 126. Eq. 132 shows us that it takes significantly less energy to thicken the crust in the foreland of a mountain belt (i.e. to widen the range) than it takes to increase the thickness of the crust in the mountain range itself (i.e. to increase the elevation of the range). Because of this, it is not necessary that convergence between two plates will stop when the gravitational extensional force F_b has reached the same magnitude as the tectonic driving force F_d acting towards the orogen. It is just that the convergence cannot be compensated anymore by *vertical* growth of the range, but will be compensated by *lateral* growth of the range towards the fore- or hinterland. Thus, active deformation in the range itself will come to a halt, the zone of active deformation propagates into the fore- and hinterland. A plateau will form in the center. In the process, the transition zone between the region where the largest principle stress is oriented horizontally and the region where it is oriented vertically will shift also towards the foreland.

Note that - despite these dramatic changes of the deformation and stress fields in the orogen - nothing has changed in the overall kinematics or stresses of the collision zone as a whole (Molnar and Lyon-Caen 1988): The driving forces have remained constant and so has the convergence between the two colliding plates. Understanding these relationships should therefore serve as a warning to structural geologists who are tempted to infer the overall kinematics of an ancient orogen from field observations on the kinematics of a few rocks.

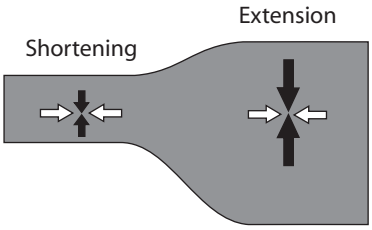

Figure 63: Distribution of horizontal and vertical stresses in a simple collisional orogen. If the topographic gradients at the surface and the base of the lithosphere are small, then the horizontal and vertical stresses σ_{xx} and σ_{zz} are parallel to the principal stresses. The horizontal stresses are constant across the orogen. However, the vertical stresses at a constant crustal level are higher in the orogen and smaller in the foreland. Thus, the largest principal stress in the foreland is given by σ_{xx}, while it is given by σ_{zz} in the orogen.

12.0.1 Mechanics on Vertical Sections

Many continental orogens are long compared to their width. In such orogens many parameters do not change very much in the direction parallel to the orogen and it is often possible to neglect this direction altogether when describing the orogen: We can characterize them with a description on a vertical cross section and the equations that must be solved to describe this are eq. 156 and eq. **??**, but omitting all terms that contain y. However, in this section we refrain from integrating these equations and simply expand on the discussion of the last section.

• **Changes in the stress field in collisional orogens** In the discussion of eq. 132 we have shown that the stress field in an orogen may change over time, even if the far field plate boundary stresses remain constant. Here we illustrate this in some more detail by looking at the changes of the stress state across a mountain belt. In this discussion we follow the logic of Dalmayrac and Molnar (1981) as well as Molnar and Lyon-Caen (1988).

If the shear stresses at the base of the lithosphere are negligible, then the *horizontal* forces in a simple orogen (simplified as shown in Fig. 63) are constant, regardless of thickness of the plate or surface elevation (Artyushkov 1973; Dalmayrac and Molnar 1981). In other words, the product of the mean horizontal stress σ_{xx} and the thickness of the plate remains a constant. Thus, if the stresses are a similar function of depth in different parts of the orogen, then the horizontal stress σ_{xx} is constant at any one depth across the orogen. This also implies that mountain ranges and plateaus transmit horizontal forces from the foreland to the hinterland of the orogen without changing their magnitude. On Fig. 63 this is indicated by the horizontal white arrows that are of the same size everywhere across the orogen.

This logic does *not* apply to the vertical stresses. Vertical stresses are the largest in regions where the overlying rock column is the thickest and the smallest where it is the thinnest (s. Fig. 57). As a consequence, the stress distribution in an orogen may be like that shown in Fig. 63. In the foreland (on the left in this figure) the *vertical* stress is *smaller* than the horizontal stress. The region is thickening, for example by thrusting. In the mountain belt (strictly: in the region of high potential energy, s. sect. 11.2), the largest principle stress is the vertical stress. The region is extending. In short: although the horizontal stress on Fig. 63 is everywhere the same, there is thickening in parts of

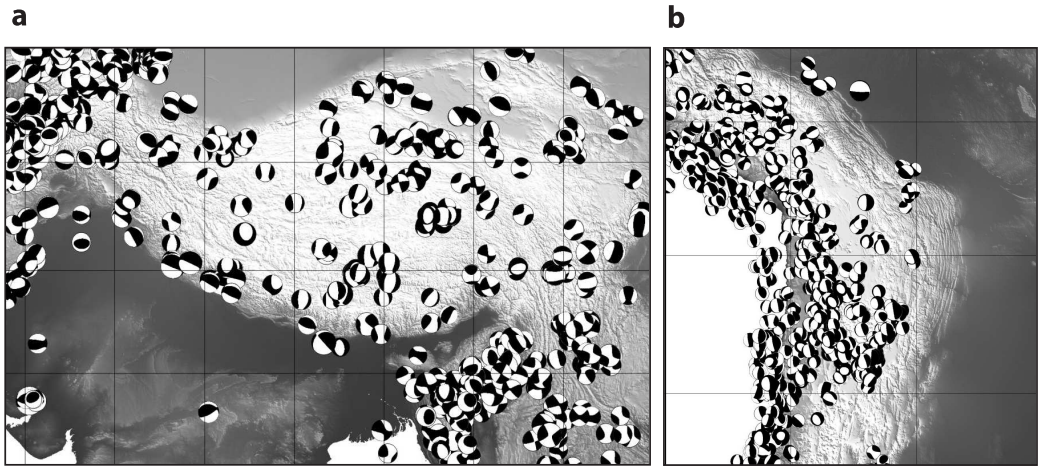

Figure 64: Fault plane solutions for the two great plateaus on this planet. **a** The Tibetan Plateau as the consequence of the India – Asia collision and: **b** the Altiplano as the consequence of the collision between the Pacific and the South American plates. Note that the majority of the fault plane solutions at low elevation regions indicate compression, while those on top of the plateau indicate largely extension.

the Figure and extension in others. On Earth, there are two orogens that have reached mechanical equilibrium and have formed plateaus. The Altiplano and the Tibetan Plateau. On both the transition from compression (in the foreland) to extension (on the plateau) can be observed (Fig. 64).

The lateral qualitative change in the deformation regime is *not* caused by changes in the horizontal- but changes in the vertical stress. This also explains why the observation of extension in mountainous regions must not occur because the surrounding plates are moving apart. The Tibetan Plateau is an example for such a situation: although the plateau is extending laterally, there is thrust tectonics in the surrounding regions (s. p. 95 and p. 98).

12.0.2 Mechanics in the Plane

Many collisional orogens have features that may only be described by considering deformation in plan view, for example processes like lateral extrusion. Because the vertical direction can then not be considered, vertically averaged assumption for lithospheric rheology and thermal structure have to be made. There are two common ways how to do this. These are the *plane strain* assumption and the *thin sheet* (plane stress) assumption. Which of the two assumptions is more appropriate for the description of orogens has been a subject of debate between the schools of Tapponier on the one side (e. g. Molnar and Tapponier 1975; 1978) and that of England, Houseman and McKenzie on the other side (e. g. England and McKenzie 1982; Houseman and England 1986a; England and Houseman 1986; 1988; Molnar and Lyon-Caen 1988).

The plane strain approximation helps to reduce three-dimensional problems to two dimensions. It assumes that all deformation is strictly two-dimensional so that all strain and displacement occurs in plane and no strain perpendicular to this plane. In plate

tectonic modeling we normally consider only the case of no volume change. Then, the total amount of shortening in one spatial direction must be compensated by stretching in the other. No area change occurs. Tapponier (e. g. 1982) has made great advances in our understanding of continental deformation using this assumption in his descriptions of the India-Asia collision. Plane strain deformation may be viewed as the deformation of a thin film of material that deforms between two fixed parallel plates. It is not *plane stress*, as the normal stresses on the surfaces of the confining plates will vary, depending on where deformation concentrates. Plane strain modeling is a good approximation when the lateral extent of deformation is much larger than the extent in the direction normal to the two modeled dimensions, e.g. crustal thickening or thinning when modeling continental deformation in plan view.

Thin Sheet Approximation When lithospheric shortening in one horizontal direction is compensated both by stretching in the second horizontal direction and by thickening (or thinning) in the vertical, the lithospheric deformation becomes three-dimensional. However, such scenarios can still be modeled in two dimensions assuming the *thin sheet* approximation (s. e.g. Houseman and England 1986a; s. however: Braun 1992). The thin sheet model is based on the assumption that the normal stresses at the surfaces of the plate are constant and that there are no shear stresses on horizontal planes. Thus, the thin sheet approximation is also called the *plane stress* approximation. As a consequence, the plate may thicken or thin in the vertical direction as to maintain the surface stresses constant but there are no vertical strain rate gradients (England and McKenzie 1982, England and Jackson 1989). Using z for the vertical spatial coordinate and $\dot{\epsilon}$ for strain rate, this can be described by:

$$\frac{\mathrm{d}\dot{\epsilon}}{\mathrm{d}z} = 0 \quad . \tag{133}$$

The thin sheet approximation is a good approximation for the description of lithospheric scale deformation when:

1. The shear stresses at the surface and the base of the lithosphere are negligible.

2. If the topographic gradients at these two surfaces are small.

Both are usually given on the scale of whole lithospheric plates and the thin sheert approximation is therefore commonly used in two dimensional orogenic scale models.

Within both the plane strain and the thin sheet model we need to consider the force balance equations (Unit 13). These may be solved for evolving orogens is a flow law is assumed. Usually this flow law is assumed to be a non-linear viscous flow according to the relationship:

$$(\sigma_1 - \sigma_3) = B\dot{\epsilon}_l^{(1/n)} \qquad \text{or :} \qquad \dot{\epsilon}_l = B^{-n}(\sigma_1 - \sigma_3)^n \tag{134}$$

in which we can recognize a simplification of the viscous relationships explained in eq. 108 and eq. 111. The constant B summarizes all temperature dependent terms of the power law (eq. 112) and represents a depth averaged value when doing thin sheet calculations. A comparison of eq. 112 with eq. 134 shows that: $B = A^{(-1/n)}\mathrm{e}^{Q/nRT}$. In short, B depends on strongly on temperature, but it can be shown that it is largely independent of the *distribution* of temperature within the lithosphere. Using the simplification of eq. 134 the

lithosphere may be considered as a simple medium deforming according to a power law relationship between stress and strain rate. Usually eq.134 is generalised in the form:

$$\tau = B\dot{E}^{(\frac{1}{n}-1)}\dot{\epsilon} \tag{135}$$

where $\dot{E}$ is the 2nd invariant of the strain rate tensor ($\dot{E} = \sqrt{\dot{\epsilon}_{ij}\dot{\epsilon}_{ij}}$) and τ and $\dot{\epsilon}$ are the deviatoric stress and strain rate tensors. Eq.135 is a proper vector equation (like eq. 108) and the flow law can now be coupled with the force balance above. The non linearity between deviatoric stress and strain rate is taken care of by introducing the deformation dependent term $\dot{E}$. In this form, eq.135 is the basis of many dynamic models for the description of continental deformation, for example those of England and McKenzie (1982) or Vilotte et al. (1982). In these models, the nature of deformation is often characterized by a single value: the Argand number.

Length scale	L	=	$U_0/\dot{\epsilon}_0$
Velocity scale	U_0	=	$L \times \dot{\epsilon}_0$
Strain rate scale	$\dot{\epsilon}_0$	=	U_0/L
Viscosity scale	B	=	$\tau_0/\dot{\epsilon}_0$
Stress scale	τ_0	=	$B \times \dot{\epsilon}_0$
Argand number	Ar	$\propto$	L/τ_0

Table 7: Scaling parameters in non dimensional viscous calculations. For simplicity, the stress exponent is assumed to be $n = 1$. Time scale t is not specifically listed here as it is simply $t = \dot{\epsilon}_0^{-1}$. In calculations where there is no Argand number, two of the top three variables and one of either viscosity- or stress scale are independent. Specifying Ar relates the top three to the next two variables, so that only two other scaling parameters must be chosen to define the system

• **The Argand number** The Argand number Ar is a measure for the ease with which the lithosphere deforms in response to gravitational stresses. It tells us if an orogen is likely to flow apart at the same rate it is being built, or if significant amounts of potential energy may be stored within it before it would collapse slowly under the influence of gravitational stress. England and McKenzie (1982) showed that these gradients in vertical stress are proportional to the square of the crustal thickness S:

$$\frac{\partial \sigma_{zz}}{\partial x} \propto \frac{\partial S^2}{\partial x} \qquad \text{or :} \qquad \frac{\partial \sigma_{zz}}{\partial x} = \left(-\frac{g\rho_c}{2L}\left(1-\rho_c/\rho_m\right)\right)\frac{\partial S^2}{\partial x} \tag{136}$$

for reasons discussed on p. 83. In eq. 136 the densities are those commonly used in this book and L is a thickness of the considered layer. If this is substituted into eq. **??** and the equation is brought into a non-dimensional form by normalizing to the length scale L, stress scale τ_0 and velocity scale U_0 (the collision velocity), then the Argand number is:

$$Ar = \frac{\rho_c g L(1-\rho_c/\rho_m)}{B(U_0/L)^{1/n}} = \frac{P_{(L)}}{\tau_0} \quad . \tag{137}$$

and may be interpreted as dimensionless ratio of the additional pressure $P_{(L)}$, that arises because of the thickness difference L between two plates and the stress τ_0, that is necessary to deform a plate with a significant rate $\dot{\epsilon}_0 = U_0/L$ (England and McKenzie 1982).

In this form, Ar may be used as an input parameter for mechanical modeling of orogens without having to explicitly consider the rheology, the material constants or the temperature profile of the lithosphere (Table 7). The additional pressure rises linearly with the thickness of the orogen and the stress τ_0 increases with the effective viscosity of the plate.

We can see that – if the effective viscosity of a plate is large, then the Argand number is small. Then, the flow properties of a mountain belt will depend largely on the orogenic boundary conditions. The belt will only begin to extend once its potential energy is very large. In contrast, if the Argand number is large (say between 10 and 20), then the effective viscosity of the range is very small and the forces caused by potential energy differences are large. The crust will quickly flow in response to applied forces. No significant thickness variations between foreland and orogen will ever develop during orogenesis.

• **Orogen parallel displacement** Collision of continents causes displacement of rocks in all three spatial directions. The *vertical* displacement results in thickening, the horizontal displacement in direction normal to the indentation direction is called loosely *lateral extrusion* and may occur in either a compressional or extensional regime.

Fig. 65a shows the collision of a plate with a rigid indenter that deforms the plate in front of it. The rocks in front of the indenter are displaced both in the direction of indentation and perpendicular to that direction. In Fig. 65a the amount of displacement decreases with distance from the indenter as the deformation there dissipates more. However, despite the orogen parallel *displacement* of rocks, all points of the indented plate are under *compression*. There is no lateral extension. This conclusion from Fig. 65a is in contrast to many observations in active collisional orogens where lateral extension *does* occur. According to England and Houseman (1989) orogen parallel extension in convergent orogens must find its nature in one of the following four processes:

1. unconstrained boundaries,

2. decrease in the convergence rate between two plates,

3. changes in the rheology of the plate,

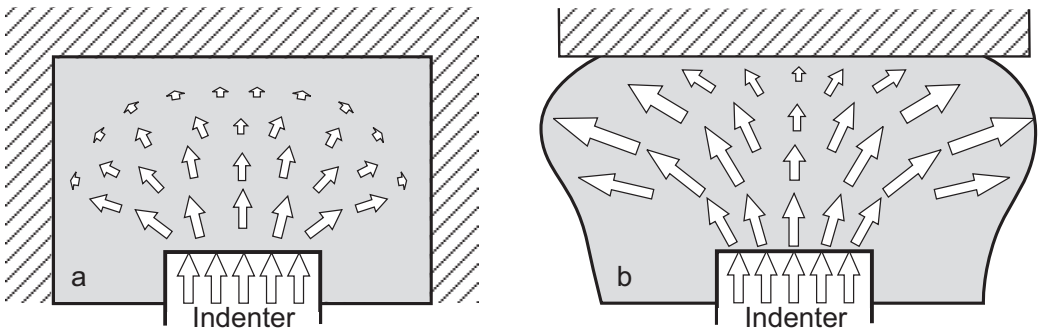

Figure 65: Different deformation regimes that occur during collision of an indenter with a much larger continental plate (gray shaded region). The arrows are velocity vectors. In **a** the plate is infinite or bound at all sides. In **b** the side boundaries of the plate are free and lateral extension occurs. The absence of confined model boundaries is one of four mechanisms that can account for orogen parallel extension during convergent plate motion.

4. external addition of potential energy to the plate.

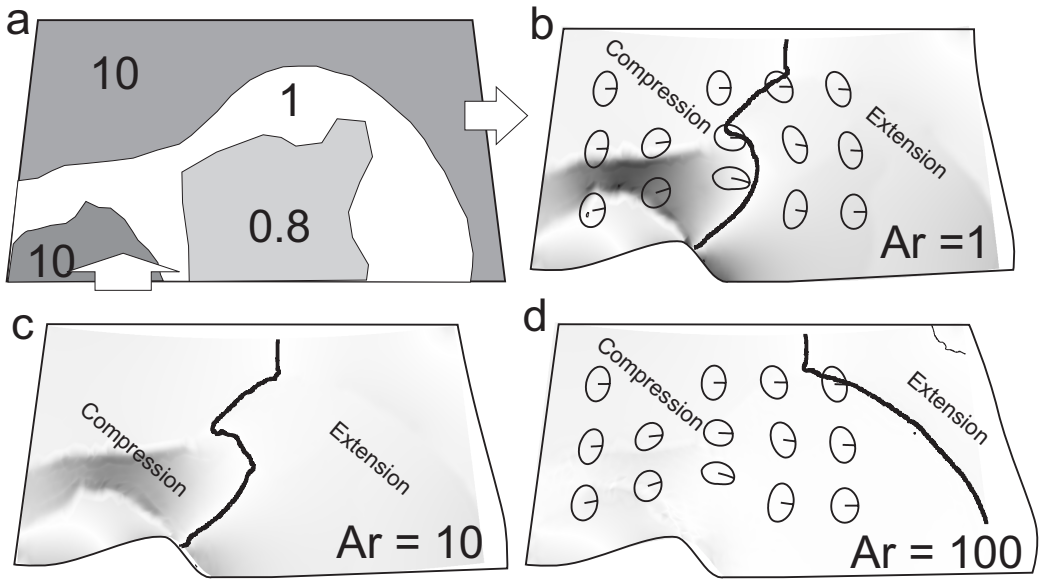

Figure 66: Model for the lateral extrusion of the Eastern Alps illustrating the influence of Argand number Ar on the deformation regime during continental indentation (after Robl and Stüwe 2005). **a** The 4 considered regions and their relative viscosity contrasts: European foreland (10), Adriatic indenter (10), Pannonian Basin (0.8) and Eastern Alps (1). For $Ar = 1$ and even for $Ar = 10$, significant topography (gray shading) is built in the Alps and lateral extrusion is exclusively due to tectonic forcing. For $Ar = 100$, lateral extrusion is increased (a little bit) by an additional contribution of extensional collapse. However – although barely any topography is suported – the extensional collapse is still in an overall compressive regime (because indentation goes on).

The first of these four processes is illustrate in Fig. 65b. There – in contrast to Fig. 65a – the gray shaded region is not bound on the sides. The other three processes may be illustrated with an analysis of eq. 117. A decrease in the convergence rate is reflected in this equation by a decrease in F_d. If F_l remains constant, the horizontal buoyancy force must decrease and extension sets in. This process is generally known as "post orogenic collapse". Changing the rheology of the plate (e. g. by heating, recrystallization, metamorphism etc.) is reflected in eq. 117 by changes in F_l. In order to maintain the force balance, strengthening of the plate must be accompanied by a decrease in the deformation rate or a decrease in the horizontal buoyancy force F_b. Extension occurs as a consequence. The external addition of potential energy, for example by delamination of the mantle part of the lithosphere may also cause the transition from compression to extension.

• **Lateral extrusion** Lateral *extrusion* of orogens is a great term that can be used when referring to lateral displacement of rocks without wanting to specify if its under a compressional or extensional regime. According to Ratschbacher et al. (1991), lateral extrusion describes lateral motion of rocks as the consequence of a combination of tectonic escape (in a compressional regime) and gravitational collapse (in an extensional regime).

While the term lateral extrusion is mechanically not specified and is a largely a kinematic description, the terms *tectonic escape* and *gravitational collapse* have well defined mechanical implications that were described by Tapponier et al. (1982) (Jones 1997) and Dewey (1988), respectively. Both processes are observed in the eastern European Alps, where extensional tectonics is observed along the east and west margins of the Tauern window) and simultaneous tectonic forcing along major strike slip lineaments has occurred (Selverstone 1988; Ratschbacher et al. 1991; Robl and Stüwe 2005).

Table 8: Definition of terms related to lateral displacement of rocks during indenter tectonics on an orogenic scale

term (key reference)	**meaning**
lateral extrusion (Ratschbacher et al. 1991)	kinematic description for displacement of rocks normal to indentation direction (stress regime: undefined)
gravitational collapse (Dewey 1988)	extension under its own potential energy (stress regime: extensional)
tectonic escape (Tapponier et al. 1982)	active lateral forcing along strike slip faults (stress regime: compressional)

13 Unit: A Reminder of Stress and Strain

In many parts of this course, we talked abotu stress and strain. Here we repeat the basics.

14 Strain - The Basics

• **Normal strain** Normal- or logitudinal strains are encountered very often in this course, for example when we talk about the thickening strains f_c and f_l. Normal strain simply relates the length of a body after deformation l to the length before deformation l_0. We define the following common terminology: The *stretch* of a rock s is the ratio of its length after deformation l to that before deformation l_0. Its *elongation* is the ratio of the change in length and the original length. We call this e. We can write the relationship between stretch (uniaxial strain), elongation and length in short:

$$s = \frac{l}{l_0} = 1 + e = 1 + \left(\frac{l - l_0}{l_0}\right) \quad . \tag{138}$$

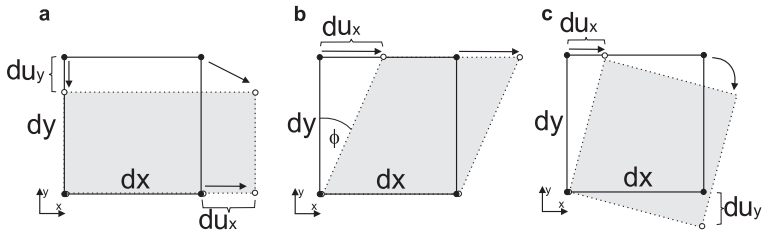

Figure 67: Deformation of a unity cube for the explanation of strain. **a** Deformation under normal strain also referred to as pure shear. **b** Deformation under shear strain also referred to as simple shear. **c** Rotation of the unity cube showing that displacement gradients can exist without internal strain.

Both s and e are often loosely referred to as "strain". It is therefore important to understand their respective meaning when we try to understand kinematics. With reference to Fig. 67a: $s = (dy + du_y)/dy$, where du_y is the displacement du in direction y.

• **Shear strain** is defined as the change in displacement with respect to a direction that is *normal* to this displacement. Shear strain is often referred to as γ and is given by the ratio of du_x to dy in Fig. 67 b so that:

$$\gamma = \tan\phi = \frac{du_x}{dy} \quad . \tag{139}$$

The angle ϕ is called the angular shear strain.

• **General displacement** In a general state of deformation (for example somewhere between Fig. 67a and b) scalar values of s and γ are insufficient to describe the deformation and we require both shear and normal displacements, both in all considered spatial

directions. In total, the deformation of a rock may be described by what is called the displacement gradient tensor D, which is a tensor containing all shear and normal gradients in displacement. This tensor is given by:

$$D = \begin{pmatrix} \frac{\partial u_x}{\partial x} & \frac{\partial u_x}{\partial y} \\ \frac{\partial u_y}{\partial x} & \frac{\partial u_y}{\partial y} \end{pmatrix} \tag{140}$$

The displacement gradient is also called the *Jacobian matrix* or the *deformation tensor* and its individual components might be abbreviated with $\partial u_i/\partial j$. This tensor describes the deformation of a unity cube perfectly well. Clearly, the examples for simple and pure shear discussed above may also be written in terms of this tensor, but several of the terms will be zero.

It is important to note that the displacement gradient tensor does *not* describe strain. For example, the rotating cube in Fig. 67c has definitely displacement gradients in both x and y direction, but it does not strain. Indeed, even for the simple shear example shown in Fig. 67b, the shear strain γ does not describe the strain of the body correctly, as it may be shown that part of the "simple shear" deformation is rigid body rotation. Fortunately (because of its symmetry), the displacement gradient tensor may always be expanded so that it can be resolved into two parts:

$$\frac{\partial u_i}{\partial j} = \frac{1}{2}\left(\frac{\partial u_i}{\partial x_j} + \frac{\partial u_j}{\partial x_i}\right) + \frac{1}{2}\left(\frac{\partial u_i}{\partial x_j} - \frac{\partial u_j}{\partial x_i}\right) \tag{141}$$

The first term on the right hand side of this equation is called the strain tensor ϵ_{ij}, the second part describes the rigid body rotation ω_{ij}. Adding a translation of the body u, we can write the full deformation of a body by:

$$u_i + du_i = u_i + \epsilon_{ij} dx_i + \omega_{ij} dx_i \tag{142}$$

Eq. 142 is a full description of deformation of rocks including their *translation* (first term), their *strain* (second term) and their *rotation* (third term). Rotational components of deformation are very much the field of structural geology and are not discussed further here. However, the strain tensor and its time derivative, the strain rate tensor, are needed in several parts of this book and we therefore write it out in full as:

$$\epsilon_{ij} = \frac{1}{2}\left(\frac{\partial u_i}{\partial x_j} + \frac{\partial u_j}{\partial x_i}\right) = \begin{pmatrix} \frac{\partial u_x}{\partial x} & \frac{1}{2}\left(\frac{\partial u_x}{\partial y} + \frac{\partial u_y}{\partial x}\right) \\ \frac{1}{2}\left(\frac{\partial u_y}{\partial x} + \frac{\partial u_x}{\partial y}\right) & \frac{\partial u_y}{\partial y} \end{pmatrix} \tag{143}$$

The strain rate tensor looks identical to eq. 143 if u is considered to be velocity and not displacement. Just like the stress tensor, the strain tensor is symmetric and the invariants of the strain tensor matrix are of some importance, for example when considering flow laws or shear heating.

14.1 The Stress Tensor

There are many excellent descriptions of stress in an abundance of good text books (e. g. Means 1976; Suppe 1985; Engelder 1993; Pollard and Fletcher 2006). Here we only summarize the definitions of a few terms related to stress (Engelder 1994).

14.1.1 Force

Force is a vector and - like all vectors - is described by a *magnitude* and a *direction*. It has the units of mass × acceleration: 1 N = 1 kg m s^{-2}. A related vector quantity is *traction*. Traction is a force (with magnitude and direction) *per area*, where the orientation of this area is not defined. Tractions may be subdivided into normal and parallel components called *normal traction* and *shear traction*. It is important to note that tractions are vectors, although they have the same units as stress. In contrast, *stress* is a tensorial quantity described by all the tractions acting on a unit cube.

14.1.2 The Stress Tensor

In three-dimensional space, the state of stress of a single point inside a rock (i.e. a unit cube) is given by nine numbers, all of which have the units of force per area. These nine numbers are all tractions acting on different planes and different directions that need to be defined by using subscripts. These nine numbers define the stress tensor which is typically written as:

$$\sigma = \begin{pmatrix} \sigma_{11} & \sigma_{12} & \sigma_{13} \\ \sigma_{21} & \sigma_{22} & \sigma_{23} \\ \sigma_{31} & \sigma_{32} & \sigma_{33} \end{pmatrix} = \begin{pmatrix} \sigma_{xx} & \sigma_{xy} & \sigma_{xz} \\ \sigma_{yx} & \sigma_{yy} & \sigma_{yz} \\ \sigma_{zx} & \sigma_{zy} & \sigma_{zz} \end{pmatrix} \tag{144}$$

The two different notations of subscript used in eq. 144 are both common in the literature. The first of the two specifying spatial indices x, y and z (or 1, 2 and 3) indicates the direction in which the stress component acts. The second index indicates the normal to the plane on which this stress component acts. We can see that the three tensor components in the diagonal of this matrix have two identical indices. They are called *normal stresses* because the surface onto which the stresses act are *normal* to the direction in which they act, (i.e. the indices for "direction in which it acts" and "plane onto which it acts" are the same). In the following we abbreviate normal stresses with σ_{n}. The remaining six components of stress in eq. 144 are *shear stresses*. In these, the stress components they describe act *parallel* to the plane onto which they are exerted. Shear stresses are abbreviated here with σ_{s}.

The stress components in a given column of eq. 144 act on the same plane, but in different directions. The rows contain stress components oriented in the same direction, but acting on different planes. In the literature, shear stresses are often abbreviated with τ and normal stresses with σ. However, this notation is somewhat confusing as all components of the tensor have the same units and should be abbreviated with the same symbol. We therefore stick to the notation of eq. 144 in particular to the use of x and y rather than 1 and 2 as subscripts and describe shear stresses with $\sigma_{i \neq j}$ or σ_{s} and normal stresses with $\sigma_{i=j}$ or σ_{n}. We reserve τ as a symbol for deviatoric stress.

The stress tensor is symmetrical, that is, each component above the diagonal has an equivalent component of equal magnitude below it: $\sigma_{yx} = \sigma_{xy}$, $\sigma_{zx} = \sigma_{xz}$, $\sigma_{yz} = \sigma_{zy}$. Thus, the stress tensor consists of only six independent numbers: three normal stresses (written in the diagonal) and three shear stresses (the off diagonal terms).

The state of stress described by eq. 144 can be expressed a bit more simply in a differently oriented coordinate system. Because of the symmetry of the stress tensor, it is always possible to assume a coordinate system with the coordinates x', y' and z', in which all shear stresses (all off diagonal terms in eq. 144) become zero. The diagonal components in this new coordinate system are called *principal stresses*. Principal stresses are denoted with a single subscript as σ_1, σ_2 and σ_3. In the Earth sciences it is common to use the

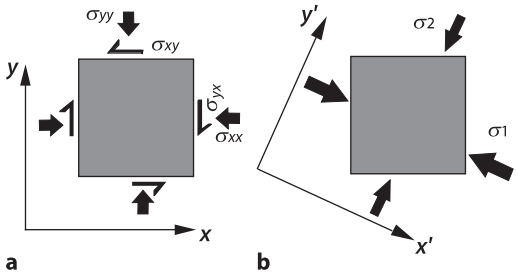

Figure 68: **a** The state of stress of a unit square within the two dimensions of this book page. In two dimensions, the stress tensor has only four independent components illustrated here by the four labeled arrows. In **b** the coordinate system x', y', z' was chosen in such an orientation so that the shear stresses become zero. The normal stresses become therefore *principal stresses*. The state of stress of the square in **a** and **b** is identical.

subscript "1" for the largest principal stress and "3" for the smallest. Thus, the state of stress at a point may always be characterized by only three principal stresses (Fig. 68):

$$\sigma' = \begin{pmatrix} \sigma'_{xx} & 0 & 0 \\ 0 & \sigma'_{yy} & 0 \\ 0 & 0 & \sigma'_{zz} \end{pmatrix} = \begin{pmatrix} \sigma_1 & 0 & 0 \\ 0 & \sigma_2 & 0 \\ 0 & 0 & \sigma_3 \end{pmatrix} \quad . \tag{145}$$

The order in which σ_1, σ_2 and σ_3 appear in eq. 145 implies that the new coordinate system was chosen here so that the x'-axis is parallel to the largest of the three principal stresses. Of course this need not be the case. Also note that the numbers denoting the three principal stresses have nothing to do with the spatial subscripts we briefly used in eq. 144. They simply refer to the largest, the intermediate and the smallest of the three principal stresses.

Fortunately, in the Earth's crust the principal stresses are often oriented roughly parallel to the vertical and the horizontal directions, because the shear stresses at the earth's surface (e.g. by wind) and at the base of the lithosphere (e.g. by mantle convection) are both negligible.

14.1.3 Mean Stress

The *mean stress* σ_m is given by the mean of the three principal stresses. It is therefore independent of the coordinate system:

$$\sigma_\mathrm{m} = P = \frac{\sigma'_{xx} + \sigma'_{yy} + \sigma'_{zz}}{3} = \frac{\sigma_1 + \sigma_2 + \sigma_3}{3} \quad . \tag{146}$$

The mean stress is also called pressure P. Strictly speaking, the mean stress is the mechanical definition of pressure, while a chemist or thermodynamicist would say that work is the product of pressure and volume change and that, therefore, pressure has the units of energy per volume (1 Pa = 1 J m^{-3}). The most common place where geologists encounter these non-intuitive units for pressure is when looking up the molar volumes of mineral phases. These are generally quoted in the units Joule per bar. As the volume change may be highly anisotropic in an anisotropic stress state, chemically defined pressure may be determined by integrating the volume change over the surface of a unit volume.

14.1.4 Differential Stress

Differential stress is a scalar value defined as the difference between the largest and the smallest principal stress:

$$\sigma_{\mathrm{d}} = \sigma_1 - \sigma_3 \quad . \tag{147}$$

It is a measure of how far the stress state deviates from the isotropic state. As such, differential stress relates directly to deviatoric stress τ. In fact, we will see that $\tau_1 = \sigma_{\mathrm{d}}/2$ and that $\tau_3 = -\sigma_{\mathrm{d}}/2$. During viscous (ductile) deformation, the application of any differential stress will cause permanent deformation.

14.1.5 Deviatoric Stress

Unlike mean stress, pressure or differential stress, *deviatoric stress* is not a single number, but a tensor, denoted commonly with τ. This tensor is defined by the deviation of the stress tensor in a general coordinate system (i.e. eq. 144) from the mean stress (i.e. pressure):

$$\tau = \begin{pmatrix} \tau_{xx} & \tau_{xy} & \tau_{xz} \\ \tau_{yx} & \tau_{yy} & \tau_{yz} \\ \tau_{zx} & \tau_{zy} & \tau_{zz} \end{pmatrix} = \begin{pmatrix} \sigma_{xx} - P & \sigma_{xy} & \sigma_{xz} \\ \sigma_{yx} & \sigma_{yy} - P & \sigma_{yz} \\ \sigma_{zx} & \sigma_{zy} & \sigma_{zz} - P \end{pmatrix} \quad . \tag{148}$$

It can be seen that the total stress tensor is the sum of the isotropic stress tensor plus the deviatoric stress tensor:

$$\begin{pmatrix} \sigma_{xx} & \sigma_{xy} & \sigma_{xz} \\ \sigma_{yx} & \sigma_{yy} & \sigma_{yz} \\ \sigma_{zx} & \sigma_{zy} & \sigma_{zz} \end{pmatrix} = \begin{pmatrix} P & 0 & 0 \\ 0 & P & 0 \\ 0 & 0 & P \end{pmatrix} + \begin{pmatrix} \sigma_{xx} - P & \sigma_{xy} & \sigma_{xz} \\ \sigma_{yx} & \sigma_{yy} - P & \sigma_{yz} \\ \sigma_{zx} & \sigma_{zy} & \sigma_{zz} - P \end{pmatrix} \quad . \tag{149}$$

This equation may also be writte in short as:

$$\sigma = P\underline{1} + \tau \quad . \tag{150}$$

where $\underline{1}$ is the identity matrix. In the viscous regime, only deviatoric stresses (right hand term in eq. 149) cause deformation. In contrast, elastic deformation occurs in response to the total stress state as described by the left hand side of eq. 149 (Fig. 69).
For a coordinate system parallel to the principal stress directions the deviatoric stress tensor may simply be written as (in analogy to eq. 145):

$$\tau' = \begin{pmatrix} \tau'_{xx} & 0 & 0 \\ 0 & \tau'_{yy} & 0 \\ 0 & 0 & \tau'_{zz} \end{pmatrix} = \begin{pmatrix} \sigma_1 - \sigma_{\mathrm{m}} & 0 & 0 \\ 0 & \sigma_2 - \sigma_{\mathrm{m}} & 0 \\ 0 & 0 & \sigma_3 - \sigma_{\mathrm{m}} \end{pmatrix} \quad . \tag{151}$$

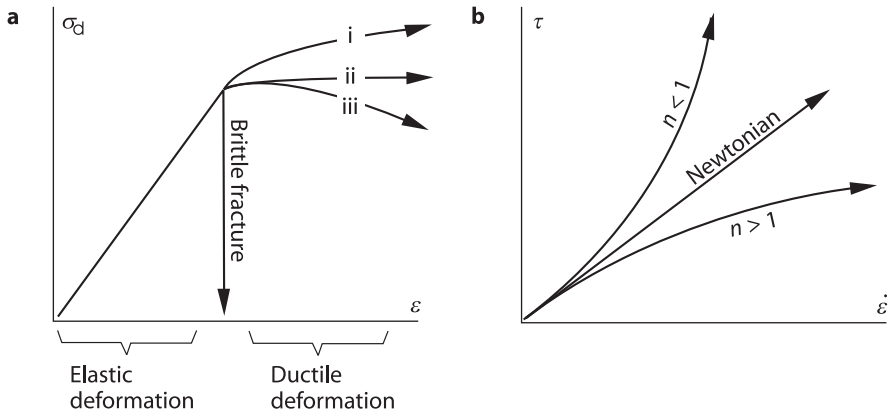

Figure 69: **a** Relationship between stress σ and strain ϵ for elastic, plastic and brittle deformation. Curve *ii* is for the ideal case of plastic (ductile) deformation; *i* is with strain hardening; *iii* with strain softening. **b** Relationship between stress and strain rate $\dot{\epsilon}$ for three different viscous materials. For a Newtonian fluid this relationship is linear. The number n is the power law exponent.

• **Simple examples for the use of deviatoric stress** The deviatoric stress tensor is important as its components cause viscous deformation. The absolute magnitude of the deviatoric stress tensor components indicates how rapidly a rock will strain (deform). A rock will *extend* in the direction in which the deviatoric stress components are negative (negative is tensional in the Earth science convention), even if all the principal stresses indicate compression (s. Fig. 70). Thus, when making cartoons of a field terrain it is always most instructive to sketch arrows for the principal components of the deviatoric stress tensor onto them, as their magnitude and direction corresponds to what is observed kinematically in the field (s. Fig. 65). Two rocks from different crustal levels may suffer the same deviatoric stresses and therefore deform similarly, but they may be in completely different states of total stress.

Let us consider a simple two dimensional example (there are only two principal stresses σ_1 and σ_2) where both σ_1 and σ_2 are positive (the rock is under compression) and the mean stress is $\sigma_\mathrm{m} = (\sigma_1 + \sigma_2)/2$. Then, according to eq. 149, the principle components of deviatoric stress are: $\tau_1 = \sigma_1 - \sigma_\mathrm{m} = (\sigma_1 - \sigma_2)/2$ and $\tau_2 = \sigma_2 - \sigma_\mathrm{m} = -(\sigma_1 - \sigma_2)/2$. We can see that the largest principal component of the deviatoric stress tensor is $\tau_1 = \sigma_\mathrm{d}/2$ and the smallest is $\tau_2 = -\sigma_\mathrm{d}/2$. We can summarize this information with a more applied example of a continent that is under horizontal compression where the principle components of stress σ_{xx} and σ_{zz} are parallel to the horizontal (x) and vertical (z) directions. There, the principle horizontal deviatoric stress is:

$$\tau_{xx} = \sigma_{xx} - \sigma_\mathrm{m} = \frac{\sigma_{xx} - \sigma_{zz}}{2} = \frac{\sigma_\mathrm{d}}{2} \quad . \tag{152}$$

Fig. 70 illustrates the state of stress of a rock cylinder as expressed in terms of the deviatoric stresses (left) and total stresses (right).

14.1.6 Strength

Strength, *failure strength* or *shear strength* are terms used to describe the critical value

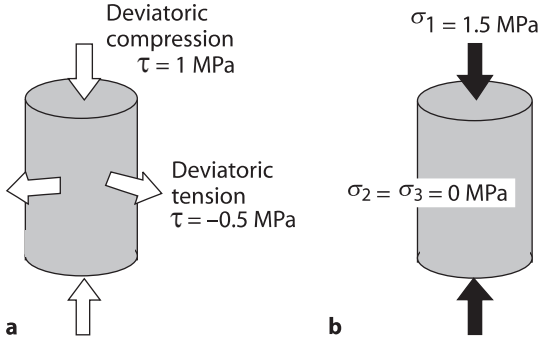

Figure 70: Cartoon illustrating a typical uniaxial deformation experiment. The state of deviatoric stress of the cylinder in **a** is identical to that of the cylinder in **b**. However, in **a** it is not specified what the confining pressure is. This may be an arbitrary number added to all deviatoric stress values. Nevertheless, if there is no additional confining pressure, then **a** is consistent with the pressure inside both cylinders being 0.5 MPa, although both σ_d and σ_1 are 1.5 MPa. In **a** the state of stress is illustrated in terms of the components of the deviatoric stress tensor. In **b** in terms of the uniaxially applied stress. Because the experiment is uniaxial, all illustrated stress components are also principal stress components both for the deviatoric stresses in **a** and the applied stress in **b** (after Engelder 1994).

which the differential stress must reach to cause permanent deformation. As such it is a material property. In the *elastic* regime, the term "strength" does not really have a meaning and it is better to refer to rigidity or other terms explained in some more detail in section 8.1 and 9.0.6. In the *brittle* regime, the strength depends directly on the magnitude of the principal stresses and is given by the stress where the curve on Fig. 69a deviates from its linear course. In the *viscous* regime, all differential stresses will lead to permanent deformation (Fig. 69). and "strength" is dependent on strain rate. Strictly, therefore, strength has no meaning in viscous deformation either and it is better to describe viscous stresses via viscosity. Nevertheless, here we use the terms "strength", "viscous strength" and "differential stress" in a similar meaning and note that they relate by a factor two:

$$\text{strength} = \frac{\sigma_\mathrm{d}}{2} \quad . \tag{153}$$

14.1.7 Stress Balance

The equations describing the balance of stresses are the basics for all mechanical descriptions of deformation. A stress balance is a generalized form of Newton's second law:

$$\text{force} = \text{mass} \times \text{acceleration} \quad . \tag{154}$$

This equation is applied to a small volume of rock which may be subjected to surface forces (applied to the surfaces of the small volume, e.g. by pushing it) and body forces (applied to the small volume itself, e.g. by gravity). Eq. 154 has its only complication in that it is a vector equation, because force is a vector. That is, it consists of three equations each of which describe a force balance in one of the three spatial directions. Also, within each of these equations, several *surface* and *body forces* must be summed up and set equal to the product of mass times acceleration on the right hand side of the equations. Also note that

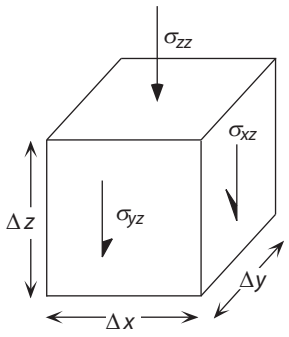

Figure 71: Different surface forces acting on a unity cube in the z direction. If z is the vertical, then there is also a body force due to gravity of the magnitude ρg. At rest, each of the three labeled forces is compensated by a force of equal magnitude but opposite direction. Other forces in the y- and x-directions are not labeled for clarity.

the equations of force balance are generally considered per unity volume so that eq. 154 is usually written in terms of force/volume = density × acceleration. The different forces acting in the z direction can be summed up from Fig. 71. The sum is:

$$\left(\sigma_{zz} + \frac{\partial \sigma_{zz}}{\partial z}\Delta z\right)\Delta x\Delta y - \sigma_{zz}\Delta x\Delta y + \left(\sigma_{zx} + \frac{\partial \sigma_{zx}}{\partial x}\Delta x\right)\Delta y\Delta z$$
$$-\sigma_{zx}\Delta y\Delta z + \left(\sigma_{zy} + \frac{\partial \sigma_{zy}}{\partial y}\Delta y\right)\Delta x\Delta z - \sigma_{zy}\Delta x\Delta z - \rho g\Delta x\Delta y\Delta z$$
$$= \rho a_z \Delta x\Delta y\Delta z \quad , \tag{155}$$

where x, y and z are the three spatial directions, ρ is density, g is acceleration due to gravity and a_z is the acceleration of the body in the z direction. Even if this equation appears enormously complicated, it should be easy to follow it using Fig. 71. It simply states that the difference in forces between any two sides of a unity cube result in acceleration. We can see that the equation has six similar looking terms on the left hand side. Every group of two terms describes a difference between the force on one side of the cube (e.g. the 2nd term in eq. 155: $\sigma_{zz}\Delta x\Delta y$) and the force on the opposite side of the cube (e.g. the 1st term in eq. 155: $(\sigma_{zz} + (\partial\sigma_{zz}/\partial z)\Delta z)\,\Delta x\Delta y$). If these are equally large, then the body does not accelerate. If this difference is finite, then the body accelerates with the rate written on the right hand side of the equation: $\rho\frac{\partial u_z}{\partial t}\Delta x\Delta y\Delta z$. Writing eq. 155 a bit shorter we can write:

$$\frac{\partial \sigma_{zx}}{\partial x} + \frac{\partial \sigma_{zy}}{\partial y} + \frac{\partial \sigma_{zz}}{\partial z} - \rho g = \rho a_z \quad . \tag{156}$$

• **Navier-Stokes equation** Eq. 156 (plus its corresponding versions for the x and y directions) can be reformulated into the famous Navier-Stokes equation if it is coupled with a viscous flow law. We will encounter this in eq. 108, but use it already here briefly to introduce this important equation. We also need the definition of strain rate from eq. 143 and the relationship between the stress and deviatoric stress tensors shown in eq. 150. Then, we can insert the definition of strain rate into eq. 108 and that into eq. 150. The resulting description of stress is then differentiated according to eq. 156 and we arrive at the Navier-Stokes equation for an incompressible medium with constant viscosity:

$$-\nabla P + \eta\nabla^2 u = \rho a + \rho g \quad , \tag{157}$$

In this form, we have placed both acceleration terms (that due to surface forces and that due to body forces) on the right hand side of the equation. In particular the surface force

related to acceleration (which is a instead of the earlier a_z meaning that acceleration may be in all three directions) can also be expressed in terms of velocity changes, but we need not do this here, as we will show below that is is negligible for most geological problems.

• **Force balance equations** In most geodynamic problems, acceleration is negligible. Then, in the horizontal directions the term $\rho\frac{\partial u_x}{\partial t} = \rho\frac{\partial u_y}{\partial t} \rightarrow 0$ and in the vertical direction $\rho\frac{\partial u_z}{\partial t} \rightarrow \rho g$, as gravitational force is still felt as a body force. Thus, eq. 155 simplifies to the following:

$$\frac{\partial \sigma_{zz}}{\partial z} + \frac{\partial \sigma_{zx}}{\partial x} + \frac{\partial \sigma_{zy}}{\partial y} - \rho g = 0 \quad . \tag{158}$$

Eq. 156 describes the equilibrium of stresses in the vertical direction and is generally applicable in the earth sciences. The first three terms of this equation are the sum of the *surface forces* acting in the z-direction, the fourth term is the *volume* or *body force* downwards. In analogous equations for the x- and y-direction this fourth term does not appear. The relationships for the x- and y-directions are formulated correspondingly, but without the accelleration term due to gravity.

14.1.8 Tectonic Relevance of Momentum

In this section we discuss the nature and relevance of momentum in tectonic processes to show that momentum is practically negligible to most geological problems. The momentum of a body I is given by the product of its mass m and its velocity v (sect. **??**):

$$I = mv \quad . \tag{159}$$

While the velocities of plate tectonic motions are very small, the mass of plates is very large and it is therefore not immediately obvious if momentum plays a role in the tectonic force balance.

Momentum is a physical quantity that is preserved: During the collision of two plates the momentum of the entire system remains constant. However, the momentum of one of the plates may be transferred to the other. This transfer of momentum occurs by a force. The magnitude of this force is given by the change of momentum ΔI per time Δt that occurs during the slowing of plate motion due to collision.

$$F = \frac{\Delta I}{\Delta t} \quad . \tag{160}$$

If a plate is slowed down due to collision very abruptly, then the force is large. If it slows over a large time period, the force is small. The slowing of a plate has also the consequence that its kinetic energy E_k decreases. Kinetic energy is given by the integrated momentum integrated over the change in velocity:

$$E_\mathrm{k} = \frac{mv^2}{2} \quad . \tag{161}$$

Let us now check if momentum, kinetic energy and the forces that arise from them could be responsible for the acceleration or slowing of plates. For this, let us hypothesize that the slowing of a continental collision is caused by a waning momentum. Lets use the India-Asia collision and make some very simple assumptions. The area of the Indo-Australian

Plate is roughly $A = 5 \cdot 10^6$ km^2. If the mean plate thickness is $z_\mathrm{l} = 100$ km and the mean density is $\rho = 3\,000$ kg m^{-3} then its mass is: $m = Az_\mathrm{l}\rho = 1.5 \cdot 10^{21}$ kg. If the relative plate velocity between India and Asia is $v = 0.1$ m y^{-1} $\approx 3.2 \cdot 10^{-9}$ m s^{-1}, then, according to eq. 159, the momentum of the collision is: $I = mv = 4.7 \cdot 10^{12}$ kg m^{-1} s^{-1} and the kinetic energy of the Indian Plate is: $E_\mathrm{k} = 7.6 \cdot 10^3$ J. If we now assume that the Indian Plate will be brought to a complete halt within one million year of the collision, then: $F = 4.7 \cdot 10^{12}/3.15 \cdot 10^{13} \approx 0.15$ N. Distributed over almost 5000 km of collision length this leaves only about: $3 \cdot 10^{-8}$ N m^{-1}. We can infer that plates would have to be brought to a halt within fractions of a second of a collision in order for momentum to have any influence on the orogenic force balance. In short, momentum is negligible in plate tectonics.

14.1.9 The Difference Between Lithostatic and Non-Lithostatic

The pressure measured by petrologists with geobarometers in metamorphic rocks is generally interpreted as the "burial pressure", that is, the pressure is directly correlated with the depth of the rocks at the time of metamorphism. This interpretation is based on the assumption that rocks have negligible strength, i.e. they cannot support any differential stress. This state of stress is called *lithostatic*. In this state, the *lithostatic pressure* is of the same magnitude as each of the principal stresses (eq. 146). The state of stress is isotropic. However, if we consider a more general state of stress (i.e. a material that *can* support differential stresses), then we can see that only part of the pressure is caused by depth. The magnitude of the difference $\sigma_1 - \sigma_3$ also contributes to pressure and the orientation of σ_1, σ_2 and σ_3 determines how pressure relates to depth. The discussion on the magnitude of the differential stress $\sigma_1 - \sigma_3$ in rocks can be summarized under the term "tectonic overpressure" (Rutland 1965; Ernst 1971).

For some special orientations of a general stress field it is possible to divide pressure into a lithostatic and a non lithostatic component. Such a division helps to illustrate the different contributions to pressure and allows us to estimate the magnitude of differential stresses under different boundary conditions. In a stress field where σ_1 and σ_3 are the maximum and minimum principle stresses and are oriented horizontally and vertically, respectively we can write:

$$P = \frac{\sigma_1 + \sigma_3}{2} = \sigma_3 + \frac{\sigma_1 - \sigma_3}{2} = \sigma_\mathrm{lith} + \frac{\sigma_\mathrm{d}}{2} = \rho g z + \tau_1 \quad . \tag{162}$$

There, σ_lith is the component of pressure caused by the weight of the overlying rock column, and the non-lithostatic component is given by the largest principal component of the deviatoric stress tensor. Of course, eq. 162 is only valid if $\sigma_2 = (\sigma_1 + \sigma_3)/2$. For other values of σ_2, or for differently oriented stress fields, this simple subdivision in lithostatic and non-lithostatic terms of pressure is not possible and non-lithostatic components of pressure can only be calculated from the complete tensor.

FRAGENKATALOG

Der im Folgenden aufgelistete Katalog an Prüfungsfragen enthält genau 10 Fragen pro Einheit. Die Fragen wurden so ausgewählt, dass die wichtigsten Teile jeder Einheit repräsentativ abgedeckt sind und kann benutzt werden um Ihr Verständnis des gesamten Lehrveranstaltungs Inhalts zu prüfen. Auch wenn ich Ihnen nicht versprechen kann, dass die Prüfungsfragen zur LV GEO.916 genau den hier aufgelisteten Fragen in Zahlenwerten und Formulierungen exakt entsprechen, so kann ich Ihnen versichern, dass Sie mit einem Verständnis dieser Fragen perfekt abschneiden werden.

1. EINHEIT: Die Diffusionsgleichung

- **1.1:** Was ist Fourier's 1. Gesetz? (ANTWORT: Der empirische Zusammenhang zwischen Wärmefluss und Temperaturgradient. Die Wärmeleitfähigkeit, k, [J/(smK)] is die Proportionalitätskonstante).

- **1.2:** (a) Wie gross ist Wärmeleitfähigkeit von Gesteinen und (b) was ist Wärmefluss? (ANTWORT: k = 2 - 5 [J/(smK)]. Wärmefluss ist die Energie die pro Zeit durch 1 m^2 fliesst. Das ist Leitfähigkeit $\times$ Temperaturgradient = [W/m^2]).

- **1.3:** Was ist Fouriers 2. Gesetz? (ANTWORT: Ein Energiegleichgewicht. Es beschreibt den Zusammenhang zwischen Rate der Temperaturänderung und räumlicher Änderung des Wärmeflusses).

- **1.4:** Wie rechnet man Wärme (H) in Temperatur (T) um? (ANTWORT: Mittels Wärmekapazität (c_p) und Dichte (ρ): $T = H/(\rho \times cp)$).

- **1.5:** Was ist Wärmekapazität? (ANTWORT: Jener physikalische Parameter, der aussagt wie viele Joule gebraucht werden um ein Kilo Masse um 1 Grad zu erwärmen. Für Steine etwa 1000 [J/(kg K)]).

- **1.6:** Wie gross ist die Dichte von Gesteinen? (ANTWORT: $\rho \approx$ 2700 (Granit) - 3300 (Mantelmaterial bei null Grad Celsius) [kg/m^3]).

- **1.7:** Was ist Diffusivität? (ANTWORT: $\kappa = k/(\rho \times cp)$. Für Diffusion von Wärme in Gesteinen ist das etwa: $\kappa = 10^{-6}$ [m^2/s]).

- **1.8:** Die Diffusivität von Kationen in Kristallen, D, ist stark Tempartur abhängig und folgt der Arrhenius Beziehung: $D_{(T)} = D_0 e^{(-Q/(RT)}$. Berechne die Kationen Diffusiviät in Granat bei 100 °C, 300 °C und 500 °C und vergleiche diese Werte mit der thermischen Diffusivität ($\kappa \approx 10^{-6}$[$m^2 s^{-1}$]). Die Materialkonstanten für Granat sind: Q = 239 000 [J mol^{-1}], $D_0 = 9.81 \cdot 10^{-9}$[m^2 s^{-1}]. Die Gas Konstante ist: R = 8.3 [J $mol^{-1} K^{-1}$]. (ANTWORT: $D_{(100)} = 2.9 \times 10^{-42}$ [m^2/s]; $D_{(300)} = 1.5 \times 10^{-30}$ [m^2/s]; $D_{(500)} = 6.5 \times 10^{-25}$ [m^2/s]. Diese Werte sind 19 - 36 Grössenordnungen kleiner als die thermische Diffusivität).

- **1.9:** Was besagt das Wort "Diffusion"? (Also: beschreiben Sie die Diffusionsgleichung in Worten). (ANTWORT: Die Rate der Temperaturänderung ist proportional zur räumlichen Krümmung des Temperatur Profils).

- **1.10:** In welchen Bereichen der Erdwissenschaften ist die Diffusionsgleichung wichtig? (ANTWORT: Hydrogeologie, Geomorphologie, Petrologie, Temperaturmodellierung).

2. EINHEIT: Kontinentale Geothermen

- **2.1:** (a) Wie gross ist die radioaktive Wärmeproduktion, $S_{\rm rad}$, an der Erdoberfläche und (b) welche Elemente verursachen sie? (ANTWORT: (a) Einige Mikrowatt pro Kubikmeter: $S_{\rm rad}$= 1 - 5 * 10^{-6} [W/m^3]); (b) Uran, Thorium und Kalium).

- **2.2:** Wie würde man erwarten, dass die radioaktiven Elemente in der Erdkruste verteilt sind ohne etwas darüber zu wissen? (ANTWORT: Weil U und Th inkombatible Elemente sind und Kalium ein wesentlicher Bestandteil von Granit ist, ist die Radioaktivität von fraktionierten Gesteinen (z.B. Rest- und Erstschmelzen) am höchsten. Daher gibt es im Mantel kaum Radioaktivität. In der Kruste nimmt die Radioaktivität mit Tiefe ab, weil Schmelzereignisse in präkambirschen Schilden diese immer wieder nach oben fraktioniert haben).

- **2.3:** (a) Was ist die messbare Evidenz dafür, dass nicht die gesamte Erdkruste (Mächtigkeit z_c) so radioaktiv ist wie die Erdoberfläche? (b) Zeige, dass im Ergebnis von (a) die Einheiten stimmen? (ANTWORT: (a) Der radiogen verursachte Wärmefluss an der Erdoberfläche, $q_{\rm rad}$, ergibt sich aus Wärmeproduktion mal die Mächtigkeit der radioaktiven Schicht. Daher: $q_{\rm rad} = S_{\rm rad} * z_c$. Bei einigen Mikrowatt pro Kubikmeter und normaler Krustenmächtigkeiten ergibt sich daraus $q_{\rm rad} \approx 0.1$ [W/m^2], also deutlich höher als der gemessene Wärmefluss an der Erdoberfläche). (b) $S_{\rm rad}$[W/m^3] $\times$ z_c [m] = [W/m^2]. Das ist die Einheit von Wärmefluss).

- **2.4:** Aus welchen 2 Beiträgen setzt sich der Oberflächenwärmefluss, q_s zusammen und wie gross sind diese Beiträge etwa? (ANTWORT: radiogen verursachter und Mantelwärmefluss: q_s (40 - 60 [mW/m^2]) = $q_{\rm rad}$ (20 - 30 [mW/m^2]) + q_m (20 - 30 [mW/m^2])).

- **2.5:** Warum ist die Annahme einer Randbedingung an der Basis der Lithosphäre (z_l) eine (a) gute und (b) schlechte Annahme für die Berechnung von stabilen kontinentalen Geothermen (ANTWORT: (a) Es ist eine gute Annahme weil die Lithosphäre thermisch definiert ist und daher definitionsgemäss die Temperaturen bei $z > z_l$ durch Konvektion vereinheitlicht werden und Wärmeleitung nicht mehr der dominierende Wärmetransportmechanismus ist. (b) Es ist eine schlechte Annahme weil wir nicht sehr gut wissen wie mächtig die Lithosphäre ist. Wir wissen viel besser über Tiefe, Wärmefluss und Temperatur der Moho bescheid).

- **2.6:** Wir haben die Diffusionsgleichung Gl.11 integriert und dabei konstante Temperatur an der Basis der Lithosphäre angenommen, um die Integrationskosntanten zu bestimmen. Eine oft bessere (weil besser bekannte) Annahme als Randbedingung ist konstanter Mantelwämefluss an der Moho. Integriere Gl.11 mit dieser Randbedingung. (Annahme: Die Wärmeproduktion ist konstant). (ANTWORT: $k\partial^2 T/\partial z^2 = -S$ daher: $k\partial T/\partial z = -Sz + C_1$. Daraus ergibt sich: $C_1 = z_c S + q_m$. Die 2. Integration ist dann trivial und mit $T = 0$ bei $z = 0$ ergibt sich: $C_2 = 0$).

- **2.7:** Das Diagramm in Abb. 6 zeigt Messdaten von Oberflächenwärmefluss und Wärmeproduktionsrate, ebenfalls an der Erdoberfläche gemessen. Wie kann man die Steigung und Verschnitt der Daten mit der q-Achse in diesem Diagramm interpretieren und wie gross sind die Werte? (ANTWORT: Zeichnung mit Beschriftung von Zahlenwerten für: Steigung: Tiefenausdehnung der radiogenen Wärmeproduktion, Verschnitt mit der q Achse ist der Mantelwärmefluss).

– **2.8:** Was ist die maximal zu erwartende Änderung des Oberflächenwärmeflusses q_s wenn die gesamte Lithosphäre gleichmässig: (a) aufs doppelte verdickt wird (b) auf die Hälfte ausgedünnt wird? (Nimm an dass radioaktiver (q_{rad}) und Mantelwärmefluss (q_m) gleich gross sind). (ANTWORT: (a) Bei der Verdickung wird der Oberflächenwärmefluss zu: $q_s = 2 \times q_{\rm rad} + 0.5 \times q_m$ (b) Bei Ausdünnung auf 50 Prozent wird $q_s = 0.5 \times q_{\rm rad} + 2 \times q_m$. D.h. Wenn $q_{\rm rad} = q_m$ ändert sich in beiden Fällen gleich viel und nur um etwa 20 Prozent).

– **2.9:** Eine radiogene Wärmequelle produziert $S_{\rm rad} = 10 \times 10^{-6}$ [W/m^3]. Was ist die Rate der Erwärmungs des Gesteins unter der Annahme normaler Dichte und Wärmekapazitäten. (ANTWORT: $dT/dt = S/(\rho c_p)$. Mit $\rho \approx 3000$ [kg/m^3] und $c_p \approx 1000$ [J/(kg K)] ist das knapp 100 Grad pro Million Jahre).

– **2.10:** Verwende Gl. 26 oder Gl. 27 um (a) die Temperatur an der Moho (bei $z = 30$ km) auszurechnen (b) um die Temperatur an der Moho in einer Lithosphäre in der die Kruste verdoppelt ist und der Mantelteil der Lithoshpäre konstant geblieben ist (ANTWORT: siehe Abb. 9).

3. EINHEIT: Ozeanische Geothermen

– **3.1:** Was ist die "Fehlerfunktion"? (ANTWORT: Es ist eine analytisch unlösbare Funktion, die bei der Integration der zeitabhängigen Diffusionsproblemen oft vorkommt. Die Fehlerfunktion von x ist bei $x = 0$ gleich Null und nähert sich für grosse x an 1 an. Bei $x = 1$ ist die Fehlerfunktion bei etwa 0.85).

– **3.2:** Skizziere die Anfangs- und Randbedingungen für die diffusive Äquilibrierung eines unendlichen Halbraumes. (ANTWORT: siehe Skizze in Abb. 72).

Figure 72: Illustration zu Frage 3.2.

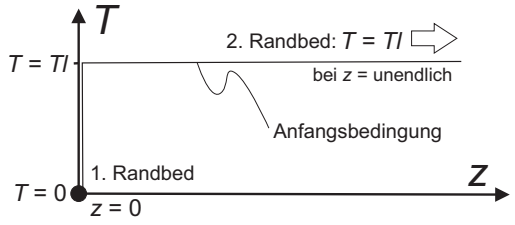

– **3.3:** Welche Randbedingungen sind eine vernünftige Annahme für die Berechnung ozeanischer Geothermen mittels der Diffusionsgleichung? (ANTWORT: Dass die Temperatur an der Oberfläche immer bei Null bleibt und in unendlicher Tiefe immer bei Asthenosphärentemperaturen um 1200°C bleibt).

– **3.4:** Welche Anfangsbedingungen werden typischerweise zur Berechnung ozeanischer Geothermen angenommen? (ANTWORT: Dass die Temperatur Verteilung mit Tiefe überall konstant ist und die Temperatur der Asthenosphäre (T_l) hat).

– **3.5:** Ein mittelozeanischer Rücken riftet mit $u = 2$ Zentimeter pro Jahr. Schätze ab wie mächtig die ozeanische Lithosphäre $x = 500$ km vom Rücken ist. (ANTWORT: Bei der Riftrate ist die ozeanische Lithoshäre 500 km vom Rücken $t = x/u = 25$ Millionen Jahre alt. Mit der Beziehung: $t_{eq} = l^2/\kappa$ ergibt sich als Schätzung $l \approx$ knapp 10 Kilometer).

- **3.6:** Sie haben gerade ein 1000 km langes Profil (weg vom mittelozeanischen Rücken x) von Wärmeflussmessungen im Atlantik gemessen und wollen Ihre Messdaten mit einer Kurve fitten. Was für eine Funktion nimmt man am besten? (ANTWORT: Eine Quadratwurzelfunktion, denn das einfachste Modell für die Entwicklung ozeanischer Lithosphäre sagt vorher, dass der Wärmefluss mit dem Abstand vom mittelozeanischen Rücken mit der Funktion $\sqrt{x}$ abnehmen sollte).

- **3.7:** Wie wurde das "Half-space-cooling" als ein erfolgreiches Modell für das altern ozeanischer Lithosphäre bewiesen? (ANTWORT: Durch Wärmeflussmessungen am Ozeanboden).

- **3.8:** Nenne eine "Eselsbrücke", die zum Umrechnen verschiedener SI Einheiten dienen können. (ANTWORT: (a) Arbeit = Kraft × Weg; ([J]=[N]×[m]); (b) Kraft = Masse × Beschleunigung ([N]= [kg]×[m s^{-2}]); (c) "E = Mc^2 " ([J]=[kg]× [m^2/s^2]). (c) Druck = Kraft/Fläche ([Pa]=[N]/[m^2]); (d) Druck = Energie/Volumen ([Pa] = [J]/[m^3])).

- **3.9:** Wieviel ist eine hfu (Heat flow Unit); 1 hfu = 10^{-6} [cal s^{-1} cm^{-2}]; 1 [cal] = 4.18 [J]) in SI Einheiten? (ANTWORT: 1 [hfu] = 0.041 [W/m^2]).

- **3.10:** Zeichnen Sie ein Profil durch einen Mittelozeanischen Rücken, beschriften Sie es mit mehreren kleinen $T - z$ Profilen an verschiedenen Stellen und kennzeichnen Sie (a) Wassertiefe, (b) Wärmefluss, und (c) Alter. (ANTWORT: Abb. 12 mit zusätzlich eingezeichneter Kruste).

4. EINHEIT: Intrusionen

- **4.1:** In kontaktmetamorphen Terrains würde man welche Beziehung aus metamorphem Grad und Alter der Metamorphose erwarten? (ANTWORT: Je höher gradig, desto früher (also älter) ist der Zeitpunkt des metamorphen Peaks).

- **4.2:** Wie gross ist die Schmelzwärme von Gesteinen? (ANTWORT: Etwa 300000 [J/kg]).

- **4.3:** Bei der Kristallisation eines Granitkörpers (a) wird wieviel Wärme frei? und: (b) Der Granit kann nicht weiter abkühlen bis nicht alle Schmelze kristallisiert ist. Wie lange dauert das? (ANTWORT: (a) L = etwa 300 kilo Joule pro Kilogramm Schmelze. (b) Bis das Äquivalent der Schmelzwärme dem Gestein entzogen wurde. In Grad Celsius ausgedrückt ist das bis der Granit $L/cp = 300°C$ weiter abgekühlt wäre).

- **4.4:** Zeichne (rein qualitativ) die mögliche Temperatur-Zeit Geschichte eines Migmatitit Terrains bei konstantem Wärme Input. (ANTWORT: Ein Temperatur-Wärmediagramm auf dem ersichtlich ist, dass die Steigung der Kurve die Einheit von Wärmekapazität hat und dass die Temperatur-Zeit Kurve am Solidus isothermal gepuffert wird).

- **4.5:** Benutze die Beziehung $t_{eq} = L^2/\kappa$ um abzuschätzen wie lange ein Granitkörper von L=3 km Durchmesser braucht um abzukühlen. Die Schmelzwärme ist dabei zu vernachlässigen. (ANTWORT: Etwa 300000 Jahre).

- **4.6:** Zeichne Temperaturprofile zu drei charakteristischen Zeitpunkten nach der Intrusion, quer über einen granitischen Gang. (ANTWORT: Abb. 17).

- **4.7:** Was ist das "Stefan Problem"? (ANTWORT: Es behandelt die diffusive Abkühlung eines Mediums mit Phasenumwandlung bei gleichzeitiger räumlicher Verschiebung des Modellrandes durch Freiwerden von Wärme an der Kristallisationsoberfläche. Das Problem wurde zuerst von Stefan 1891 am Beispiel von frierendem Meerwasser quantifiziert).

- **4.8:** Was ist die Problematik von LPHT metamorphen Terrains? (ANTWORT: Dass das Verhältnis aus Peak Druck und Temperatur zu klein ist, als dass diese Terrains entlang einer monoton steigenden Geotherme gebildet wurden, aber dass die Evidenz für Kontaktmetamorphose erzeugende Intrusiva oft fehlt).

- **4.9:** Wieviel zusätzliche Joule bringt ein V=5 km^3 umfassender Pluton von 700°C in ein 300°C warmes Gebiet? Nehmen Sie Schätzwerte für Dichte ρ und Wärmekapazität c_p an (ANTWORT: Energie $= V \times \rho(c_p \times \delta T + L) = 9.45 \times 10^{18}$ [J]).

- **4.10:** Benutze die Beziehung: $T = T_\mathrm{b} + (T_\mathrm{i} - T_\mathrm{b})/2\left(\mathrm{erfc}(z/(\sqrt{4\kappa t})\right)$ um die Temperatur in 100 m Entfernung vom Kontakt eines sehr grossen Granitplutons 1000 Jahre nach dem Intrusionszeitpunkt zu berechnen. (T_b = 400°C; T_i = 700°C; $\kappa = 10^{-6}$ [m^2/s]). (ANTWORT: Mit Zuhilfenahme der Abb. 11 ergibt sich: 596°C).

5. EINHEIT: Wärmeproduktion und Advektion

- **5.1:** Kernreaktionen sind die einzigen Prozesse bei denen Masse in Energie verwandelt wird. Wie lange kann eine 60 W Glühbirne mit der Energie brennen, die bei der Umwandlung von 1 g Masse in Energie frei wird? (Zur Erinnerung: Energie = Masse × Lichtgeschwindigkeit^2. Die Lichtgeschwindigkeit ist: $\approx$300 000 [km s^{-1}]). (ANTWORT: Etwa 50000 Jahre).

- **5.2:** Diskutiere die geodynamische Wichtigkeit von Wärmeproduktion. (ANTWORT: Wärme kann radioaktiv (S_{rad}), chemisch (S_{chem}) und durch Reibung (S_{mec}) erzeugt werden. S_{rad} ist einige microwatt pro Kubikmeter an der Erdoberfläche und nimmt nach unten schnell ab. Trotzdem verursacht S_{rad} etwa 50% des Wärmebudgets der Kruste. S_{chem} ist nur für Prozesse wichtig wo Phasen umgewandelt werden, z.B. beim Schmelzen. Dort ist es ein wichitger Pufferprozess. S_{mec} ist schlecht erfasst, aber könnte bei hohen Verformungsraten und Spannungen durchaus grösser sein als S_{rad}).

- **5.3:** Ein Granitkörper produziert $S_\mathrm{rad} \approx 100$ Microwatts pro Kubikmeter. Schätzen Sie ab wie heiss der Körper nach t= 10^5 Jahren werden kann wenn man die Ableitung von Wärme vernachlässigt, c_p=1 000 [J kg^{-1}K^{-1}] and ρ = 2 700 [kg m^{-3}].

- **5.4:** Ein Migmatit enthält 30% Schmelze die alle am Solidus entstanden ist. Das Gestein kühlt von seiner Peak Temperatur weit über dem Schmelzpunkt mit einer konstanten Abkühlrate von $s = 100\,[^\circ\mathrm{C\,my}^{-1}]$ ab. Bestimme wie lange das Gestein am Solidus bleiben wird? Benutze dazu die Überlegungen von Gl.49 bis Gl.- 52 (Schmelzwärme ist: 320 000 [J kg^{-1}], Dichte: of ρ =2 700 [kg m^{-3}] und Wärmekapazität: c_p=1 000 [J kg^{-1} K^{-1}]). (ANTWORT: Die Zeit ergibt sich aus $t = LV/(sc_p) = 0.1$ my).

- **5.5:** Ein regionalmetamorphes Ereignis erfasst die ganze Kruste von L = 30 km Dicke. Gleichzeitig erodiert das dabei entstandene Gebirge an der Erdoberfläche und exhumiert die metamorphen Gesteine zur Erdoberfläche. Schätze mit Hilfe der Pecletzahl ($Pe = uL/\kappa$) ab, ob die thermische Entwicklung des Orogens nur mit der Wärmeleitungsgleichung beschrieben werden könnte oder ob die Advektion von Wärme durch die Erosion auch berücksichtigt werden müssten. Nimm an, dass die Erosionsrate folgende Werte

hat: (a) $u = 100$ m my^{-1}; (b) $u = 1\,000$ [m my^{-1}]; (c) $u = 5\,000$ [m my^{-1}]. Die Diffusivität $\kappa = 10^{-6}$[m^2/s]. (ANTWORT: Für (b) ist die Pecletzahl $Pe = 1$. Advektion und Leitung von Wärme sind beide relavant und müssen berücksichtigt werden. In (a) ist $Pe = 0.1$ sodass angenommen werden kann, dass Wärmeleitung dominiert und Advektion vernachlässigt werden kann. Für (c) ist das umgekehrt ($Pe = 5$, also deutlich grösser als 1.)).

– **5.6:** Zeige, dass das Produkt von Spannung und Verformungsrate die Einheiten von Wärmeproduktion hat. (ANTWORT: Spannung ist in [Pa]; Verformungsrate in [s^{-1}]. Daher: [Pa/s]= [N/(m^{2}s)] = [kg/(s^{3}m)]. Mit der Beziehung "Energie = Masse × Geschwindigkeit^2" ergibt sich: [kg/(s^{3}m)]= [W/m^3]).

– **5.7:** Das Molvolumen von Granat is etwa 11.5 [J bar^{-1}]. Wieviele Kubikzentimeter sind das? (1 bar = 10^5 Pascal). (ANTWORT: 115 Kubikzentimeter).

– **5.8:** Skizziere die Form von Isothermen in einem Profil um eine vertikale Störung deren rechte Seite mit 1 cm pro Jahr nach oben bewegt (und oben aberodiert) wird. Der geothermische Gradient vor der Bewegung war 20°C/km. Benutze die Pecletzahl um die Krümmung der Isothermen richtig zu zeichnen und beschrifte den Maßstab der Skizze).

– **5.9:** Welche Prozesse können Wärme in der Kruste advektieren? (ANTWORT: Erosion, Deformation, Fluide und Magma).

– **5.10:** Wieviel Masse wird beim Verbrennen von 5 [kg] Holz in Energie verwandelt? (ANTWORT: Gar nichts! (Es ist ja keine Kernreaktion). Alle 5 kg sind nachher in der Form von CO_2 und Wasser noch vorhanden. Die freiwerdende Energie ist ausschliesslich Reaktionswärme, so wie sie auch bei metamorphen Reaktionen frei bzw. konsumiert wird).

6. EINHEIT: Zusammenfassung und ausgewählte Probleme

– **6.1:** Skizziere die Temperaturverteilung in den obersten 3 Metern einer Bodenprofils zu 4 verschiedenen Jahreszeiten. (ANTWORT: Siehe Skizze Abb. 27).

– **6.2:** Was ist eine "analytische Lösung" einer Differentialgleichung? (ANTWORT: Die ausintegrierte Gleichung).

– **6.3:** Welche Methoden sind die bekanntesten um unlösbare Differentialgleichungen zu verwenden? (ANTWORT: Numerische Methoden wie finite Differenzen oder finite Elemente).

– **6.4:** Fassen Sie zusammen welche Wärmetransportmechanismen in der Lithosphäre relevant sein können? (ANTWORT: 1. Wärmeleitung (sehr langsam: $t = l^2/\kappa$); 2. Wärmeproduktion $S = S_{rad} + S_{mech} + S_{chem}$, wobei S_{rad} auf dem Maßstab der Kruste sehr viel ausmacht, S_{mech} eigentlich unbekannt ist weil die Scherfestigkeiten von Gesteinen so schlecht bekannt sind und S_{chem} ist nur als Puffer bei der Erwärmungs- oder Abkühlgeschichte von Migmatiten oder Intrusiva relevant. 3. Wärmeadvektion durch Magma, Erosion, Deformation (durch Fluide ist irrelevant). Die Pecletzahl $Pe = uL/\kappa$ hilft um den Maßstab abzuschätzen).

– **6.5:** Worauf ist bei der Interpretation von Spaltspuren- oder (U-Th)/He Datierungen im Hochgebirge zu achten und warum? (ANTWORT: Diese 2 Systems datieren 100°C bzw. 60°C. Diese Isothermen knnen im Hochgebirge (bei einem Relief von 2-3 km) bereits genug in die Topografie gebogen sein, sodass Erosionsraten aus Höhe-Alter Profilen überschätzt werden).

– **6.6:** Was sind (a) "Peclet Zahl" und (b) "Thermische Zeitkonstanten"? (ANTWORT: (a) Die Pecletzahl ist ein Maßder relativen Wichtigkeit von Advektion und Diffusionsprozessen. Sie ist durch $Pe = U \times L/\kappa$ gegeben. Die thermische Zeitkonstante ist ein Maßder Dauer der diffusiven Äquilibrierung. Sie ist $t_{eq} = L^2/\kappa$ gegeben).

– **6.7:** Skizziere einen Berg mit einem Probenahmeprofil vom Tal bis zum Gipfel und ein Alter-Höhe Diagramm daneben in dem hypothetische Spaltspuren Alter eingetragen sind die illustrieren warum man aus diesem Diagramm die Erosionsrate ablesen kann. (ANTWORT: siehe Skizze in Abb. 73).

Figure 73: Illustration zu Frage 6.7.

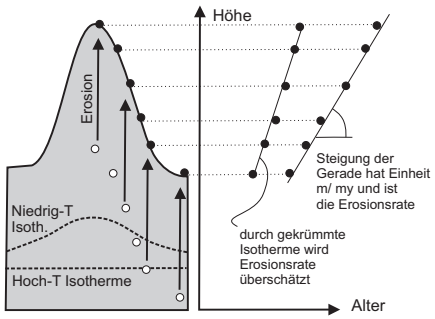

– **6.8:** Was sind (a) Randbedingungen und (b) Anfangsbedingungen in Zusammenhang mit der Lösung von Differentialgleichungen? (ANTWORT: Randbedingungen sind Informationen am räumlichen Modellrand, die notwendig snd um die Integrationskonstanten zu evaluieren. Anfangsbedingungen beschreiben bei zeitabhängigen Problemen die Ausgangssituation).

– **6.9:** Skizziere ein Tiefe-Temperatur Profil im Boden aus dem ersichtlich ist warum es in Österreich in mehr als 1 m Tiefe nie friert. (ANTWORT: Abb. 27).

– **6.10:** Welche Vorteile und (b) Nachteile haben analytische Lösungen von Differentialgleichungen gegenüber numerischen Lösungen? (ANTWORT: Analytische Lösungen haben den Vorteil, dass sie (im Sinne guter wissenschaftlicher Methode) sehr einfach sind und die kontrollierenden Parameter eines Prozesses klar interpretiert werden können. Numerische Lösungen haben den Vorteil, dass Prozesse mit viel wirklichkeitsnäheren Rand- und Anfangsbedingungen beschrieben werden können).

7. EINHEIT: Die Höhe von Gebirgen

– **7.1:** Was ist Isostasie? (ANTWORT: Ein Spannungsgleichgewicht in der senkrechten Richtung. Das Gleichgewicht der Spannungen erfolgt in der "isostatischen Kompensationstiefe". In dieser Tiefe sind die Gewichte alles darüber liegenden Materials gleich).

– **7.2:** McKenzie hat vor etwa 40 Jahren berechnet, bei welchem Verhältnis aus Kruste und Gesamtlithosphäre gleichmässige Dehnung *keine* Veränderungen in der isostatisch

kompensierten Seehöhe der Erdoberfläche ergibt. Berechne dieses Verhältnis mit der Gleichung $H = \delta z_c(f_c - 1) - \xi z_l(f_l - 1)$ (z_c und z_l sind die Mächtigkeiten von Kruste und Gesamtlithosphäre, f_c und f_l die Verdickungsparameter, δ das Dichteverhältnis $(\rho_m - \rho_c)/\rho_m)$ und $\xi = \alpha T_l/2$. Die Zahlenwerte für δ und ξ sollten Sie in etwa wissen. (ANTWORT: Für $H = 0$ und $f_c = f_l$ ergibt die Gleichung: $z_c/z_l = \xi/\delta = 12$ prozent).

- **7.3:** Wie lange braucht isostatische Angleichung und warum wird isostatisches Gleichgewicht nicht sofort hergestellt? (ANTWORT: Isostatisches Gleichgewicht wird auf dem Maßstab von 10^4 Jahren erreicht. Es braucht so lange weil das Asthenosphärenmaterial verdrängt bzw. nachfliessen muss. Trotzdem ist auf geologischen Zeitmaßstäben isostatische Angleichung als sofortig zu betrachten).

- **7.4:** Wie kann man nachweisen ob ein Gebirge isostatisch kompensiert ist? (ANTWORT: Nachdem die Massen im isostatischen Gleichgewicht überall gleich sind, kann das Gleichgewicht mit gravimetrischen Messungen bewiesen werden).

- **7.5:** Was ist Isostasie nach Airy und nach Pratt? (ANTWORT: Nach Airy sollte jede topografische Erhebung an der Erdoberfläche durch eine Krustenwurzel kompensiert sein. Nach Pratt sind topografisch hohe Bereiche, Bereiche geringerer Dichte und es gibt keine Wurzel in der Tiefe).

- **7.6:** Welche Prozesse tragen zur isostatisch kompensierten Höhe eines Gebirges bei? (ANTWORT: Die Kruste hat aufgrund ihrer relativ geringen Dichte einen positiven Auftrieb. Der Mantelteil der Lithosphäre hat aufgrund seiner kühleren Temperatur einen negativen Auftrieb. Die 2 Beiträge sind vergleichbar wichtig).

- **7.7:** Um isostatisch kompensierte Höhen zu berechnen brauche ich Mächtigkeiten der Kruste, der Mantellithosphäre, die Dichten, und den thermischen Ausdehnungskoeffizient. Wie gross sind diese Parameter und was sind ihre Einheiten? (ANTWORT: Krustenmächtigkeit: $= 3 \times 10^4$ [m]; Mantellithosphäre: $= 10^5$ [m]; Dichte Kruste: $\rho_c = 2700$ [kg/m^3]; Dichte Mantellithosphäre (bei Null Grad): $\rho_m = 3200$ [kg/m^3]; thermischer Ausdehnungskoeffizient: $\alpha = 10^{-5}$ [°C]).

- **7.8:** Zeichne ein Diagramm in dem die Mächtigkeit der Kruste gegen die Mächtigkeit der Gesamtlithosphäre aufgetragen ist, konturiere es (schematisch) für isostatisch kompensierte Seehöhe und zeichne typische orogene Entwicklungspfade z.B. für die Alpen und die Indien-Asien Kollisionszone ein. (ANTWORT: Abb. 35).

- **7.9:** Die mittlere Höhe der Zentralalpen ist etwa 2000 m und die Kruste ist dort fast 60 km mächtig. Benutze die Beziehung $H = \delta z_c(f_c - 1) - \xi z_l(f_l - 1)$ um die isostatisch kompensierte Mächtigkeit der Mantellithosphäre zu berechnen. z_c und z_l sind die Mächtigkeiten von Kruste und Gesamtlithosphäre (Achtung: Mantellithosphäre $= z_l - z_c$), f_c und f_l die Verdickungsparameter und δ= 0,15 und ξ= 0.018 fassen die Materialkonstanten zusammen.

- **7.10:** Wenn Sie mit der Gleichung $H = \delta z_c(f_c - 1) - \xi z_l(f_l - 1)$ isostatisch kompensierte Höhen berehchnen, *was* genau sind das für Höhen? (ANTWORT: Die Höhe über der undeformierten Referenz lithosphäre).

8. EINHEIT: Die Wassertiefe der Meere

- **8.1:** Wir haben den Flexurparameter α erwähnt und gesagt, dass er eine Zusammenfassung der Materialkontanten ist, die bei der Anwendung der Flexurgleichung auf die

elastische Biegung ozeanischer Platten oft vorkommen. Er ist: $\alpha = (4D/(g(\rho_m - \rho_w))^{0.25}$. Welche Einheit hat α und wie gross ist er etwa? (Nimm: $D \approx 10^{23}$ [Nm]; $\rho_m = 3200$ [kg m^{-3}]; $\rho_w = 1000$ [kg m^{-3}] und $g = 10$ [m s^{-2}]).

- **8.2:** Beschreibe in Worten wie Sie eine Gleichung zur Berechnung der Wassertiefe der Ozeane als Funktion vom Mittelozeanischen Rücken aufstellen würden. (ANTWORT: Nachdem die ozeanische Kruste gleichmässig dick und vernachlässigbar mächtig ist, ist nur die Mantellithosphäre und Wasser zu berücksichtigen. Die Dichte der ozeanischen Mantelltihosphäre kann mit dem half-space cooling Modell berechnet werden. Integration dieser Dichte über Tiefe und Vergleich mit dem Mittelozeanischen Rücken ergibt die Wassertiefe. Sie ist eine Quadratwurzelfunktion vom Alter der ozeanischen Platten).

- **8.3:** Welche mathematischen Funktionen beschreiben die elastisch gebogene Form von Platten? (ANTWORT: Sinusfunktionen, die durch eine negative Exponentialfunktion gedämpft sind).

- **8.4:** Wie breit muss eine topografische Erscheinung an der Erdoberfläche (z.B. ein Gebirge) sein damit man es vernünftigerweise als isostatisch kompensiert betrachten kann? (ANTWORT: Nachdem die elastische Mächtigkeit der Lithosphäre etwa 40 - 80 km ist, ist die Biegung wohl auch zumindest so breit und ein Gebirge sollte so um etwa das 3-fache breiter sein (also 150 - 250 km breit damit es auch isostatisch kompensiert ist).

- **8.5:** Die flexurelle Rigidität D ergibt sich aus: $D = Eh^3/(12(1 - \nu^2))$. Bestimme die elastische Mächtigkeit der Lithosphäre h für eine typische Rigidität von $D = 10^{24}$ [N/m] und diskutiere warum sie anders ist als die thermisch oder mechanisch definierte Lithosphäre. Die Materialkonstanten sind $E = 10^{11}$[Pa] und $\nu = 0.25$. (ANTWORT: Es ergibt sich $h \approx 50$ km. Die Mächtigkeit ist deutlich geringer als nach anderen Deformationen, weil die oberste Kruste spröd bricht und die unterste Lithosphäre ist sehr weich. Daher ist nur der Kern der Lithosphäre elastisch).

- **8.6:** Die Pazifische Platte hat eine Rigidität von $D = 10^{24}$ [N/m]. Um Hawai bildet der Tiefseeboden der Pazifik Platte einen elastischen Buckel, der etwa x=250 km von der Inselkette entfernt liegt. Benutze diese Beobachtung und die Gleichung $w = w_o \exp(-x/\alpha)(\cos((x/\alpha) + \sin((x/\alpha))$, um die Rigidität der Pazifik Platte zu bestimmen. (Obwohl dies eine ausgesprochen schwere Frage ist, ist genau dieses Problem recht berühmt aus den Anfängen der Plattentektonik und soll daher hier angeführt werden!). (Tip: Auf dem elastischen Buckel ist die Steigung Null. D.h. es gilt: $dw/dx = 0$ (ANTWORT: Eine Ableitung der Gleichung nach x ergibt: $dw/dx = -2w_o/\alpha \times \exp(-x/\alpha)\sin(x/\alpha))$. Dies gleich Null gesetzt ergibt: $x = \pi\alpha$ und daraus ergibt sich der Flexurparameter sowie die Rigidität).

- **8.7:** Bei der Anwendung der Flexurgleichung auf die Lithosphäre sind innere und äussere Lasten zu berücksichtigen. Was ist damit gemeint? (ANTWORT: die *äussere Last* ist die Topografie eines Gebirges das auf der Platte liegt. *Innere Last* ist die leichte Krustenwurzel deren Auftrieb der äusseren Last entgegen wirkt (siehe Abb. 40).

- **8.8:** Es ist allgemein bekannt, dass 90% eines Eisberges unter Wasser liegen. Benutze diese Beobachtung und die Definition von Isostasie um die Dichte von Eis zu bestimmen. (Die Dichte von Wasser ist $\rho_w = 1000$ [kg/m^3]). (ANTWORT: Die Isostasiebeziehung besagt, dass die integrierte Dichte überall gleich ist. Daher gilt für Eis und Wasser mit

konstanter Dichte (nach Abb. 33): $0.1 = (\rho_w - \rho_{eis})/\rho_w$. Daraus ergibt sich die Dichte mit $\rho_{eis} = 900$ kg/m^3).

- **8.9:** Gesteine sind angeblich recht komprimierbar (Poissons Ration zwischen $\nu = 0.1$ - 0.3). Macht das Sinn? (Siehe auch Einheit 9). (ANTWORT: Ja! Komprimierbarkeit ist nicht mit Elastizität oder Verformbarkeit zu verwechseln! Komprimierbar heisst, dass Gesteine bei Druck Volumen verlieren. Das ist nur deshalb nicht so offensichtlich, weil Gesteine sehr hoche Elastizitätsmodule haben. Daher ist der Gesamtverformung die sie elastisch aufnehmen sehr gering (aber ein Teil derselben geht eben in Volumsverringerung).

- **8.10:** Nenne zwei Stellen in kontinentaler Lithosphäre wo man elastisches Verhalten beobachten kann und illustriere mit einer Skizze die Biegung der Platte. (ANTWORT: Vorland Becken und Great Escarpments. An beiden gibt es elastische Buckel).

9. EINHEIT: Deformationsmechanismen

- **9.1:** Was ist Hooke's Gesetz? (ANTWORT: Das lineare Elastizitätsgesetz: $\sigma = E \times \epsilon$ (Spannung und Verformung sind proportional). Die Proportionalitätskonstante E (Youngs Modul) ist für Steine etwa 10^{10} - 10^{11} Pascal).

- **9.2:** Was ist der *Elastizitätsmodel* und was die *Poissons Ratio*? (ANTWORT: Der Elastizitäts- oder Youngs Modul ist die Proportionalität zwischen Spannung und Verformung in Hooke's Gesetz. Die Poissons Ratio ist das Verhältnis aus Verkürzung in eine Richtung und Ausdehnung in die anderen 2 Richtungen und ist somit ein Maßder Kompressibilität von Gesteinen).

- **9.3:** Was ist die Grundaussage des Mohr Coulomb Kriterions? (ANTWORT: Dass die Bruchspannung eines spröd brechenden Mediums proportional zur Normalspannung ist. Die Proportionalitätskonstante heisst *innerer Reibungskoeffizient*. Die Kohäsion muss zu dieser Beziehung dazu addiert werden).

- **9.4:** Was ist eine Newton'sche Flüssigkeit? (ANTWORT: Ein Flüssigkeit mit linearer Beziehung aus deviatorischer Spannung und Verformungsrate. Die Proportionalitätskonstante wird als Viskosität bezeichnet).

- **9.5:** Wie unterscheidet sich das duktile Verhalten von Gesteinen von einer Newton'schen Flüssigkeit? (ANTWORT: durch eine starke Nicht-Linearität. Der Powerlaw Exponent zwischen deviatorischer Spannung und Verformungsrate ist etwa 3. Das heisst, bei doppelter Kraft verformt sich das Material etwa 8 mal so schnell).

- **9.6:** Ein Gestein verformt sich duktil nach der Beziehung: $\sigma_d = (\dot{\epsilon}/A)^{(1/n)} \times \mathrm{e}^{Q/(nRT)}$. Die Materialkonstanten Q, A und n wurden mit: $Q = 1,9 \times 10^5$ [J/mol] und $A = 5 \times 10^{-6}$ [MPa^{-3}s^{-1}] n=3 bestimmt. Mit welcher Rate wird sich das Gestein bei 500°C verformen wenn eine Differentialspannung von 50 MPa angelegt wird? (ANTWORT: Mit $\dot{\epsilon} = 8,78 \times 10^{-14}$ [s^{-1}]).

- **9.7:** Byerlee hat empirisch festgestellt, dass $\mu = 0.85$ ein guter Schätzwert für den Reibungskoeffizient auf Krustenmaßstab ist. Schätze ab wir hohe Scherspannungen an der Moho (in 30 km Tiefe) aufgebracht werden müssen um ein Gestein spröd zu zerbrechen. (ANTWORT: Die Moho liegt etwa 30 km tief. Die Normalspannung ist dort: $\sigma_{zz} = \rho_c g z_c$ also etwa 8.1 kbar. Die spröde Festigkeit ist daher dort etwa 680 MPa).

- **9.8:** Sie sind am viskosen (duktilen) Verformungsverhalten von einem Staurolit- Granat-Biotit-Muskovit Glimmerschiefer interessiert. Von welchem Gestein oder Mineral suchen Sie sich die Mterialkonstanten dazu heraus? (ANTWORT: Das Deformationsverhalten eines Gesteins wird von der weichesten vernetzten Phase bestimmt. In Glimmerschiefern ist das in der Regel Quarz und daher brauche ich die Materialkonstanten von Quarz).

- **9.9:** Wovon hängt das Deformationsverhalten bei (a) Sprödbruch und (b) Viskoser Verformung ab? (ANTWORT: Spröd: abhängig vom Gesamtdruck, unabhängig vom Material, Temperatur oder Verformungsrate. Viskos: abhängig vom Material, Temperatur und Verformungsrate, aber unabhängig vom Druck).

- **9.10:** Bestimme die Einheiten aller Parameter in der folgenden Gleichung: $\sigma_d = (\dot{\epsilon}/A)^{(1/n)} \times e^{Q/(nRT)}$. (ANTWORT: σ_d= [Pa]; ($\dot{\epsilon}$ = [s^{-1}]; Q= [J/mol]; R= [J/mol/K]; T= [K]; A=[(Pa/s)$^{1/n}$]).

10. EINHEIT: Rheologie und Kräftegleichgewicht

- **10.1:** Mit welchem (einzigen) Verformungsmechanismus beschreibt man die Rheologie der Lithosphäre am besten? (ANTWORT: Nicht-linear viskoses Verhalten dominiert (bis auf den spröd brechenden Teil oberhalb der brittle- duktile Transition) 90% der Lithosphäre und dieser Mechanismus ist daher eine gute Annäherung für das Verhalten der gesamten Lithosphäre).

- **10.2:** Beschreiben Sie eine einfache Beziehung eines orogenen Kräftegleichgewichtes. (ANTWORT: Festigkeit der Lithosphäre = Plattentektonische Antriebskraft - Horizontale gravitative Kraft des Gebirges ($F_l = F_d - F_b$)).

- **10.3:** Zeichnen Sie ein schematisches rheologisches Profil durch die Lithosphäre und beschriften Sie eine Reihe von wichtigen Aspekten desselben. (ANTWORT: Skizze so wie Abb. 47 - 50 mit Beschriftung von: (a) Horizontalachse: Differentialspannung (von 0 - 1 GPa); (b) Vertikalachse: Tiefe (von 0 - 150 km); (c) Brittle Ductile Transition; (d) viskose Kurven für langsame und schnelle Verformung; (e) Sprödkurve an der Moho etwa bei gleicher Spannung wie die viskose Kurve. (f) Fläche unter dem Profil = Festigkeit der Lithosphäre).

- **10.4:** Was bezeichnet man als "effektive plattentektonische Antriebskraft"? (ANTWORT: Die externe Antriebskraft minus die potentielle Energie (pro Quadratmeter) des davor liegenden Orogens. Dieser Wert hat die Einheiten [N/m]).

- **10.5:** Zeichnen Sie ein schematisches rheologisches Profil durch die ozeanische Lithosphäre aus dem erkenntlich ist warum die ozeanische Lithosphäre höhere Differentialspannungen unterstützt (also: härter ist) als kontinentale, obwohl sie dünner ist. (ANTWORT: Vergleichsskizzen so wie Abb. 50 und Abb. 51, die zeigen, dass die Fläche unter der Kurve in Abb. 51 grösser ist).

- **10.6:** Wie gross ist die Festigkeit der Lithosphäre (f_l) etwa und welche Einheit hat sie? (ANTWORT: Bei normalen kontinentalen Verformungsraten etwa $f_l = 5 \times 10^{12}$ [N/m]).

- **10.7:** Wenn Sie nichts über die rheologische Stratifizierung der Lithosphäre wissen würden, welche Hinweise gibt es trotzdem auf die Grössenordnung des Zahlenwertes für die Festigkeit von Gesteinen (ANTWORT: Die Tatsache, dass das Altiplano und

das Tibetische Plateau die limitierende Seehöhe erreicht haben zeigt, dass die mittlere Festigkeit der Lithosphäre gross genug sein muss, um diese Plateaus aufzubauen. Aus dem Gewicht solcher Plateaus (plus deren Krustenwurzel) ergeben sich Werte zwischen 50 - 70 MPa, gemittelt über eine 100 - 150 km mächtige Lithosphäre).

- **10.8:** Die rheologischen Daten für Quarz sind $Q = 1.9 \times 10^5$ [J/mol]; $A = 5 \times 10^{-6}$ [MPa^{-3} s^{-1}] und $n = 3$. Jene für Olivin sind: $Q = 5.2 \times 10^5$ [J/mol]; $A = 7 \times 10^4$ [MPa^{-3} s^{-1}] und $n = 3$. Berechne mit der Beziehung $\sigma_d = (\dot{\epsilon}/A)^{1/n} \times \exp(Q/(nRT))$ die wievielfache Differentialspannung (σ_d) Olivinhältige Gesteine als Quarzhältige Gesteine bei 1000°C aushalten. (ANTWORT: $\sigma_d(olivin)/\sigma_d(quarz) = (A_q/A_o)^{1/n} \times \exp((Q_o - Q_q)/(nRT)) = 73$. Olivin ist also um knapp das hundertfache härter).
- **10.9:** Wenn ein Gebirge hoch genug ist sodass sein gravitatives Gewicht (F_b) gleich gross ist wie die plattentektonische Antriebskraft (F_d), dann ist die effektive Antriebskraft gleich Null ($F_{eff} = F_d - F_b$) und die Festigkeit der Lithosphäre ebenfalls Null. Was passiert in diesem Fall wenn die Konvergenz weiter anhält? (ANTWORT: Das Gebirge wird nicht mehr höher, aber wird beginnen in die Breite zu wachsen).
- **10.10:** Zeige anhand einer schematischen Skizze eines rheologischen Profils durch die Lithosphäre warum (und wieviel) Kontinente in Dehnung weicher sind als in Kompression? (ANTWORT: An den viskosen Kurven ändert sich nichts, aber die Sprödbruchkurve ist um dadurch wird die Lithosphäre in Dehnung (bei gleichbleibender Temperatur und Verformungsrate) insgesamt um etwa 10% weicher).

11. EINHEIT: Plattentektonische Antriebskräfte

- **11.1:** Was hat potentielle Energie mit plattentektonischen Antriebskräften zu tun? (ANTWORT: Nachdem die Lithosphäre von viskosem Verhalten dominiert wird, hat sie im lithostatischen Zustand auch keine Festigkeit. Daher ist die seitlich ausgeübte Kraft in jeder Tiefe gleich gross wie die Normalspannung. Die insgesamt horizontal ausgeübte Kraft der Lithosphäre ist gleich der Summe aller Normalspannungen über Tiefe. Dieser Wert ist ident mit der potentiellen Energie der Lithosphäre pro Quadratmeter Fläche).
- **11.2:** Vom Aspekt des Spannungsansatzes, auf welche 2 fundamental verschiedene Wege kann man Käfte in ein Orogen übertragen? (ANTWORT: Durch Scherspannung an der Unterseite (nur relevant auf relativ kleinem Maßstab z.B. in Akkretionskeilen), Normalspannungen (Gebirgsbildung auf Plattenmaßstab).
- **11.3:** Diskutiere den Unterschied des Spannungsfeldes bei Platten Kollision (Gebrigsbildung) und Kontinentaler Dehnung (ANTWORT: Bei Kollision ist die grösste Hauptnormalspannung σ_1 horizontal orientiert, bei Dehnung ist σ_1 vertikal orientiert. In beiden Fällen sind jedoch alle drei Hauptnormalspannungen positiv (sie zeigen also aufeinander zu).
- **11.4:** Plattentektonische Prozesse können Subjekt von zwei mechanisch verschiedenen Randbedinungen sein. Welchen? (ANTWORT: (a) Die orogene Entwicklung kann durch *Spannungen* am Orogenrand kontrolliert werden (und die Geschwindigkeiten ergeben sich aus den Spannungen). (b) die orogene Entwicklung hängt von *Geschwindigkeiten* der Konvergenz ab (unabhängig von den Spannungen) (Himalaya).
- **11.5:** Bestimmen Sie grafisch die plattentektonische Kraft die sich aus den potentiellen Energie Unterschieden von Säule A auf Säule B ergibt (ANTWORT: siehe Skizze in Abb. 74).

Figure 74: Illustration zu Frage 11.5.

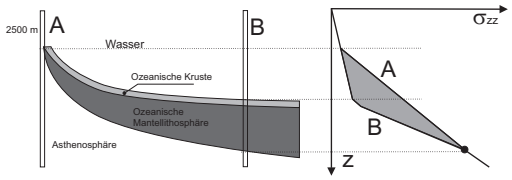

– **11.6:** Zeichne, nebeneinander, zwei Skizzen für die Situation aus Abb. 33: (a) Dichte gegen Tiefe und (b) Vertikale Normalspanung (σ_{zz}) gegen Tiefe. Achten Sie darauf, dass die Skizzen in der gleichen Tiefen den richtigen Werten entsprechen und diskutieren Sie welche Flächen welchen Werten entsprechen (ANTWORT: siehe Abb. 76).

Figure 75: Illustration zu Frage 11.6.

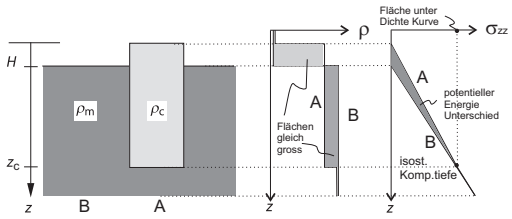

– **11.7:** Die Seehöhe eines Gebirges im isostatischen Gleichgewicht wird durch die Dichte und Mächtigkeit der Lithosphäre bestimmt. Was ist der grundlegende Unterschied von potentieller Energie im Vergleich zur Isostasie? In anderen Worten, welche zusätzliche Info braucht man um die plattentektonische Antriebskraft zu bestimmen? (ANTWORT: Für Isostasie brauche ich nur Mächtigkeiten und Dichten. Für potentielle Energie ausserdem die *Verteilung* von Dichte mit Tiefe in der Lithosphäre).

– **11.8:** Für eine ganz einfache, einschichtige Lithosphäre, ergibt sich die Kraft, die ein Gebirge auf sein Vorland ausübt (pro Meter Orogenlänge) (oder auch: die potentielle Energie pro Quadratmeter) durch: $F_b = \rho_c g H(H/2 + z_c + w/2)$, wobei H die Seehöhe, g die Erdbeschleunigung, w die Mächtigkeit der Krustenwurzel und z_c die Mächtigkeit der Kruste ist. Was kann man aus dieser Beziehung lernen? (ANTWORT: (a) F_b nimmt quadratisch mit der Seehöhe des Gebirges zu. Es ist also deutlich schwerer ein Gebirge von 3000 m auf 3001 m zu heben, als es ist von 1000 m auf 1001 zu heben. (b) Der dritte Ausdruck dieser Gleichung ist deutlich grösser als der 1. Das heisst, die Mächtigkeit der Wurzel bestimmt den potentiellen Energieunterschied maßgeblich).

– **11.9:** Wie gross ist Ridge Push und (ANTWORT: die Ridge Push Kraft nimmt linear mit dem Alter der ozeanischen Lithosphäre zu und ist für 100 mio J alte ozeanische Platten etwa 3 10^{12} [N/m] gross).

– **11.10:** Was wissen wir über "Slab Pull"? (ANTWORT: Nicht sehr viel! Das Gewicht ozeanischer Platten, das diese nach unten zieht ist natürlich gut berechenbar, aber der Reibungswiderstand der Asthenosphäre lässt sich kaum abschätzen und daher ist nicht gut bekannt ob Slab Pull deutlich grösser oder vernachlässigbar kleiner als Ridge Push ist).

12. EINHEIT: Dynamische Entwicklung von Gebirgen

- **12.1:** Was ist die "Thin Sheet" Annäherung? (ANTWORT: Die Thin Sheet Annäherung wird auch als "Plane Stress" Annäherung bezeichnet, weil in ihr die Annahme getroffen wird, dass die Scherspannungen an der Ober- und Unterseite der Platte Null sind und die Normalspannungen an diesen Oberflächen überall konstant ("plane") sind. Dadurch sind keine Verformungsraten Gradienten in senkrechter Richtung möglich. Sie bildet die bestmögliche Annäherung plattentektonische Prozesse auf Plattenmaßstab in 2-D zu modellieren).

- **12.2:** Was bedeutet "Plane Strain" und warum ist plane strain nicht "Plane Stress"? (ANTWORT: "Plane Strain" bedeutet strikte 2-Dimensionalität, also Flächenkonstanz. Wenn man sich Plane Strain Verformung als einen verformenden Film zwischen 2 Glasplatten vorstellt, ist leicht ersichtlich, dass der Druck auf die Glasplatten in horizontaler Richtung variiert).

- **12.3:** Zeichnen Sie auf dem beiliegenden Profil im Becken, Vorland und Orogen Vektoren (also Länge und Grösse) für die Hauptnormalspannungen ein (Nehmen Sie 2-Dimensionalität an (also: es gibt nur σ_1 und σ_3) und die Thin sheet Annäherung (also: σ_1 und σ_3 sind entweder vertikal oder horizontal orientiert) (ANTWORT: Die horizontalen Spannungen sollten an allen drei Stellen gleich gross sein. Im Orogen sollte die vertikale Spannung grösser sein, im Becken kleiner).

Figure 76: Illustration zu Frage 12.3.

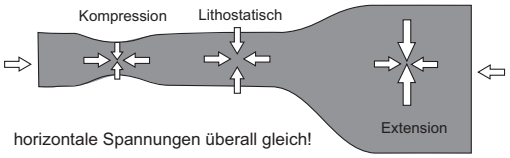

- **12.4:** Was ist die Argand Zahl? (ANTWORT: Die Argandzahl ist das Verhältnis aus vertikalen und horizontalen Spannungen bei der Orogenese. Sie ist ein Maßfür die "Zerrinnbarkeit" eines Orogens. Für kleine Argandzahlen überwiegen die horizontalen Spannungen und Gebirgsbildung ist duch die Randbedingungen kontrolliert. Bei grossen Argandzahlen überwiegen die vertikalen Spannugen und ein Orogen wird etwa gleich schnell zerfliessen wie es aufgebaut wird, d.h. es baut sich kaum Topografie auf. Die Argandzahl kann als input Parameter für numerische Modelle verwendet werden ohne Annahmen über Temperaturverteilung oder Rheologie treffen zu müssen).

- **12.5:** Wie kann es zur Dehung während der Kontinent-Kontinent Kollision kommen? (ANTWORT: Durch offene Ränder, (ii) Durch zusätzlichen input von potentieller Energie (z.B. durch Delamination der Mantellithosphäre), (iii) durch Verringerung der Konvergenzgeschwindigkeit).

- **12.6:** Der potentielle Energie Unterscheid, der nötig ist um eine Gebirge entweder aufs doppelte zu verbreitern oder aufs doppelte zu heben haben wir bestimmt. Er ist: $\Delta E_{p(hoch-breit)} = (\rho_c \rho_m / (\rho_m - \rho_c) \times glH^2$. Diskutiere anhand dieser Gleichung wie die Entwicklung eines Kollisionsorogens aussehen wird. (ANTWORT: Nachdem die Breite linear eingeht und die Höhe quadratisch ist es klar, dass ein Gebirge mit zunehmender

Höher schwerer wachsen kann und dass die Deformation ins Vorland propagieren wird um das Gebirge in die Breite zu wachsen).

– **12.7:** Bestimme grafisch die Ridge Push Kraft anhand der hier angeführten Skizze. Beschrifte die Achsen gut genug mit Zahlen, sodass aus Ihrer Grafik ein etwaiger Zahlenwert für Ridge Push abgelesen werden kann. (ANTWORT: Siehe Abb. 77).

Figure 77: Illustration zu Frage 12.7.

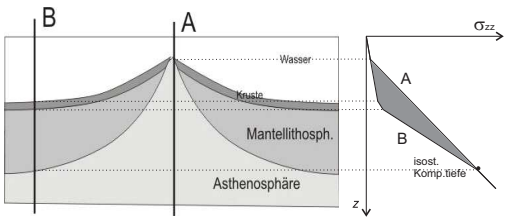

– **12.8:** Was ist "Lateral Extrusion" und welche mechanischen Prozesse beinhaltet sie? (ANTWORT: Lateral Extrusion bezeichnet die Bewegung eines Gebirges senkrecht zur Konvergenz Richtung. Der Prozess beinhaltet gravitativen Kollaps (laterale Extension) und "tectonic forcing" (in Kompression). In den Ostalpen sieht man beides (wahrscheinlich nicht genau zeitgleich): Extension entlang N-S streichenden Abschiebungen (Brenner, Katschberg) und "tectonic forcing" (konjugierte Lavanttal und Mur-Mürz Störungs systeme).

– **12.9:** Was ist mit "effektiver Viskosität" gemeint? (ANTWORT: Viskosität in einer Newton'schen Flüssigkeit hat die Einheiten [Pa × s]. In nicht-linearer viskoser Verformung hat die Proportionalitätskonstante die Einheit $[(\text{Pa} \times \text{s})^n]$ und wird oft mit A abgekürzt (Also: $\tau_s^n = A\dot{\epsilon}$). Die "effektive Viskosität" ist - in Analogie zur Newton'schen Viskosität - durch das Verhältnis aus deviatorischer Spannung und Verformungsrate definiert. Sie ergibt sich als: $\eta_{eff} = A^{1/n} \times \dot{\epsilon}^{(1/n)-1}$).

– **12.10:** Berechne wie viel potentielle Energie pro Meter Orogenlänge (ΔE_p) aufgebracht werden muss, um ein Gebirge der Breite l= 100 km und der Höhe H = 3000 m aufzubauen. Benutze die Gleichung: $\Delta E_p = \rho_c g H l(H/2 + z_c + w/2)$ mit w = 30000 m und Standartwerte Ihrer Wahl für dichte, Beschleunigung und Krustenmächtigkeit. (ANTWORT: Zahlenwerte ergeben etwa 4 $\times 10^{12}$ [N/m]. Das ist ein durchaus normaler Wert für plattentektonishce Antriebskräfte.).

13. EINHEIT: Basis Prinzipien von Spannung und Verformung

– **13.1:** Was ist Druck? (ANTWORT: Die mittlere Spannung. Druck ergibt sich aus dem Mittelwert der 3 Hauptnormalspannungen: $P = (\sigma_1 + \sigma_2 + \sigma_3)/3$).

– **13.2:** Was ist Differentialspannung? (ANTWORT: Es ist der Unterschied zwischen grösster und kleinster Hauptnormalspannung: $\sigma_d = (\sigma_1 - \sigma_3)$).

– **13.3:** (a) Was ist deviatorische Spannung und (b) warum ist sie so praktisch? (ANTWORT: (a) Es ist die Abweichung des Spannungszustandes vom Druck. (b) Deviatorische Spannungen sind in Vorzeichen und Grösse equivalent zu den Beobachtungen über Verformung und Verformungsrate).

- **13.4:** Was ist die Navier Stokes Gleichung? (ANTWORT: Es ist die wichtigste Gleichung der Fluid Dynamik. Sie koppelt die Gleichungen des Spannungsgleichgewichtes mit einem viskosen Fliess Gesetz).

- **13.5:** Was ist Hauptnormalspannung? (ANTWORT: Es sind die Normalspannungen in einem Koordinatensystem, das so orientiert ist, dass alle Scherspannungen gleich Null sind).

- **13.6:** Ist den "Schwung" von Platten, also der Impuls wichtig für Gebirgsbildung? (ANTWORT: Impuls ergibt sich aus Masse $\times$ Geschwindigkeit. Nachdem die Masse von Platten sehr gross ist, aber die Geschwindigkeit sehr klein ist die Wichtigkeit von Impuls nicht von vornherein offensichtlich. Die Kraft die durch Impuls ausgelöst wird, ist die Impulsänderung pro Zeit. Es stellt sich heraus, dass diese auf tektonischem Maßstab vernachlässigbar kleine Kräfte bewirkt).

- **13.7:** Was ist tektonischer Überdruck? (ANTWORT: Es ist jene Komponente im Druck, die nicht durch Überlagerung verursacht wird. Er ist in der Regel von der Größenordnung $(\sigma_1 - \sigma_3)/2)$).

- **13.8:** Wie gross sind: (a) die Differentialspannung σ_d, (b) der Druck P; (c) die deviatorischen Hauptnormalspannungen τ_1 und τ_2 und: (d) ist der tektonische Überdruck in einem Gestein in einem kompressiven Orogen, in dem die vertikalen Normalspannung $\sigma_3 = 100$ MPa und die horizontale Normalspannung $\sigma_1 = 300$ MPa ist. (Wir nehmen 2-Dimensionalität an, also berücksichtigen kein σ_2). (ANTWORT: (a) $\sigma_d = \sigma_1 - \sigma_3 =$ 200 MPa; (b) $P = (\sigma_1 + \sigma_3)/2 = 200$ MPa; (c) $\tau_1 = \sigma_1 - P = +$ 100 MPa; $\tau_3 = \sigma_3 - P =$ - 100 MPa; (d) Überdruck $= P - \sigma_3 = 100$ MPa).

- **13.9:** Was ist Normalverformung ("Normal Strain") und was ist Scherverformung ("Shear Strain")? (ANTWORT: Normalverformung hat die Einheiten von (Länge nach der Verformung (l) / (Länge vor der Verformung (l_0)) und ist somit einheitslos. Wir unterscheiden "Streckung" $= l/l_o$ und "Elongation" $= (l - l_o)/l_o)$. Scherverformung hat die Einheiten von horizontalem Versatz pro Länge senkrecht zur Versatzrichtung, also $\tan\phi$).

- **13.10:** Was ist der Zusammenhang von Geschwindigkeiten und Verformungsraten? (ANTWORT: Geschwindigkeiten sind in [m/s], Verformungsraten in $[s^{-1}]$. Verformungsraten ergeben sich aus den räumlichen Gradienten der Geschwindigkeiten).